

The Role of Tubedown in Ocular Endothelial Permeability

By

©Kindra R. Grozinger

A thesis submitted to the School of Graduate Studies in partial fulfillment of the requirements of the degree of Master of Science

**Division of Biomedical Sciences
Faculty of Medicine
Memorial University**

July 2012

St. John's

Newfoundland

ABSTRACT

Tubedown (Naa15) is a protein that associates with the acetyltransferase Arrest defective protein 1 (Naa10) and is involved in the regulation of vascular homeostasis of the retina. In endothelial cells Tubedown interacts with the actin-binding protein Cortactin. Cortactin is a known regulator of the permeability of molecules through cells (transcytosis) and between cells (paracytosis). Transcytosis is enhanced by the phosphorylation of Cortactin at tyrosine residues. Recent studies have shown that stable suppression of Tubedown expression leads to increased endothelial cell permeability. Increased permeability leading to pathological angiogenesis is observed within patients with wet age-related macular degeneration (AMD), proliferative diabetic retinopathy (PDR), and retinopathy of prematurity (ROP). Previous studies have revealed that patients with wet AMD, PDR, and ROP, have decreased levels of Tubedown in correlation with areas of pathological angiogenesis. The present work aims to investigate Tubedown's mechanistic involvement in retinal permeability pathways, to further elucidate its role in ocular neovascular diseases.

Immunoprecipitation and western blotting techniques were used to explore possible interactions between Tubedown and known regulators of permeability pathways: Dynamin, Afadin-6 (AF-6), Y421-Phospho-Cortactin, c-Src, and Zona Occludins-1 (ZO-1). These results provided evidence that the mechanism by which permeability is regulated by Tubedown does not likely involve an interaction with Dynamin, AF-6, c-Src, or ZO-1. The specific interaction of Tubedown with non-phosphorylated Cortactin but not Y421-Phospho-Cortactin suggests that Tubedown may attenuate phosphorylation

of Cortactin and subsequently decrease transcytosis. Furthermore, *in vitro* transient and stable knockdown techniques for Tubedown expression were combined with immunofluorescence microscopy to determine if reduced Tubedown levels affect the distribution of the paracytosis regulator ZO-1 in cultured rhesus macaque retinal-choroidal endothelial cells. While stable Tubedown knockdowns showed decreased ZO-1 cell perimeter expression, transient Tubedown knockdowns had no effect on ZO-1 cell perimeter distribution. Tubedowns effect on ZO-1 perimeter distribution remains inconclusive.

ACKNOWLEDGEMENTS

I would like to thank my supervisors, Drs. H el ene Paradis and Robert Gendron, for their guidance, support, and financial assistance throughout the pursuit of my M.Sc. program. I would also like to thank Kerri Smith and Dr. Jules Dor e for their helpful training which enabled me to successfully complete my research. Also, thanks to my supervisory committee member, Dr. Ann Dorward, for her invaluable guidance and encouragement.

I would like to thank all lab members, Dr. Ewa Miskiewicz, Jackie Walker, Danielle Gardiner, and Krista Squires for their assistance within the lab. Thank you, Nhu Ho for all your support throughout my entire M.Sc. program.

Thank you to my family, Mimi Grozinger, Ken Grozinger, Kim Smith, and Kyle Grozinger for your support, encouragement, and love throughout the completion of my research. Thank you to my friend, Travis Gitau, for guidance and encouragement at all times.

Lastly, I would like to thank the School of Graduate Studies, Faculty of Medicine, and CIHR for their financial support as a graduate student.

TABLE OF CONTENTS

| | |
|--|------|
| ABSTRACT..... | ii |
| ACKNOWLEDGEMENTS..... | iv |
| TABLE OF CONTENTS..... | v |
| LIST OF TABLES..... | vii |
| LIST OF FIGURES..... | viii |
| LIST OF ABBREVIATIONS..... | x |
| 1.0 INTRODUCTION..... | 1 |
| 1.1 Eye Sight..... | 1 |
| 1.2 Ocular Vasculature..... | 3 |
| 1.3 Neovascular Retinopathies..... | 4 |
| 1.4 Molecular Pathways of Endothelial Permeability..... | 8 |
| 1.4.1 Transcellular Permeability (Transcytosis)..... | 8 |
| 1.4.2 Paracellular Permeability (Paracytosis)..... | 11 |
| 1.5 Tubedown: Homeostatic Regulator of the Ocular Vascular Systems through Endothelial Permeability Regulation..... | 12 |
| 1.5.1 Tubedown, In Vitro..... | 14 |
| 1.5.2 Tubedown, In Vivo..... | 16 |
| 1.6 Rationale for Project..... | 17 |
| 1.7 Hypothesis..... | 21 |
| 2.0 MATERIALS AND METHODS..... | 22 |
| 2.1 Antibodies..... | 22 |
| 2.2 Cell Culture..... | 23 |
| 2.3 In Vitro Transcription/Translation..... | 24 |
| 2.4 C-Src Purification..... | 25 |
| 2.5 Immunoprecipitation..... | 25 |
| 2.6 Western Blot Analysis..... | 27 |
| 2.7 siRNA Knockdown..... | 28 |
| 2.8 Coverslip Preparation/Immunofluorescence Staining..... | 29 |
| 2.9 Transient Transfection GFP Quantitation..... | 30 |
| 2.10 Transient Transfection Protein Quantitation..... | 30 |
| 2.11 ZO-1 Perimeter Quantitation..... | 31 |
| 2.12 Data Analysis and Statistics..... | 31 |
| 2.13 Sequence Alignment Analysis..... | 32 |
| 3.0 RESULTS..... | 33 |
| 3.1 Specificity of Tubedown Antibodies..... | 33 |
| 3.2 Analysis of Tubedown/Dynamin Interaction..... | 36 |
| 3.3 Analysis of Tubedown/AF-6 Interaction..... | 38 |
| 3.4 Analysis of Tubedown/Y421-Phospho-Cortactin Interaction..... | 40 |
| 3.5 Analysis of Tubedown/c-Src Interaction..... | 45 |
| 3.6 Analysis of Tubedown/ZO-1 Interaction..... | 53 |
| 3.7 Analysis of ZO-1 Distribution in Tubedown Knockdowns..... | 54 |
| 4.0 DISCUSSION..... | 65 |

| | |
|----------------------|----|
| 5.0 SUMMARY | 79 |
| 6.0 REFERENCES | 80 |

LIST OF TABLES

Table 2.1 Antibody Inventory 22

LIST OF FIGURES

| | |
|---|-----------|
| Figure 1. 1 Schematic Depicting Structures of the Eye..... | 2 |
| Figure 1. 2 Transcellular and Paracellular Permeability: Molecular Interactions in Endothelial Cells | 9 |
| Figure 1. 3 Structural Domains of Tubedown..... | 13 |
| Figure 3. 1 Specificity of Tubedown Antibodies | 35 |
| Figure 3. 2 Dynamin and Tubedown: Western Blot Analyses of Tubedown Immunoprecipitation..... | 37 |
| Figure 3. 3 AF-6 and Tubedown: Western Blot Analyses of Tubedown Immunoprecipitation..... | 39 |
| Figure 3. 4 Y421-Phospho-Cortactin and Cortactin: Western Blot Analyses of Cortactin Immunoprecipitation | 43 |
| Figure 3. 5 Y421-Phospho-Cortactin, Cortactin, and Tubedown: Western Blot Analyses of Tubedown Immunoprecipitation. | 44 |
| Figure 3. 6 Tubedown and c-Src: Western Blot Analyses of Tubedown Immunoprecipitation..... | 49 |
| Figure 3.7 Tubedown and c-Src: Western Blot Analyses of Tubedown | 50 |
| Figure 3. 8 Tubedown and c-Src: Western Blot Analyses of c-Src and Myc-Tag Immunoprecipitations | 51 |
| Figure 3. 9 Tubedown, c-Src, and Ard1: Photon Emissions and Western Blot Analysis of ³⁵S-Tubedown-Myc-His and ³⁵S-Ard1-Myc-His Immunoprecipitations Incubated with Purified c-Src..... | 52 |
| Figure 3. 10 ZO-1 and Tubedown: Western Blot Analyses of ZO-1 Immunoprecipitation..... | 56 |
| Figure 3. 11 GFP Transfection Efficiency in Transiently Transfected RF/6A Endothelial Cells | 57 |
| Figure 3. 12 Tubedown and Tubulin: Western Blot Analyses of WCL from Transient Tubedown Knockdowns | 58 |

| | |
|--|-----------|
| Figure 3. 13 Quantitative Analysis: Tubedown Expression in Transient Tubedown Knockdowns. | 59 |
| Figure 3. 14 ZO-1 and Tubulin: Western Blot Analyses of WCL from Stable and Transient Tubedown Knockdowns | 60 |
| Figure 3. 15 Quantitative Analysis: ZO-1 Expression in Transient Tubedown Knockdowns | 61 |
| Figure 3. 16 Quantitative Analysis: ZO-1 Expression in a Stable Tubedown Knockdown Clone..... | 62 |
| Figure 3. 17 Fluroescent Staining: ZO-1 Distribution in Stable and Transient Tubedown Knockdowns | 63 |
| Figure 3. 18 ZO-1 Cell Perimeter Quantitation of Stable and Transient Knockdowns of Tubedown..... | 64 |
| Figure 4. 1 BLAST Analysis of Control siRNA and MMP20 Homology..... | 72 |
| Figure 4. 2 BLAST Analysis of Control siRNA and P2RY12 Homology. | 72 |
| Figure 4. 3 Hypothesized Mechanism for Tubedown's Regulation of Transcytosis | 76 |

LIST OF ABBREVIATIONS

| | |
|-------------|--|
| Ab | Antibody |
| ADIP | Afadin and α -actinin binding protein |
| AF | Afadin |
| AJ | Adherens junctions |
| AMD | Age-related macular degeneration |
| Ard1 | Arrest defective protein 1 |
| ARP | Actin related protein |
| <i>ASTB</i> | <i>Antisense Tubedown</i> |
| BSA | Bovine serum albumin |
| BLAST | Basic local alignment search tool |
| ° C | Celsius |
| c-Src | Cellular Src |
| DAPI | 4',6-diamidino-2-phenylindole |
| DMEM | Dulbecco's Modified Eagle Medium |
| ECL | Enhanced chemiluminescence |
| EDTA | Ethylenediaminetetraacetic acid |
| FBS | Fetal bovine serum |
| FITC | Fluorescein isothiocyanate |
| GFP | Green fluorescent protein |
| gp60 | 60 kDa glycoprotein |
| His | Polyhistadine tag |

| | |
|---------|--|
| HRP | Horseradish peroxidase |
| IEM | Immortalized endothelial cells |
| JAM | Junctional adhesion molecule |
| kDa | Kilodalton |
| MAGUK | Membrane guanylate kinase-like homologue |
| mAmp | Milliamp |
| μ g | Microgram |
| ml | Millimeter |
| μ l | Microliter |
| mm | Millimeter |
| mM | Millimolar |
| μ M | Micromolar |
| MMP | Metallopeptidase proteins |
| mNAT-1 | Mouse <i>N</i> -terminal acetyltransferase |
| Myc-Tag | c-Myc epitope tag |
| NATH | <i>N</i> -acetyltransferase 1 protein |
| NARG1 | NMDA receptor regulated gene 1 |
| NEAA | Non-essential amino acid |
| Neo | Neocin |
| ng | Nanogram |
| NMDA | <i>N</i> -Methyl- <i>D</i> -aspartate |
| PDR | Proliferative diabetic retinopathy |

| | |
|-------------|--|
| PVDF | Polyvinylidene fluoride |
| ROP | Retinopathy of prematurity |
| SDS | Sodium dodecyl sulfate |
| SDS-PAGE | Sodium dodecyl sulfate polyacrylamide gel electrophoresis |
| SFK | Src family kinase |
| T-SNARES | N-ethylmaleimide-sensitive factor attachment protein receptor family |
| Tbdn | Tubedown |
| TBS | Tris buffered saline |
| TBST | Tris buffered saline tween |
| TJ | Tight junction |
| TnT | Transcription and translation |
| TPR | Tetratricopeptide repeat |
| VE-Cadherin | Vascular endothelial Cadherin |
| VEGF | Vascular endothelial growth factor |
| WCL | Whole cell lysate |
| Y | Tyrosine |
| ZO | Zona occludens |

The Role of Tubedown in Ocular Endothelial Permeability

1.0 INTRODUCTION

1.1 Eye Sight

The eye is a complex organ capable of receiving refractive light and commencing the energy exchange necessary to perceive an image. The formation of an image begins with light reflecting off the surface of an object entering the eye and passing through the cornea and lens optimizing it to be inversely projected onto the macula, the center of the retina (Pylyshyn et al., 2003) [Fig. 1.1]. The retina is a multi-layered, light-sensitive tissue that lines the inner surface of the eye. It is located in-between the choroidal tissue and the vitreous humor. The retina is a highly regulated tissue containing rods, cones, bipolar, horizontal, amacrine, ganglion, and Müller cells (Kolb, 1995). These cells are responsible for converting light energy into chemical energy for transference to the visual cortex of the brain (Jackson et al., 2003; Roberts, 1995). Damage to the retina can inhibit the conversion of energy and consequently decrease visual acuity eventually leading to complete blindness.

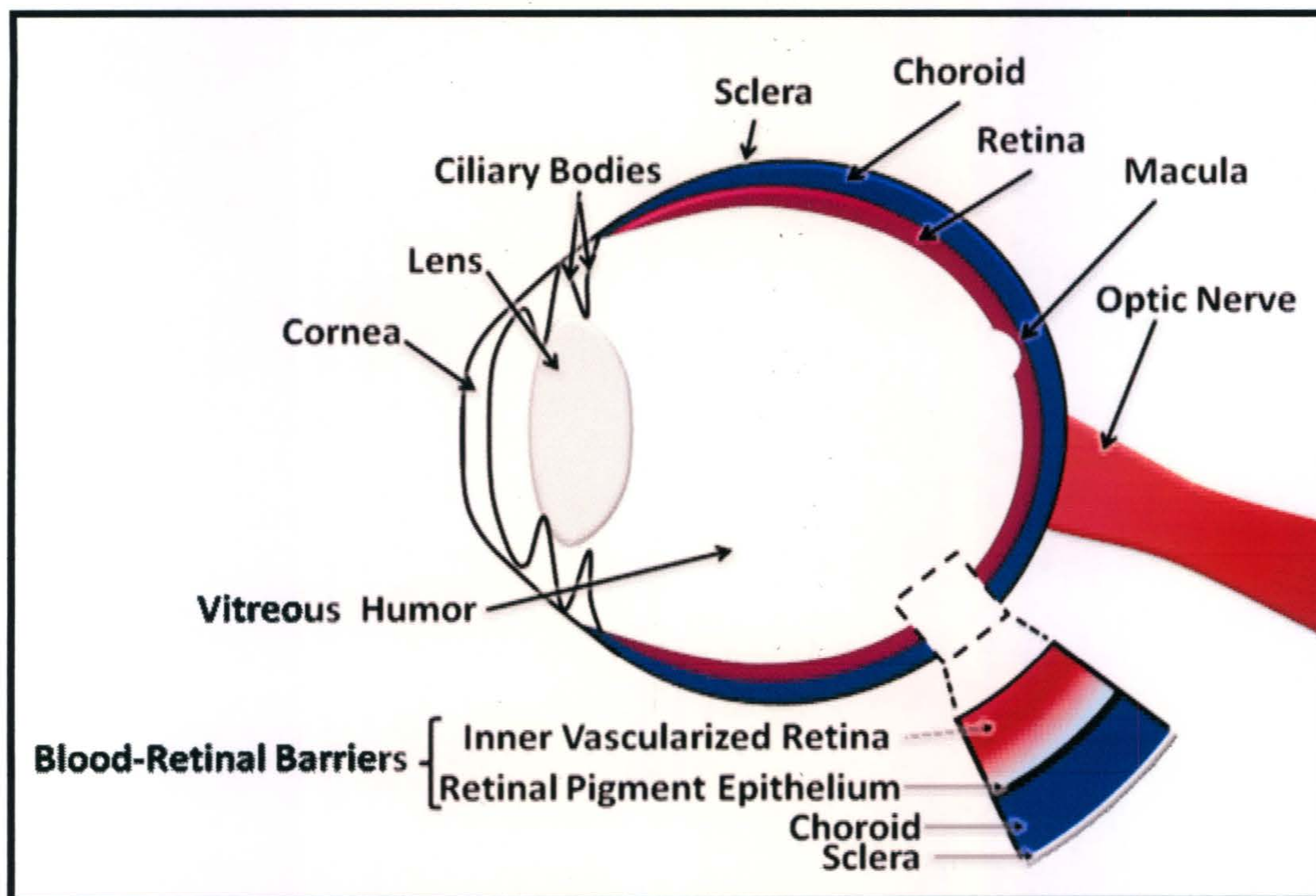


Figure 1. 1 Schematic Depicting Structures of the Eye.

1.2 Ocular Vasculature

The ocular vasculature plays a vital role in the clarity of eyesight. There are specific avascular and vascularized tissues within the eye, which must be maintained for optimum eyesight. The retina requires a constant supply of oxygen and nutrients from blood vessels in order for it to be functional. The inner retinal layers, closest to the vitreous humor, are vascularized while the outer layers of the retina, closest to the choroid, are relatively avascular (Wanek et al., 2011). The retina receives the necessary nutrients and oxygen from two discrete circulatory systems. Fenestrated capillaries within the choroid allow for rapid diffusion of molecules to supply the outer retina with nutrients while the inner retina is supplied by the central retinal artery which branches out to supply the entire inner retina (Roh et al., 2010).

The eye contains blood-ocular barriers that are much like the blood-brain barrier, which control the movement of molecules from within the vessel to the outer tissues. The two blood-ocular barriers include the blood-aqueous barrier and the blood-retinal barrier. Ciliary epithelium and capillaries of the iris control the blood-aqueous barrier (Wanek et al., 2011). The blood-retinal barrier is controlled by tight-junctions between retinal endothelial and epithelial cells which comprise the inner and outer components of the blood-retinal barrier, respectively [Fig. 1.1] (Wanek et al., 2011). The inner component of the blood-retinal barrier consists of tight junctions between endothelial cells lining the central retinal blood vessel located in the inner most part of the retina (Cunha-Vaz et al., 2010). The outer component of the blood-retinal barrier consists of tight junctions between epithelial cells that comprise the retinal pigment epithelium and

the most outer portion of the retina (Cunha-Vaz et al., 2010). Damage to the blood-retinal barrier is associated with ocular neovascular diseases (Roh et al., 2010).

1.3 Neovascular Retinopathies

In, general vessel growth in healthy adults is restricted to periods of wound healing, hair growth, pregnancy, and menstruation (Witmer et al., 2003). However, ocular angiogenesis, the process of growth of blood vessels, within a healthy individual ceases after birth (Chan-Ling and Stone, 1992). However, angiogenesis is commonly seen with diseases of the eye such as wet age-related macular degeneration (AMD), proliferative diabetic retinopathy (PDR), and retinopathy of prematurity (ROP). The pathological cascade of ocular angiogenesis begins with vasodilatation and increased permeability mediated by vascular endothelial growth factor (VEGF) (Nagy et al., 2007). Increased permeability causes the endothelium to undergo differentiation and proliferation (Dvorak et al., 1995). The extracellular matrix is then degraded by matrix metalloproteases (MMP) and urokinase-type plasminogen receptor, allowing the endothelial cells to migrate (Witmer et al., 2003). These pathological consequences allow the endothelium to form tube-like structures, which generate the basement membrane of new vessels.

In neovascular retinopathies areas of the eye undergo angiogenesis due to hypoxic stimuli or an imbalance between inhibitory and inducing angiogenic factors. The hypoxic stimuli and imbalanced inhibitory and inducing angiogenic factors are known to cause an increase in permeability of endothelial cells, which is known to lead to

angiogenesis (Fischer et al., 1999; Nagy et al., 2007). These newly formed vessels are weak and can hemorrhage, leaking fluids into the eye that cause lesions, scar tissue build-up, and retinal detachment that can lead to subsequent blindness.

AMD left untreated is the leading cause of blindness in individuals age 65 and older (Age-Related Eye Disease Study Research Group, 2001). Dry and wet are the two forms of AMD with wet also being known as neovascular AMD. Dry AMD results from atrophy of the retinal pigment epithelium underlying the retina (Itoh et al., 1999; Nowak, 2006). Wet AMD is the more advanced and more threatening form of AMD (Nowak, 2006). Wet AMD is caused by damage to the macula from abnormal vessel growth due to an imbalance of inhibitory vs. inducing angiogenic factors (Rajappa et al., 2010). The macula is the center of the retina containing the highest concentration of cone cells within the eye and is responsible for high resolution of vision (Kolb, 1995). In patients with wet AMD angiogenesis begins under the macula within the choroidal tissue and can extend into the retina damaging the outer blood-retinal barrier (Cunha-Vaz et al., 2010). Increased VEGF production followed by increased permeability of the endothelium causes a build-up of fluid under and in the retina (Ng and Adamis, 2005). In the early stages, patients begin seeing dark spots within their central vision and straight lines can become wavy; furthermore, wet AMD can advance to complete blindness within as little as three months (Wong et al., 2008).

Diabetic retinopathy affects over 6 % of Canadians (Maberley et al., 2006). Decreased retinal blood flow, inflammation, endothelial cell loss and capillary basement membrane thickening signify early stage diabetic retinopathy, also named

nonproliferative diabetic retinopathy. More advanced retinal ischemia causes pathological angiogenesis throughout the retina and is referred to as PDR (Durham and Herman, 2011). The neovascularization within PDR can cause damage to the inner blood-retinal barrier leading to increased permeability (Cunha-Vaz et al., 2010). Patients with PDR have hazy vision with dark spots, which can advance to complete blindness.

Retinopathy of prematurity is a complication affecting 13 % of premature babies within the United States (Mataftsi et al., 2011). Healthy fetal ocular vessel growth begins in the optic disc at gestation week 18 and ends at full term on week 40. ROP occurs in two phases, the first is delayed vessel growth followed by uncontrolled vessel growth within the second phase. When a baby is born prematurely they are introduced to a hyperoxic environment more suddenly than a full term baby delaying normal neovascularization, the formation of microvascular networks. As a result, uncontrolled neovascularization occurs throughout the eye to compensate for the lack of oxygen. The uncontrolled vessel growth causes damage to the inner blood-retinal barrier leading to increased permeability (Chan-Ling and Stone, 1992). While ROP can be spontaneously repaired 40 % of infants are left with a moderate decrease in visual acuity, and 18 % develop severe ROP having possible retinal detachment and concurrent blindness (Phelps, 1995).

Wet AMD, PDR, and ROP can all attribute vision loss to increased vascular permeability leading to vessel growth and leaky vessels damaging the blood-retinal barrier (Schlingemann and van Hinsbergh, 1997). Therefore, these diseases are all treated similarly with anti-angiogenic therapeutics. In early stages of wet AMD, PDR,

and ROP, surgery or photodynamic therapy may be used. However, in advanced stages anti-angiogenics are now the most effective therapeutic for all three diseases whether it is alone or in combination with other treatments (Meyer and Holz, 2011; Orozco-Gomez et al., 2011; Age-Related Eye Disease Study Research Group, 2001; Bressler, 2009). The most effective anti-angiogenic therapeutics target the VEGF protein or receptor (Bayes et al., 2002). VEGF is a key mediator of vessel growth that stimulates increased endothelial cell migration, permeability, and survival. Therefore, in order to decrease side effects at normal vascularized beds, anti-angiogenic drugs are directly injected into the eye. Intravitreal injections can lead to adverse effects such as corneal abrasion, ocular inflammation and 1.5 % of patients have consequential injury to the lens or complete retinal detachment (Shima et al., 2008; Simo et al., 2008). Several reports have showed that as high as 17 % of patients who receive anti-angiogenic intravitreal injections have retinal pigment epithelial tears that subsequently decrease visual acuity (Chang et al., 2007; Nicolo et al., 2006; Yeh and Ferrucci, 2011). Anti-angiogenic treatments can pass into the blood stream leading to possible side effects of hypertension, proteinuria and cardiovascular events (Simo et al., 2008). Moreover, after 2 years of treatment with anti-angiogenics, some patients no longer respond to therapy (Rosenfeld et al., 2011). Enhancements to anti-angiogenic therapeutics that avoid intravitreal injections could be achieved by targeting other regulators of the permeability pathway that are specific to the retina. In addition, therapies that address the underlying physiological cause of neovascular retinopathies could aid in repairing damage to the retina and prevent loss of

visual acuity. Therefore, defining the mechanisms leading to abnormal neovascularization of the eye is pertinent to develop new therapies.

1.4 Molecular Pathways of Endothelial Permeability

The endothelium is a semi-permeable barrier lining all vessels within the body, and controls the fluid and solute exchange between the blood and surrounding tissues. Permeability of the endothelium is required for endothelial cells to receive nutrients and eliminate metabolic waste products. However, disruption of endothelial cell homeostasis leading to hyper-permeability is a known cause of pathological angiogenesis (Dvorak et al., 1995). Transcellular and paracellular are the two types of endothelial permeability [Fig.2]. Transcellular permeability (transcytosis) is movement of molecules through a cell. Paracellular permeability (paracytosis) is the movement of molecules between cells.

1.4.1 Transcellular Permeability (Transcytosis)

Transcytosis is selective to macromolecules such as albumin, albumin-bound ligands, hormones, insulin, and lipids (Komarova and Malik, 2010). Transcytosis begins with a macromolecule binding to its corresponding receptor initiating endocytosis [Fig. 1.2]. Endocytosis involves a flask-like invagination at the cell membrane of endothelial cells being formed and cinched off, creating a lipid bilayer raft known as a vesicle. The vesicle is actively transferred to the other side of the cell where it undergoes exocytosis. Exocytosis is the process of a vesicle docking and fusing onto the baso-lateral membrane, thereby releasing its contents into the surrounding tissues. Vesicles may be coated in caveolin or clatherin protein. Within endothelial cells caveolin-coated rafts known as

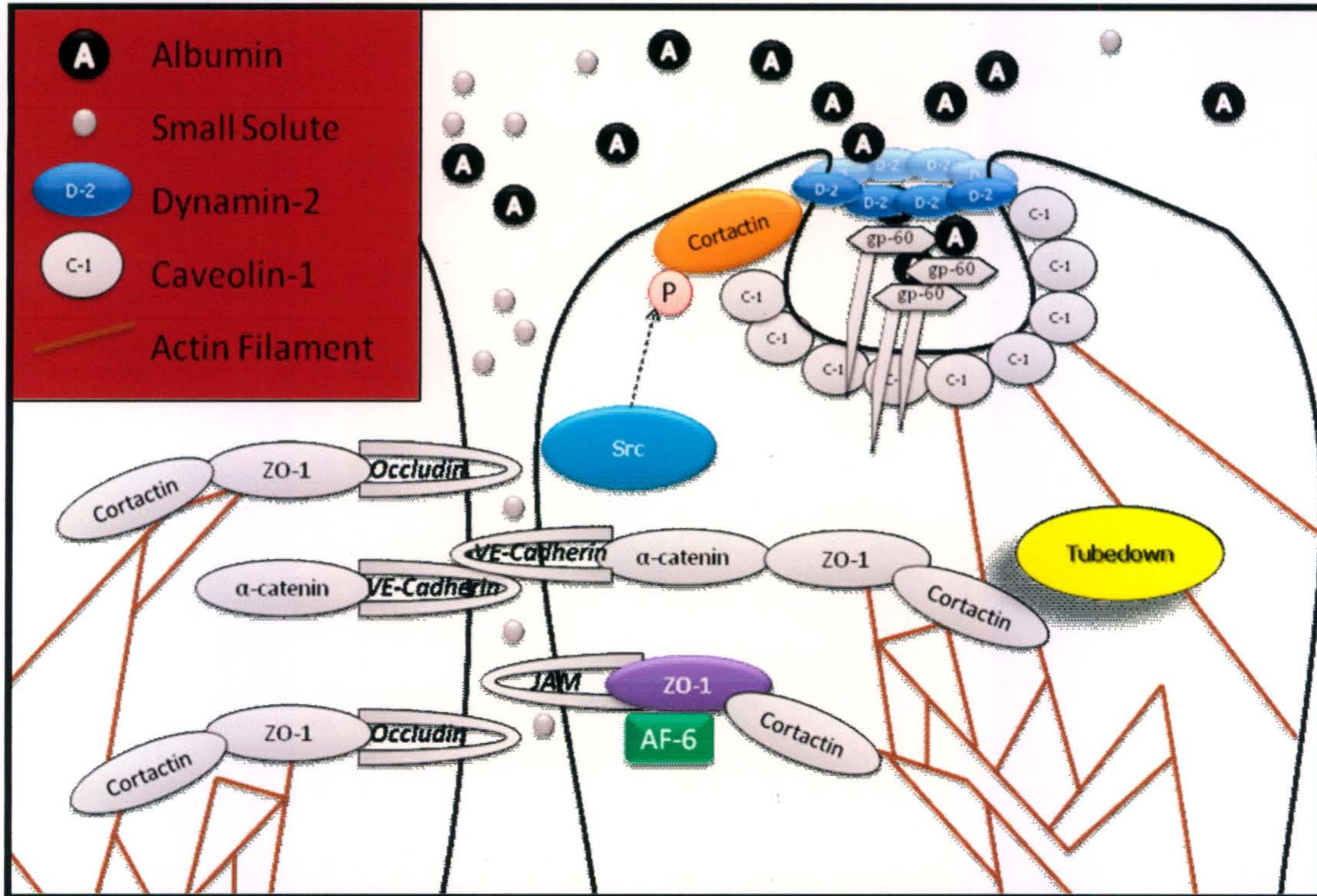


Figure 1. 2 Transcellular and Paracellular Permeability: Molecular Interactions in Endothelial Cells. Transcytosis is initiated by albumin (A) binding to gp-60 and Caveolin-1 (C-1) oligomerization at the plasma membrane. C-Src tyrosine kinase phosphorylates Cortactin and Dynamin-2 enhancing their interaction required for transcytosis. Dynamin-2 (D-2) wraps around neck of caveolae cinching them from the membrane and creating a vesicle. Cortactin bound to the actin cytoskeleton advocates endocytosis and caveolae transport from the apical to basal side of the endothelial cell. The caveolae undergo exocytosis and its contents are released into the surround tissues. In paracytosis ZO-1 recruits the inter-endothelial junctional proteins VE-cadherin, JAM and Occludin to the plasma membrane which bind to the actin cytoskeleton restricting the passage of solutes larger than 3 nm.

caveolae comprise over 97 % of vesicular transport (Predescu et al., 2007). The transcytotic signaling cascade is best defined by the caveolae exclusive transport of albumin. The transcytosis of albumin begins with its binding to one of its cell surface receptors, such as glycoprotein-60 (gp-60), followed by the cytosolic monotropic membrane protein Caveolin-1 oligomerization at the cell membrane (Vogel et al., 2001) [Fig. 1.2]. Oligomerization of Caveolin-1 enables the formation of the flask-like invagination of the membrane (Minshall et al., 2002). The interaction between the guanosine triphosphate-ase (GTPase) protein Dynamin-2 and actin-bound Cortactin at the cell membrane regulates actin reorganization aiding in the formation of the invagination (Schafer et al., 2002). Once the invagination is formed Dynamin-2 wraps around the neck separating the vesicle from the membrane (Jones et al., 1998). The cargo within the caveolae is then shuttled from the apical side of the cell to the basal side of the cell. The transport of caveolae from apical to basal surface of the endothelial cell is process that requires Src family kinases (SFK) and Cortactin (Shajahan et al., 2004; Zhu et al., 2007). The caveolae then undergoes exocytosis, which requires syntaxin and target soluble N-ethylmaleimide-sensitive factor attachment protein receptor family (t-SNARES) (Littleton et al., 1998). Furthermore, phosphorylation of Caveolin-1 and Dynamin-2 by c-Src, a member of SFK, facilitates transcytosis and initiates vesicle fission (Hu et al., 2008). In addition, c-Src phosphorylation of Dynamin-2 and Cortactin enhances their interaction with each other that is required for transcytosis (Cao et al., 2010).

1.4.2 Paracellular Permeability (Paracytosis)

Paracytosis is controlled by inter-endothelial junctions bound to the actin cytoskeleton, which form a barrier restricting passive diffusion of solutes larger than 3 nm in-between cells. There are two types of endothelial junctions, adherens junctions (AJ) and tight junctions (TJ) [Fig. 1.2]. AJs are the more predominate junction within endothelial cells (Mehta and Malik, 2006). AJs are largely comprised of vascular endothelial cadherin (VE-cadherin) (Dejana et al., 2008). VE-cadherin homophilically binds creating cell-cell adhesion between cells (Chappuis-Flament et al., 2001). The cytoplasmic tail of VE-cadherin contains a highly conserved cadherin domain that binds alpha and beta-catenins, which are in turn bound to the actin cytoskeleton (Vestweber et al., 2009). Reorganization of the actin cytoskeleton can stabilize or destabilize AJs (Dudek and Garcia, 2001). TJs are composed of the membrane spanning proteins Occludin, Claudin, and Junctional Adhesion Molecule (JAM). TJ proteins bound to the actin cytoskeleton are critical for regulation of paracytosis.

An essential protein that is part of both AJ and TJ in paracellular permeability is Zona Occludins-1 (ZO-1). ZO-1 is required for both the formation of AJs and as a scaffold protein for the arrangement of TJs, thereby playing a pivotal role in paracellular barrier function in endothelial cells (Umeda et al., 2004; Ikenouchi et al., 2007). ZO-1, -2, -3 are a subfamily of membrane guanylate kinase-like homologue (MAGUK) family (Umeda et al., 2006). The ZO subfamily has one Src homology 3 domain (SH3), one guanylate kinase-like domain (GuK), and three PDZ domains (Umeda et al., 2006). The SH3 and GuK domains of ZO-1 bind actin, AF-6, and Alpha-Catenin, and are critical for

Claudin polymerization. ZO-1's interaction with actin, AF-6 and Alpha-Catenin allows for the transduction of extracellular signal, provides mechanistic stability, recruits proteins to TJ's to regulate cell-cell contacts, and links AJs to the actin cytoskeleton for stability (Yamamoto et al., 1997; Ebnet et al., 2000; Rimm et al., 1995). Claudin polymerization is involved in TJ formation and ZO-1 is necessary for the location of Claudin polymerization (Umeda et al., 2006; Furuse et al., 1999). The PDZ domain within ZO-1 is named because post synaptic density protein, *Drosophila* disc large tumor suppressor, and ZO-1 were the first three proteins in which the domain was discovered (Kennedy et al., 1995). The PDZ domain of ZO-1 interacts with all three membrane proteins that form TJs; Occludins, Claudins, and JAMs (Itoh et al., 1999; Furuse et al., 1994; Bazzoni et al., 2000).

1.5 Tubedown: Homeostatic Regulator of the Ocular Vascular Systems through Endothelial Permeability Regulation

Mammalian homologues of the Tubedown protein were first reported in the year 2000 (Gendron et al., 2000). In the literature, Tubedown may also be referred to as mouse *N*-acetyltransferase 1 (mNat1), *N*-acetyltransferase human (NATH), or *N*-methyl-*D*-aspartate receptor regulated gene 1 (NARG1). However, it has recently been renamed Naa15 (N-alpha-acetyltransferase 15) (Polevoda et al., 2009). Tubedown exists mainly as a 100 kDa isoform, containing three tetratricopeptide repeat (TPR) motifs, a linker region, and a syntaxin-18 homology domain [Fig. 1.3] (Gendron et al., 2000; Dr. H. Paradis [Memorial University of Newfoundland], personal communication (Gendron et al., 2000; Mullen et al., 1989). In yeast, Nat1 is known to interact with arrest-defective

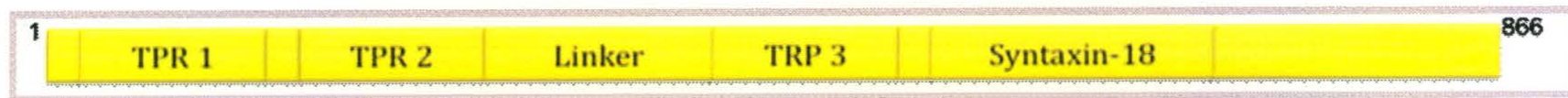


Figure 1.3 Structural Domains of Tubedown. Tubedown contains 3 tetratricopeptide repeat (TPR) structural motifs, a linker region, and a syntaxin-18 homology domain (Dr. H. Paradis [Memorial University of Newfoundland], personal communication).

protein 1 (Ard1) and form an essential part of the NatA complex, which conducts N-terminal α -acetylation on nascent polypeptides protruding from the ribosome (Park and Szostak, 1992). Tubedown has also been shown to interact with Ard1, co-purify with acetyltransferase activity within mammalian cells, and Ard1 is co-downregulated with Tubedown (Paradis et al., 2008; Arnesen et al., 2005; Gendron et al., 2000). While 30 % of mammalian proteins are acetylated, the outcome of acetylation is it still not completely understood (Meinzel et al., 2005). Post translational modifications like N-terminal α -acetylation has many molecular consequences. For example, N-terminal α -acetylation can stimulate the degradation of a protein or protect a protein from degradation (Arnesen et al., 2009; Min et al., 2010). Tubedown is transiently expressed during embryogenesis in the developing endothelium and vasculature (Gendron et al., 2000). In adults, expression is limited to the endothelium of a few vascular beds with highest expression seen in the ocular vasculature (Gendron et al., 2000; Gendron et al., 2001). A second human isoform of Tubedown exists having an 81 % similarity with the primary human isoform of Tubedown (Arnesen et al., 2009; Sugiura et al., 2003).

1.5.1 Tubedown, In Vitro

Stable knockdown retinal-choroidal endothelial cell clones of Tubedown (*ASTB*) generated with an antisense cDNA fragment in Drs. Paradis and Gendron's laboratory (Memorial University of Newfoundland in St. John's, NL) have a ~50 % decrease in Tubedown expression (Paradis et al., 2002). The *ASTB* lines were generated in rhesus macaque retinal-choroidal endothelial cells (RF/6A). *In vitro*, Tubedown suppression leads to increased capillary formation in both the RF/6A endothelial cell clones and an

immortalized murine endothelial cell (IEM) clonal line (Paradis et al., 2002; Gendron et al., 2000). Tubedown suppression showed increased permeability to both albumin and 40 kDa-dextran which are transported by transcytosis and paracytosis, respectively (Paradis et al., 2008; Dr. H. Paradis [Memorial University of Newfoundland], personal communication). In addition, Asami et al. found that co-expression of mammalian Tubedown and Ard1 suppressed transcytosis of the Alzheimers β -amyloid precursor protein (2005). *In vitro*, work with Tubedown provides evidence that Tubedown regulates ocular endothelial permeability.

To explore the mechanism in which Tubedown may regulate endothelial permeability co-immunoprecipitation and co-localization techniques were completed and Tubedown was found to interact with the actin-binding protein Cortactin (Paradis et al., 2008). Cortactin is known to regulate F-actin polymerization through its interaction with actin-related protein 2 and 3 complex (Arp2/3) (Urano et al., 2001). Alterations to the actin-cytoskeleton are known to change endothelial cell shape which can alter inter-endothelial junctions leading to increased permeability (Osborn et al., 2006; Dudek and Garcia, 2001). Actin-cytoskeleton reorganization by Cortactin is required for membrane internalization which is essential for vesicle formation in transcytosis (Zhu et al., 2007).

Preliminary studies have shown decreased Tubedown expression may be linked to an increase in tyrosine 416 (Y416)-Phospho-Src, a member of Src family kinase family (SFK), in endothelial cells (Whelan, 2011). In humans, the normal cellular protein for Src is referred to as cellular Src (c-Src). Y416 and Y527 are two significant sites on c-Src that can be phosphorylated and control its activation. C-Src is activated with

phosphorylation at Y416 or by dephosphorylation of Y527 (Schlessinger, 2000).

Therefore, Tubedown seems to be regulating the activation of c-Src. Currently, further characterization of decreased Tubedown expressions affect on Y416-phospho-Src is being carried out by another master's student, Nhu Ho (Dr. H. Paradis [Memorial University of Newfoundland], personal communication).

1.5.2 Tubedown, In Vivo

In vivo, research with bitransgenic endothelial specific Tubedown knockdown mice show increased retinal albumin leakage, retinal and choroidal neovascularization, retinal thickening, and lesions within the retina (Wall et al., 2004; Paradis et al., 2008; Gendron et al., 2010). Furthermore, the pathological consequences seem to be restricted to the retina and choroid (Wall et al., 2004). *In vivo* pathological features of Tubedown knockdown mice mimic the pathological features of human patients with wet AMD, PDR, and ROP.

Patients with PDR and ROP show decreased Tubedown expression in the retinal vasculature correlating with the areas of pathological angiogenesis seen within patients (Gendron et al., 2001; Gendron et al., 2006). Patients with AMD show decreased Tubedown expression within the choroidal vasculature, which again parallels with the area of neovascularity observed in affected patients (Gendron et al., 2010). The cumulative evidence suggests that Tubedown is regulating ocular endothelial permeability and therefore ocular vascular homeostasis; however, Tubedown's mechanistic role in the regulation of endothelial permeability remains incompletely understood.

1.6 Rationale for Project

Suppression of Tubedown causes increased retinal-choroidal endothelial permeability and angiogenesis. Tubedown interacts with the actin-binding protein Cortactin which is known to regulate both paracellular and transcellular permeability. Tubedown shows marked suppression in AMD, PDR, and ROP in correlation with areas of increased permeability and vascularity seen in patients (Ng and Adamis, 2005; Cunha-Vaz et al., 2010; Chan-Ling and Stone, 1992). It is a possibility that decreased Tubedown expression is the underlying cause or mechanistic outcome observed in ocular neovascular diseases. There have been no reported mutations in Tubedown; however, a human mutation in the Tubedown binding protein Ard1 has been shown to cause severe developmental defects ultimately due to reduced protein acetylation (Rope et al., 2011). Therefore, it is possible that Tubedown's role in the acetylation complex with Ard1 plays a role in the developmental defects seen with Ard1 mutations.

TPR motifs are known to act as interaction scaffolds in a range of cellular processes including protein translocation (Allan and Ratajczak, 2011). Since Tubedown contains three TPR motifs I was interested in protein interactions Tubedown might have with other prominent regulators of the permeability pathways: Dynamin, AF-6, Y421-Phospho-Cortactin, c-Src, and ZO-1.

Dynamin is a large GTPase that regulates endocytosis in transcellular permeability. Dynamin can independently catalyze fission of the membrane in endocytosis by wrapping around the neck of a vesicle. Dynamin contains a GTPase domain, a pleckstin homology domain, a GTPase effector domain, and a proline-rich

domain (Low and Lowe, 2010). There are three mammalian forms of Dynamin that each have distinct expression patterns: Dynamin-1 is neuronal-specific, Dynamin-2 is ubiquitously expressed and Dynamin-3 is expressed in testis, lung, and brain (Cook et al., 1996). Therefore, only Dynamin-2 is expressed within the ocular endothelium. Since, Dynamin-2 is a key transcellular regulator it was hypothesized to be a potential binding partner with Tubedown.

Afadin (AF-6) localizes to adherens junctions, is required for the ZO-1 recruitment to nectin-based AJs and is essential for structural organization of both AJs and TJs (Mandai et al., 1997; Yokoyama et al., 2001; Ikeda et al., 1999; Zhadanov et al., 1999). Previous liquid chromatography mass spectrometry analysis revealed that the afadin dilute domain-interacting protein (ADIP), an afadin- and α -actinin-binding protein, had high identity with a protein that co-immunoprecipitated with Tubedown (Dr. H. Paradis [Memorial University of Newfoundland], personal communication). While ADIP's role is poorly characterized, it is known to take part in platelet derived growth factor-induced cell movement that requires AF-6's interaction (Fukumoto et al., 2011). We speculated that AF-6 and Tubedown might interact. Therefore, co-immunoprecipitation in combination with western blotting techniques were used to test this hypothesis.

While Tubedown and Cortactin bind, no work has shown how Cortactin phosphorylation affects their interaction. Cao et al. recently showed that c-Src tyrosine phosphorylation of Cortactin was necessary for efficient transcytosis of transferrin (Cao et al., 2010). Lambotin et al. also showed in 2005 that phosphorylation of Cortactin is

necessary for incorporation of the *Neisseria meningitides* into endothelial cells (Lambotin et al., 2005). These results along with others suggest phosphorylation of Cortactin enhances transcellular permeability (Huang et al., 1998; Yang et al., 2006). Cortactin can be phosphorylated by proteins such as Rac, myosin light-chain kinase, and extracellular signaling-regulator kinase; however, most well studied is tyrosine phosphorylation by c-Src (Lua and Low, 2005). Cortactin phosphorylation by c-Src occurs at tyrosine residues 421, 466, and 482 (Huang et al., 1998). C-Src phosphorylation of Cortactin has been linked to increased actin assembly and polymorphonuclear leukocyte transmigration (Tehrani et al., 2007; Yang et al., 2006). Furthermore, c-Src phosphorylation of Cortactin at tyrosine residues is progressive whereby Y421 precedes Y466 phosphorylation (Head et al., 2003). Since tyrosine phosphorylation of Cortactin is important for its function in regulating transcytosis, it would be important to determine if phosphorylated Cortactin, at c-Src specific Y421, binds Tubedown. Co-immunoprecipitation and western blotting techniques were used to determine whether Y421-Phospho-Cortactin and Tubedown interact.

C-Src is a member of SFK, which are non-receptor cytoplasmic membrane associated tyrosine kinases (Hu and Minshall, 2009). C-Src plays a critical role in transendothelial permeability by acting as a 'switch' to regulate caveolar transport (Hu and Minshall, 2009). For example, c-Src is known to phosphorylate Caveolin-1 and Dynamin-2 enhancing their interaction and initiating vesicle fission (Hu et al., 2008). In addition, as mentioned above, c-Src is known to phosphorylate Cortactin and lead to increased permeability (Tehrani et al., 2007; Yang et al., 2006). Recently, it was found

that decreased Tubedown expression may correlate with an increased quantity of Y416-Phospho-Src within endothelial cells (Dr. H. Paradis and N. Ho [Memorial University of Newfoundland], personal communication; (Whelan, 2011). Currently, another master's student has taken on the project of confirming if decreased Tubedown expression correlates with increased Y416-Phospho-Src *in vivo*. Since c-Src is known to play such a critical role in transcellular permeability, I hypothesized that Tubedown may be regulating transcellular permeability through an interaction with c-Src. Co-immunoprecipitation and western blotting techniques were used to determine whether c-Src and Tubedown interact.

ZO-1 has been shown to recruit inter-endothelial junctions to the membrane, bind numerous permeability regulators, and is involved in maintaining the structure of paracellular permeability proving it to be a key regulator of paracellular permeability (Umeda et al., 2004; Ikenouchi et al., 2007; Yamamoto et al., 1997; Ebnet et al., 2000; Rimm et al., 1995). Electron microscopy of tight junctions within the retinal-blood barrier show extensive amounts of ZO (Cunha-Vaz, 1976). ZO-1 is known to interact with the Tubedown binding partner Cortactin (Katsube et al, 1998). Since ZO-1 plays such an important role in paracellular permeability, it was speculated that Tubedown might bind ZO-1. Again, immunoprecipitation followed by western blotting techniques were used to test this hypothesis. In addition, previous unpublished work in Drs. Gendron and Paradis' laboratory has shown decreased ZO-1 cell perimeter expression with immunofluorescence in *ASTB* clones (Dr. H. Paradis [Memorial University of Newfoundland], personal communication). These results suggest that Tubedown may

recruit ZO-1 to inter-endothelial junctions to regulate paracellular permeability. However, further validation was needed to prove Tubedown's involvement in the regulation of ZO-1 perimeter expression. A transient Tubedown knockdown protocol was developed for the RF/6A endothelial cell line for comparison with the stable Tubedown knockdown *ASTB* cell clone for further investigation of Tubedown's influence over ZO-1 expression at the cell membrane.

1.7 Hypothesis

I hypothesize that Tubedown is interacting with other protein regulators of the permeability pathways to decrease endothelial cell permeability: Dynamin-2, AF-6, Y421-Phospho-Cortactin, c-Src, and ZO-1. In addition, I hypothesize that Tubedown may be regulating the endothelial permeability pathways through relocation ZO-1 to the cell membrane.

2.0 MATERIALS AND METHODS

2.1 Antibodies

Table 2.1 Antibody Inventory

| Antibody | Target | APPLICATION | | | Origin |
|--|----------------------------|-------------|----|----|--|
| | | WB | IP | IF | |
| Rabbit Polyclonal LE C10-20 | Tubedown | X | X | | Custom (Paradis et al., 2007) |
| Rabbit Polyclonal MI-C755 | Tubedown | X | X | | Custom (Paradis et al., 2007) |
| Mouse Monoclonal Narg1 | Tubedown | X | X | | Santa Cruz Bio. Inc. (Santa Cruz, CA) |
| Mouse Monoclonal AF-6 | AF-6 | X | X | | Santa Cruz Bio. Inc. (Santa Cruz, CA) |
| Mouse Monoclonal Cortactin (p80/85) (clone 4F11) | Cortactin | X | X | | Upstate Cell Signaling Solution (Lake Placid, NY) |
| Rabbit Polyclonal Y421-Phospho- Cortactin | Y421-Phospho- Cortactin | X | | | Cell Signaling Tech. (Pickering, Ontario) |
| Mouse Monoclonal Dynamin | Dynamin | X | | | BD Transduction Lab. (Lexington, KY) |
| Mouse Monoclonal ZO-1 (clone 1A12) | ZO-1 | X | X | X | Invitrogen (Carlsbad, CA) |
| Mouse Monoclonal ZO-1 (clone R40.76) | ZO-1 | | X | | Santa Cruz Bio. Inc. (Santa Cruz, CA) |
| Rhodamine Red-X Anti-Mouse Conjugate | Primary Antibody | | | X | Jackson Immuno Research Lab. Inc. (West Grove, PA) |
| Negative Control Anti- Mouse IgG ₁ | Primary Antibody | | X | X | Dako (Mississauga, Ontario) |
| Anti-Mouse IgG HRP | Primary Antibody | X | | | Promega (Fitchberg, WI) |
| Anti-Rabbit IgG HRP | Primary Antibody | X | | | Promega (Fitchberg, WI) |
| Mouse Monoclonal Tubulin (clone DM1A) | Tubulin | X | | | Sigma (St. Louis, MO) |
| Anti-Myc Tag (Clone 4A6) | Myc Tag | X | X | | Millipore (Billerica, MA) |
| Anti-Mouse c-Src (clone 327) | c-Src | X | X | | Abcam (Cambridge, MA) |

*Western Blot (WB), Immunoprecipitation (IP), Immunofluorescence (IF), Horseradish peroxidase (HRP)

2.2 Cell Culture

RF/6A endothelial cells are immortalized rhesus macaque choroid-retinal endothelial cells which were originally obtained from American Type Culture Collection. RF/6A endothelial cells were cultured in low glucose Dulbecco's Modified Eagle Media (DMEM) (Invitrogen) supplemented with 10 % of heat inactivated fetal bovine serum (FBS), 50 μ M non-essential amino acids (NEAA), and 2 μ M glutamine. The *ASTB* clones created previously with a pcDNA/Zeo 3.1 antisense construct designed to knockdown *Tubedown* expression have previously been described (Paradis et al., 2002). The *ASTB* clones from RF/6A endothelial cells were cultured in the same manner as the parental RF/6A endothelial cells with the addition of 100 μ g/ml of Zeocin to maintain expression of the transgene. The RF/6A *Tubedown*-Myc-His and *Ard1*-Myc-His clones created previously were designed with a pcDNA/Neo/Myc-His 3.1 vector containing either *Tubedown* or *Ard1* coding sequences, respectively (Dr. H. Paradis [Memorial University of Newfoundland], personal communication). The RF/6A *Tubedown*-Myc-His and *Ard1*-Myc-His clones were cultured in the same manner as parental RF/6A endothelial cells with the addition of 300 μ g/ml and 750 μ g/ml of Neocin to maintain expression of the transgenes, respectively (Dr. H. Paradis [Memorial University of Newfoundland], personal communication).

Immortalized mouse embryonic endothelial (IEM) cells were obtained and cultured as previously described (Gendron et al., 2000). IEM cells were cultured in the same manner as the RF/6A endothelial parental cells without adding NEAA. All cells were maintained at 37 °C in an atmosphere containing 10 % CO₂.

RF/6A parental and cell clones were plated at 0.75×10^6 cells per 100 mm plate for 48 hours of cell growth. IEM cells were plated at 1.5×10^6 cells per 100 mm plate for 48 hours of cell growth. At the time of collection, cells were washed with cold tris-buffered saline (TBS) containing 50 mM Tris-hydrochloric acid pH 7.6, 150 mM NaCl, treated with a protein lysis buffer (50 mM Tris pH 7.6, 150 mM NaCl, 0.5 % Brij 96) with protease and phosphatase inhibitors (1 mM Sodium Orthovanadate, 0.3 U/ml Aprotinin, 10 $\mu\text{g}/\mu\text{l}$ Leupeptin, 1 mM Phenylmethylsulfonyl fluoride (PMSF), 25 mM NaF, 10 mM β -glycerophosphate). Whole cell lysates were agitated on a rotating stage at 4 °C for 1 hour, centrifuged for 10 minutes at 4 °C at 10,000 X g, and supernatant collected. Protein was then quantified using Bio-Rad Protein Assay (Bio-Rad Laboratories, Hercules, CA) using bovine serum albumin as standard and protein extracts were frozen at -80 °C until assayed.

2.3 *In Vitro* Transcription/Translation

TnT Quick Coupled Transcription/Translation System from Promega was used to transcribe and translate two different pcDNA3.1/Neo/Myc-His vectors (Invitrogen) that harbor either *Tubedown* or *Ard1* coding sequences (provided by Dr. H. Paradis) to generate ^{35}S -labeled Tubedown and Ard1, respectively. ^{35}S -labeled protein samples were generated using 40 μl TnT Quick Master Mix, 4 μl [^{35}S]-methionine/cysteine (11 mCi/mL, Perkin Elmer (Santa Clara, CA)), 1 μg plasmid, and 5 μl diethylpyrocarbonate (DEPC) treated H_2O . Samples were incubated at 30 °C for 90 minutes while gently mixing every 30 minutes. This method generated Myc-His tagged, ^{35}S -labeled

Tubedown and Ard1, respectively. Samples created using the ^{35}S -labeled Tubedown and Ard1 TnT samples were run on 8 % sodium dodecyl sulfate polyacrylamide gels (SDS-PAGE) directly or used for immunoprecipitation (described below). Gels were then either transferred as described in *Western Blot Analysis* (Section 2.6) or dried using a gel dryer model 583 (Bio-Rad Laboratories, Hercules, CA). Dried gels or gels transferred onto nitrocellulose membranes were then exposed to small, multi-sensitive storage phosphor screen (Life Sciences, Boston, MA). Storage phosphor screens were exposed for 1 week to dried gels or nitrocellulose membranes, scanned with the Cyclone Storage Phosphor Scanner and analyzed with OptiQuant software version 03.10 from Life Sciences (Boston, MA).

2.4 C-Src Purification

Purified c-Src was a generous gift from Dr. N Lydon. In short, c-Src was purified by recombinant pp60c-Src baculovirus lacking the myristoylation site at codon 2 was transfected into Sf9 cells to produce non-myristoylated pp60c-Src (Lydon et al., 1992). Non-myristoylated pp60c-Src was used to increase production and provide a more stable form of c-Src (Lydon et al., 1992). This method generates 95 % pure c-Src (Lydon et al., 1992).

2.5 Immunoprecipitation

All immunoprecipitation manipulations were conducted at 4 °C. Protein-G sepharose beads (Amersham, Buckinghamshire, England) were prepared by washing 2 X with 5 volumes of TBS, and then twice with 5 volumes of 50 mM Tris-HCl pH 7.6, 150

mM NaCl, 0.5% Brij 96 (0.5 % TNB). A 50 % protein-G sepharose bead suspension was created with 0.5 % TNB. Depending on recommended amounts for the antibody being used 500-1000 μ g protein or 20 μ l 35 S-labeled Tubedown-Myc-His or 35 S-labeled Ard1-Myc-His were used per immunoprecipitation. Samples were brought to a volume of 250 μ l with 0.5 % TNB, and incubated overnight on a rotating stage at 4 °C. Antibody-antigen complexes were mixed with 55 μ l 50 % Protein-G. Samples were centrifuged for 1 minute at 1000 X g and visualized for equal amounts of beads. Samples were then placed on rotating stage for 75 minutes, centrifuged for 1 minute at 1000 X g and the supernatant aspirated. Beads were washed 4 X with 500 μ l of 0.5 % TNB. Supernatant was discarded and 12 μ l 5 X protein loading buffer (50 mM Tris- HCl (pH 6.7), 2 % SDS, 10 % Glycerol, 1 % β -mercaptoethanol, 12.5 mM Ethylenediaminetetraacetic acid (EDTA), 0.02 % Bromophenol Blue) was added. Samples were kept at 4 °C until electrophoresis. Bead-antibody-antigen complexes were boiled for 5 minutes at 100 °C before loading in 7 % SDS-PAGE. Immunoprecipitation of 35 S-labeled proteins were analyzed on Cyclone Storage Phosphor Scanner as described above.

Double and triple immunoprecipitations were performed using double and triple the amount of antibody, protein, and beads, respectively. All immunoprecipitations manipulations were completed as one and samples were split at the last wash for downstream application.

2.6 Western Blot Analysis

Protein extracts were prepared as described previously in *Cell Culture* (Section 2.2). Non-immunoprecipitation protein samples were prepared in 0.5 % TNB and boiled for 3 minutes at 100 °C. All samples were separated on a 7 % SDS-PAGE overnight at 4 mA. Gels were soaked in 25 mM Tris Base and 192 mM glycine for 15 minutes. Sponges, 0.2 µm nitrocellulose/PVDF membrane (Bio-Rad), and 3 MM whatman paper were soaked in 25 mM Tris Base, 192 mM glycine, and 18 % methanol until saturated. Both nitrocellulose membranes (0.2 µm) and polyvinylidene fluoride (PVDF) membranes were used. Once transferred, membranes were placed into H₂O for rinsing before being blocked in 2 % enhanced chemiluminescence (ECL) advance block (General Electric, Mississauga, Ontario) in TBS with 0.05 % Tween 20 (TBST), for 1 hour at 55 °C. Membranes were incubated overnight with primary antibody at room temperature in 2 % ECL advance block in TBST. Membranes were then washed 7 X for 5 minutes in 100 ml TBST, then incubated for 1.5 hours with a horseradish peroxidase (HRP) conjugated secondary antibody in 2 % ECL advance block in TBST. Membranes were again washed 7 X for 5 minutes in TBST. Western blots were revealed by chemiluminescence that was detected using Lumiglo Reserve (Mandel, Guelph, Ontario), ECL Plus (Tubulin western blot analysis only) (General Electric), or ECL Advanced (c-*Src* western blot analysis only) (General Electric) substrates based on antibody sensitivity and protein amounts. Images and densitometry analysis were performed using Kodak Gel Logic Imaging System (Eastman Kodak Company, Rochester, New York). Band intensities were analyzed with Kodak Molecular Imaging Software (Eastman Kodak Company).

To strip antibodies from the membrane in preparation for re-probing the membranes were placed in 60 mM Tris-HCl (pH 6.7), 2 % SDS, 0.7 % 2-mercaptoethanol, and 34 ml water for 1 hour at 55 °C. The membrane would then be washed 7 X for 5 minutes each in TBS before re-blocking the membrane for further western blot analysis.

2.7 siRNA Knockdown

RF/6A transient Tubedown knockdowns were formed by electroporation using a Neon Transfection Kit purchased from Life Technologies (Carlsbad, California). RF/6A endothelial cells were collected and counted with a hemocytometer after 24 hours of growth. Cells were then centrifuged and supernatant aspirated. Cell pellets were re-suspended with 10 ml of sterile 37 °C phosphate buffered saline per 10^7 cells for washing. Suspensions were then centrifuged for 5 minutes at 150 X g at room temperature. Supernatants were aspirated and cell pellets re-suspended in sterile Buffer R (from Neon Transfection Kit) so that cells were at a final density of 1.33×10^6 cells/110 μ l Buffer R. Neon apparatus was assembled and 3 ml Buffer E2 (from Neon Transfection Kit) was added. Electroporation tubes from Neon Transfection Kit were replaced when different materials were electroporated or tubes had been used for 10 electroporations.

Cells were transfected with a combination of: 0-20 nM rhesus macaque Tubedown100 siRNA target Rhe-Tbdn703 (5'-TGCGAGATCTTGAGGGTTA-3') (Dharmacon, Lafayette, Colorado), 0-20 nM scrambled control siRNA SC47 (5'-

GATCCGTTTCATCGTCACTA-3') (Dharmacon, Lafayette, Colorado), 0.5 µg of plasmid maxFP-Green expressing a variant of the green fluorescent protein maxGFP (Amaya Biosystems, Gaithersbury, Massachusetts), and 110 µl of Buffer R suspension plus cells (1.33×10^6 cells/sample). Electroporation was conducted with 2 pulses of 1150 volts and a pulse width of 30. These electroporation guidelines were determined to give the best maxFP-Green expression with low cell death using the RF/6A endothelial cell line. Once electroporated, samples were placed directly into RF/6A cell culture media, re-suspended and plated at 1.33×10^6 cells/100 mm plate or 0.3325×10^6 cells/well in 12-well chamber plate with 18 mm round glass coverslips at the bottom of each well. After 72 hours of cell growth plates and coverslips were retrieved. Whole cell lysates from growth plates were prepared as described above in *Cell Culture* (Section 2.2) and protein quantitation conducted using Bio-Rad assay.

2.8 Coverslip Preparation/Immunofluorescence Staining

After 72 hours of growth wells from 12-well culture plates containing coverslips were washed 2 X with 1 ml cold TBS buffer. Coverslips were allowed to air dry then placed in 4 % paraformaldehyde in phosphate buffered saline for 15 minutes and transferred into 80 % ethanol for storage until staining was performed. Samples were not stored in ethanol at 4 °C for longer than 4 weeks to preserve antigenicity.

For immunofluorescent staining coverslips were washed 2 X for 5 minutes in TBS and blocked for 1 hour at room temperature in 2 % ECL block (General Electric, Mississauga, Ontario) in TBS plus 0.2 % TritonX-100 to permeabilize cell membranes.

Coverslips were then incubated with either ZO-1 (1A12) antibody at a 1:100 dilution or IgG₁ negative control antibody at 5µg/ml in 2 % ECL block in TBST overnight at room temperature. Then coverslips were washed 3 X for 5 minutes in TBST before secondary antibody incubation with anti-mouse rhodamine red antibody at a 1:100 dilution in 2 % ECL block (General Electric, Mississauga, Ontario). Coverslips were washed 3 X for 5 minutes each in TBST before being mounted with vectashield medium containing 4',6-diamidino-2-phenylindole (DAPI) (Vector Laboratories, Burlingame, California) for nuclear detection. Coverslips were inverted onto clear slides and sealed with clear nail polish the next day. Fluorescence was visualized using the Leica DMIRE2 microscope with a brightfield 40 X objective using a Qimaging RETIGA Exi camera. Images were processed with Improvision Openlab software version 5.50.

2.9 Transient Transfection GFP Quantitation

Transient transfection efficiency was determined by visualizing cells after 72 hours of culture using the Leica DMIRE2 microscope with green fluorescent protein (GFP) and brightfield 10 X objectives using a Qimaging RETIGA Exi camera. Cells from a 20 mm x 20 mm field from each image taken were counted and cells that expressed GFP were divided by total number of cells. A minimum of 20 cells from each transfection replicate were counted.

2.10 Transient Transfection Protein Quantitation

Tubedown and ZO-1 protein quantitation from transient transfections were conducted by visualizing western blot bands with a Kodak Gel Logic 2200 Imaging System followed by densitometric analyses of bands with Kodak Molecular Imaging Software 4.0.

2.11 ZO-1 Perimeter Quantitation

Quantitation of cell perimeter ZO-1 expression was determined by counting cells that intensely expressed ZO-1 at the perimeter of the cell. Intensities were evaluated using Improvision Openlab Software version 5.50. Cells with less than an average of 60 % contact with other cells were not counted due to decreased tight junction assembly at paracellular contacts (Siliciano, J.D. 1988). Cells undergoing mitosis or having mis-shaped nuclei were also not counted because this also could affect ZO-1 expression. No less than 100 cells per transfection group were quantitated for ZO-1 perimeter expression.

2.12 Data Analysis and Statistics

Statistical differences in data sets completed from quantitations were determined with analysis of variance between groups (ANOVA) using GraphPad Prism Version 4.0. Statistical differences of controls that were set to 100 % were determined using the T-test function of Microsoft Excel 2008, version 12.2.0 with unadjusted numbers within each data set. While ANOVA is a more precise method when determining statistical differences between the means of multiple data sets, when the control is adjusted to 100 % all data sets would then be statically different from the control. Therefore, T-test scores were completed from original values within individual data sets and the average used for accuracy of control comparison. Significant differences were considered for $p < 0.05$ and are designated by an asterisk (*) within graphs.

2.13 Sequence Alignment Analysis

The Basic Local Alignment Search Tool (BLAST) algorithm version 2.2.26+ was used to evaluate possible homologies with siRNA constructs (Altschul et al., 1990). Query sequences were 'BLASTed' into nucleotide BLAST (BLASTn) using the reference RNA sequences (refseq_rna) database accession Mmul_1 (Pruitt et al., 2009). *Macaca mulatta* was used as the organism because RF/6A endothelial cells are *macaca mulatta* derived. BLASTn automatically adjusts parameters to a short input sequence. Sequences showing a significant alignment were evaluated based on Expect (E) value that estimates the number of matches expected to occur randomly with a score equal to or higher than a given score. Simply put, the lower the E-value the greater chance of a 'hit' leading to siRNA interaction with an mRNA causing protein knockdown. The threshold of significance differs from study to study. Since short sequences were 'BLASTed' in this case an E value less than 15 was considered significant. After review of the E value protein matches were then further evaluated using Ensembl genome browser to determine significant regions within the protein. Genomic and siRNA input candidate sequences were aligned using Sequencher Software, version 4.10.1, from Gene Codes Corporation for visualization of homology.

3.0 RESULTS

Testing potential Tubedown binding partners to elucidate its mechanistic role in the regulation of ocular endothelial permeability.

3.1 Specificity of Tubedown Antibodies

To confirm that the Narg1 commercial antibody recognizes the Tubedown protein, immunoprecipitations of ³⁵S-labeled Tubedown-Myc-His transcription and translation (TnT) lysates were conducted with the Narg1 antibody. ³⁵S-labeled Tubedown-Myc-His and ³⁵S-labeled Ard1-Myc-His lysates were generated from transcription and translation (TnT) of pcDNA3.1/Neo/Myc-His construct containing either *Tubedown* or *Ard1* coding sequences, respectively. Immunoprecipitations using LE C10-20 (Tubedown; Paradis et al., 2008) and Myc-Tag antibodies from ³⁵S-labeled Tubedown-Myc-His lysates were used for comparison. Immunoprecipitation from ³⁵S-labeled Tubedown-Myc-His TnT lysate with no antibody was the control. Immunoprecipitations were exposed to phosphor screen and photon emissions analyzed. The photon emission band at 108 kDa in the Narg1 immunoprecipitation proves that the Narg1 antibody can immunoprecipitate Tubedown-Myc-His from ³⁵S-labeled Tubedown-Myc-His TnT lysates permitting it to be used for further analyses of Tubedown [Fig. 3.1].

³⁵S-labeled Ard1-Myc-His TnT lysates were used as a positive control for comparisons to the Tubedown immunoprecipitations. Immunoprecipitations of ³⁵S-labeled Ard1-Myc-His TnT lysates were conducted using either the Myc-Tag antibody or no antibody as control. The 36 kDa band in the Myc-Tag immunoprecipitation shows

that the Myc-Tag antibody can immunoprecipitate the Ard1-Myc-His protein from TnT
³⁵S-labeled Ard1-Myc-His lysates.

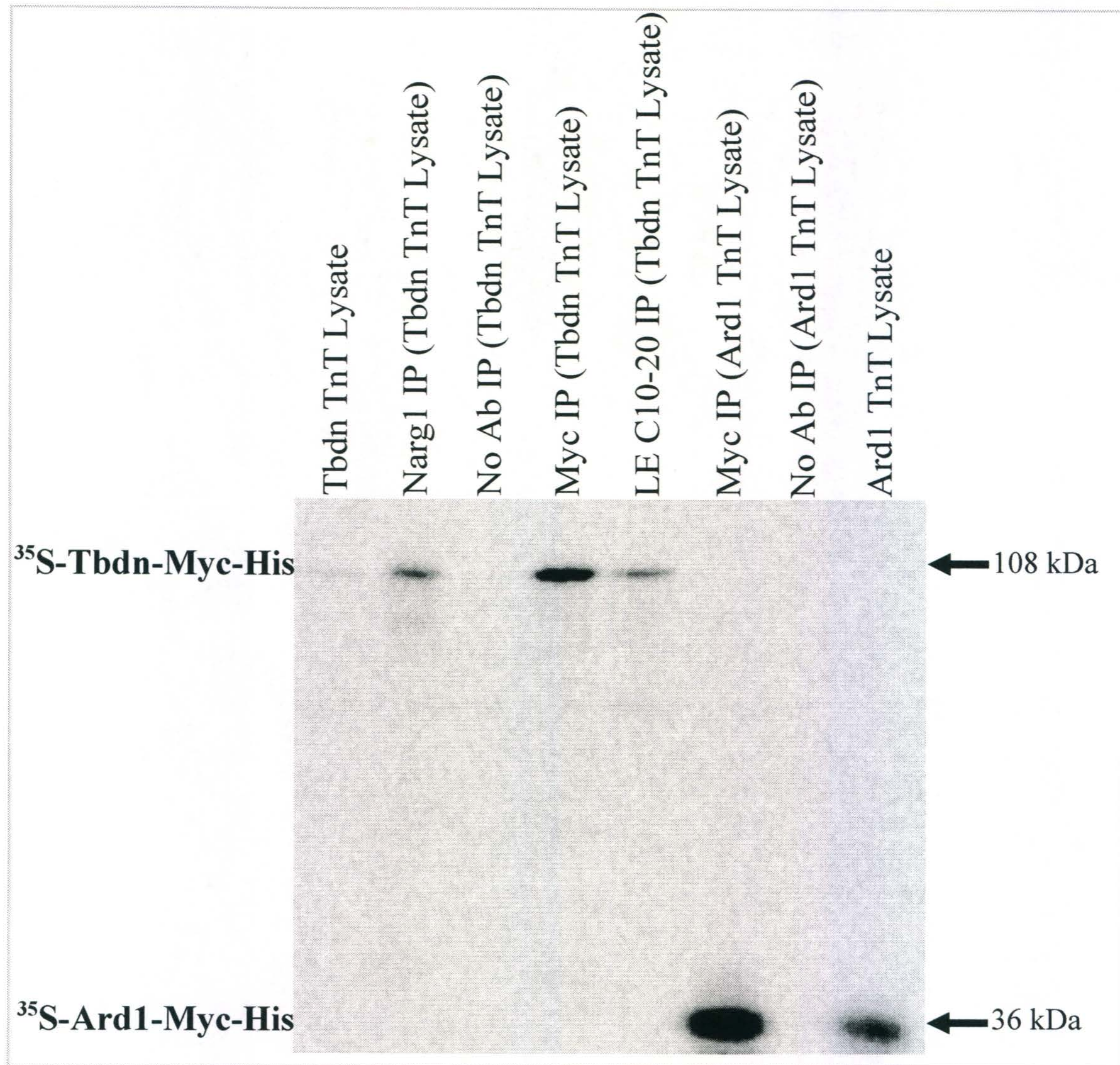


Figure 3. 1 Specificity of Tubedown Antibodies. Ard1-Myc-His were prepared from TnT lysates of two different pcDNA3.1/Neo/Myc-His constructs containing either *Tubedown* or *Ard1* coding nucleotide sequences. TnT ^{35}S -labeled Tubedown-Myc-His was immunoprecipitated with Narg1 (Narg1 IP), LE C10-20 (LE C10-20 IP), and Myc-Tag (Myc IP) antibodies, and no antibody (No Ab IP) as control. Immunoprecipitations were analyzed by SDS-PAGE and by reading photon emissions from a phosphor screen after 1 week of exposure to radioactive gels. TnT ^{35}S -labeled Tubedown-Myc-His and Ard1-Myc-His lysates were used for comparison (Tubedown TnT and Ard1 TnT lanes, respectively). ^{35}S -labeled Ard1-Myc-His was immunoprecipitated using the Myc-Tag antibody (Myc IP) and no antibody (No Ab IP) as control. ^{35}S -labeled Tubedown-Myc-His and ^{35}S -labeled Ard1-Myc-His are indicated with arrows at 108 kDa and 36 kDa, respectively. Photon emission bands at 108 kDa in Narg1 and LE C10-20 immunoprecipitations proves that these antibodies recognize Tubedown (Experiments completed = 1).

3.2 Analysis of Tubedown/Dynamin Interaction

To verify that endothelial cells express Dynamin, western blot analyses on whole cell lysates (WCL) from RF/6A retinal endothelial cells were performed with Dynamin antibody [Fig. 3.2, WCL lanes]. Western blot analysis with Dynamin shows a band at 100 kDa confirming endothelial cells express Dynamin.

To determine if Tubedown and Dynamin interact together, immunoprecipitations were prepared using LE C10-20 (Tubedown) antibody followed by western blot analyses with Dynamin (Fig. 3.2, bottom panel) and Narg1 (Tubedown) antibodies (Fig. 3.2, top panel) from RF/6A endothelial cell extracts [Fig. 3.2]. A double immunoprecipitation was performed followed by two separate western blot analyses because both Dynamin and Tubedown are 100 kDa. Control immunoprecipitations were prepared with rabbit pre-immune serum. Immunoprecipitations of Tubedown followed by Dynamin western blot analyses showed no band in the migration area of Dynamin (100 kDa) suggesting that Tubedown and the Dynamin-2 endothelial isoform do not interact within RF/6A endothelial cells [Fig. 3.2].

Other combinations of immunoprecipitations followed by western blot analyses were performed using the Narg1 antibody (Tubedown) for immunoprecipitation, and a second endothelial cell line (IEM) to further detect possible Tubedown and Dynamin interactions (results not shown). Immunoprecipitation using Dynamin antibody could not be performed because the antibody was not suitable for immunoprecipitations. Tubedown interaction with Dynamin was not observed following any of the immunoprecipitations / western blot analyses tested.

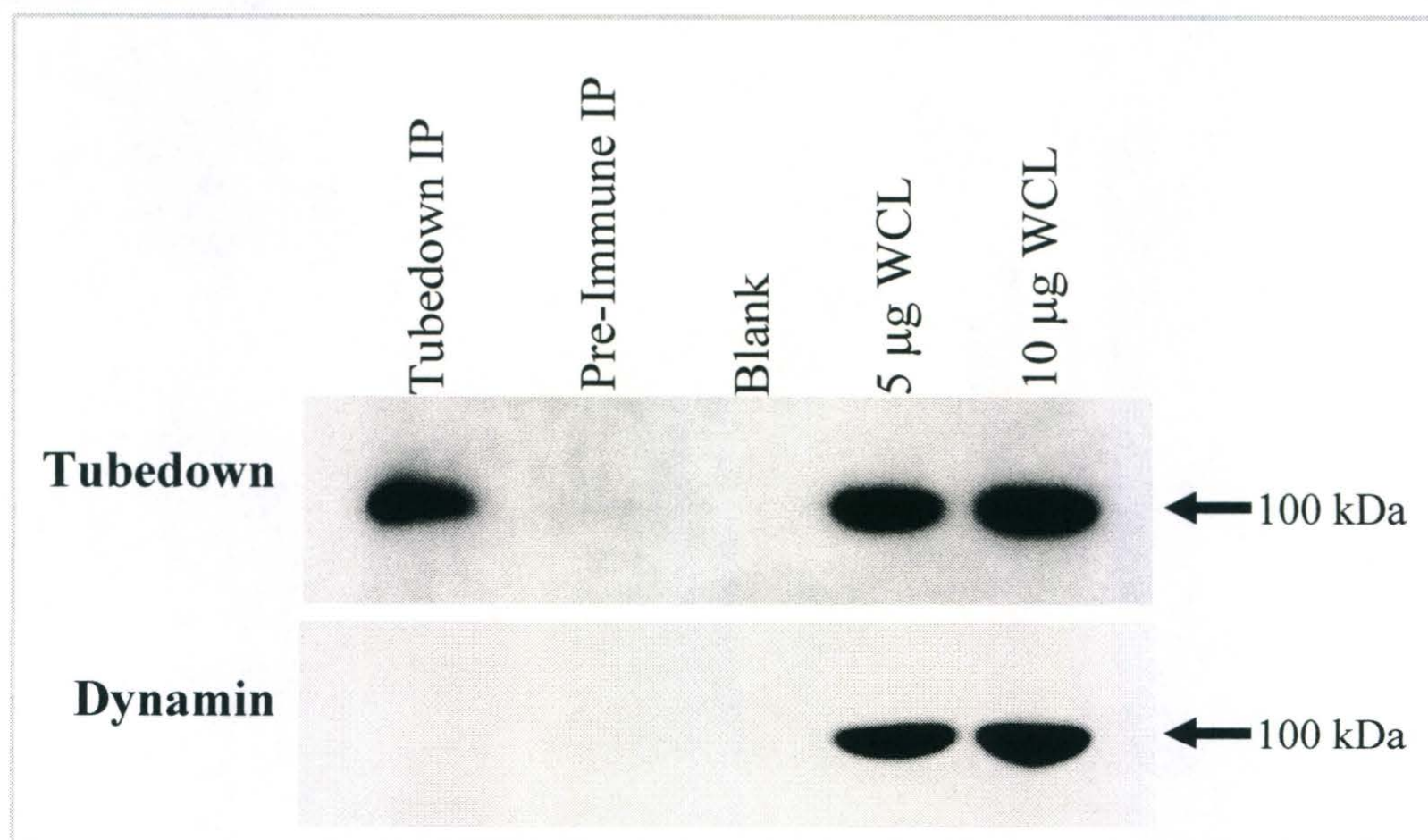


Figure 3. 2 Dynamin and Tubedown: Western Blot Analyses of Tubedown Immunoprecipitation. Immunoprecipitations (IP) prepared from RF/6A endothelial cell extracts using LE C10-20 (Tubedown IP) antibody or pre-immune rabbit serum (Pre-Immune IP) as control were analyzed by western blotting for Tubedown or Dynamin. Lanes with 5 µg and 10 µg of whole cell lysate (WCL) were used for protein amount comparison. Western blot analyses were conducted using Narg1 (Tubedown) antibody and Dynamin antibody (top and bottom panel, respectively). Tubedown and Dynamin are both at 100 kDa as indicated by arrows. An empty lane (blank) was left in between immunoprecipitations and WCL lanes to detect possible run-over of lanes when loading gel. Dynamin does not co-immunoprecipitate with Tubedown suggesting no interaction between Dynamin and Tubedown. Representative results are shown (Experiments completed = 5).

3.3 Analysis of Tubedown/AF-6 Interaction

To verify that AF-6 is expressed in endothelial cells, western blot analyses of WCL from IEM cells were performed using AF-6 antibody (Fig. 3.3, WCL lanes). Western blot analysis with AF-6 shows a band at 200 kDa confirming endothelial cells express AF-6.

To determine if Tubedown binds to AF-6, immunoprecipitations were performed with AF-6 antibody from IEM cell extracts followed by western blot analyses with AF-6 (Fig. 3.3, bottom panel) or Narg1 (Tubedown) antibodies (Fig. 3.3, top panel) [Fig. 3.3]. Immunoprecipitations with IgG₁ negative control antibody were used as a control. AF-6 western blot analyses of Narg1 (Tubedown) immunoprecipitation showed no band in the migration area of AF-6 (200 kDa) suggesting that Tubedown and AF-6 do not bind within IEM cells [Fig. 3.3].

Other immunoprecipitations were performed with RT C10-20 (Tubedown) antibody. In addition, reciprocal experiments were performed using the AF-6 antibody. All immunoprecipitations were followed by western blot analyses with AF-6 and Narg1 (Tubedown) (results not shown). Tubedown and AF-6 interactions were not detected with any immunoprecipitations/western blot analyses.

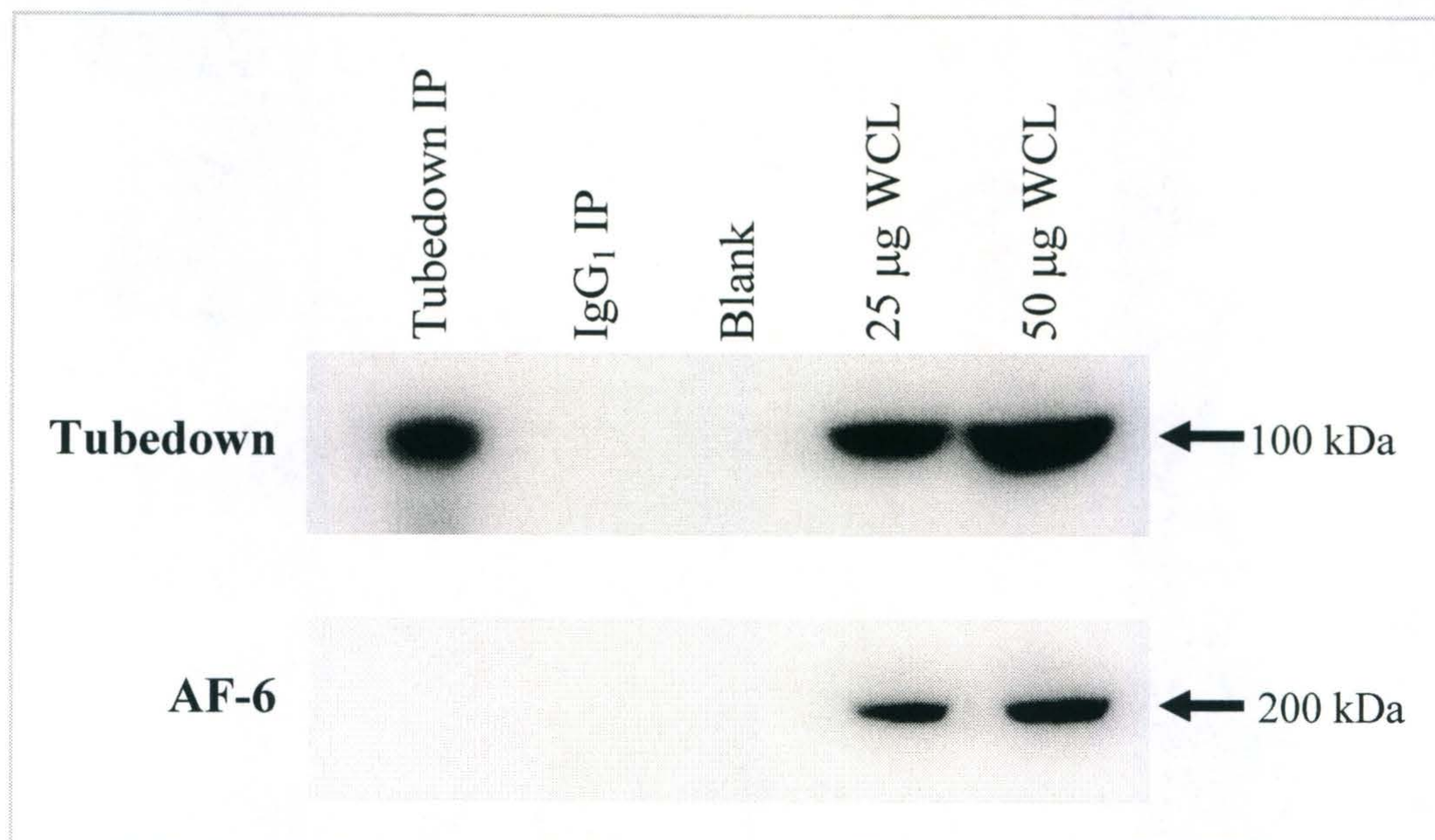


Figure 3.3 AF-6 and Tubedown: Western Blot Analyses of Tubedown Immunoprecipitation. Immunoprecipitations (IP) prepared from IEM cell extracts using Narg1 (Tubedown IP) antibody and IgG₁ negative control (IgG₁ IP) antibody were analyzed by western blot analysis for Tubedown or AF-6. Lanes with 25 µg and 50 µg of whole cell lysates (WCL) were used for protein amount comparison. Western blot analyses were conducted using Narg1 antibody (Tubedown) and AF-6 antibody (top and bottom panels, respectively). Tubedown and AF-6 are indicated with arrows at 100 kDa and 200 kDa, respectively. An empty lane (blank) was left in between immunoprecipitations and WCL lanes to detect possible run-over of lanes when loading gel. Lack of AF-6 in Tubedown immunoprecipitation suggests no interaction between AF-6 and Tubedown. Representative results are shown (Experiments completed = 3).

3.4 Analysis of Tubedown/Y421-Phospho-Cortactin Interaction

To verify that the levels of Y421-Phospho-Cortactin are high enough to be detected in endothelial cells, western blot analyses on WCL of IEM cells were performed using the Y421-Phospho-Cortactin antibody [Fig. 3.4 & 3.5, WCL lanes]. Western blot analysis with Y421-Phospho-Cortactin shows a band at 100 kDa confirming endothelial cells express Y421-Phospho-Cortactin.

To determine if immunoprecipitation manipulations allowed for detection of Y421-Phospho-Cortactin by western blot analysis, immunoprecipitations and western analyses were completed in IEM cell extracts. Immunoprecipitation of Cortactin using 4F11 antibody followed by western blot analyses with Y421-Phospho-Cortactin antibody (Fig. 3.4, top panel) and Cortactin (4F11) antibody (Fig. 3.4, bottom panel) were conducted [Fig. 3.4]. Western blot analyses were first conducted with Y421-Phospho-Cortactin antibody (Fig. 3.4, middle panel) and the membrane was then stripped and re-probed with Cortactin 4F11 antibody (Fig. 3.4, bottom panel). Immunoprecipitation with IgG₁ negative control antibody was used as control. An 80 kDa band corresponding to the molecular weight of Cortactin was detected in the immunoprecipitation of Cortactin followed by western blot analysis with Y421-Phospho-Cortactin, verifying that immunoprecipitation manipulations allowed the detection of Y421-Phospho-Cortactin within IEM cells [Fig. 3.4].

To determine if Tubedown and Y421-Phospho-Cortactin interact together, immunoprecipitation of Tubedown was performed followed by western blot analyses of Y421-Phospho-Cortactin, Cortactin, and Tubedown within IEM cell extracts. A triple

immunoprecipitation of Narg1 (Tubedown) was performed and three separate western blot analyses were conducted. Western blot analyses were completed with Y421-Phospho-Cortactin antibody (Fig. 3.5, middle panel), Cortactin 4F11 antibody (Fig. 3.5, bottom panel), and Narg1 (Tubedown) antibody (Fig. 3.5, top panel) [Fig. 3.5]. Cortactin western blots (Fig. 3.5, bottom panel) were stripped and reprobed with Narg1 (Tubedown) antibody (Fig. 3.5, top panel) to confirm the presence of Tubedown. Immunoprecipitation with IgG₁ negative control antibody was used as control. Immunoprecipitation of Tubedown followed by Cortactin western blot analyses showed the binding between Cortactin and Tubedown. However, immunoprecipitation of Tubedown followed by Y421-Phospho-Cortactin western analyses shows no band. These results suggest the interaction between Tubedown and Cortactin does not occur in IEM cells when Cortactin is phosphorylated at Y421 [Fig. 3.5].

Immunoprecipitations were also carried out using LE C10-20 (Tubedown) and RT C10-20 (Tubedown) antibodies followed by western analyses for both with Y421-Phospho-Cortactin and Narg1 (Tubedown) antibodies (results not shown). Immunoprecipitation of Narg1 (Tubedown) antibody with double antibody and double protein concentrations were also completed to detect minimal amounts of Y421-Phospho-Cortactin interaction with Tubedown. Western blot analyses were also conducted on WCL of RF/6A endothelial cells with Y421-Phospho-Cortactin antibody verifying Y421-Phospho-Cortactin can be detected in retinal-choroidal endothelial cells (results not shown). Immunoprecipitations with Y421-Phospho-Cortactin antibody could not be performed because antibody is not suitable for immunoprecipitations. Tubedown and

Y421-Phospho-Cortactin binding could not be detected in any of the immunoprecipitation / western blot analyses performed.

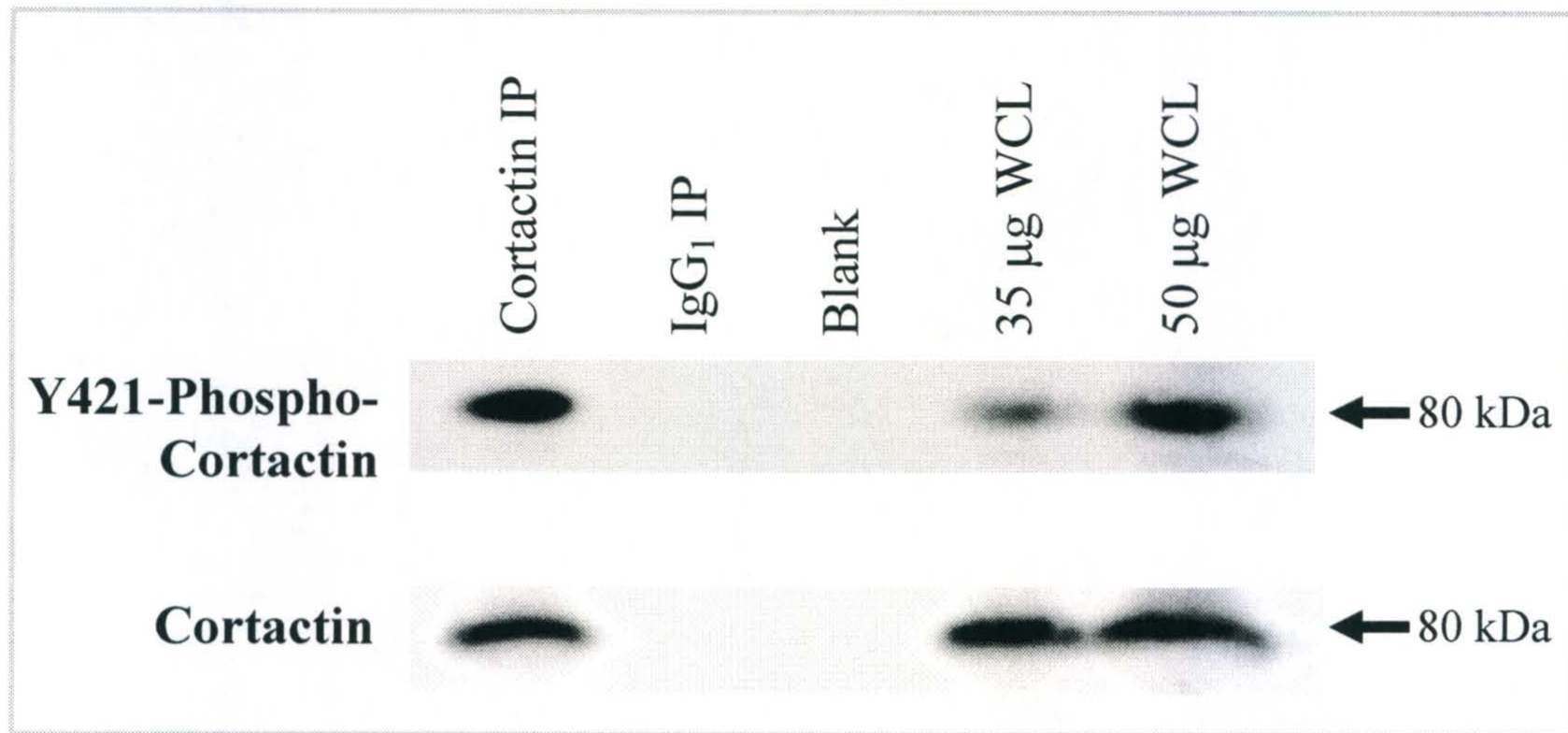


Figure 3. 4 Y421-Phospho-Cortactin and Cortactin: Western Blot Analyses of Cortactin Immunoprecipitation. Immunoprecipitations (IP) were prepared from IEM cell extracts using Cortactin (Cortactin IP) and IgG₁ negative control (IgG₁ IP) antibodies. Immunoprecipitations were analyzed by western blotting using Y421-Phospho-Cortactin antibody and Cortactin antibody (top and bottom panels, respectively). Arrows at 80 kDa indicate Y421-Phospho-Cortactin and Cortactin. Lanes with 35 µg and 50 µg of whole cell lysates (WCL) were used for protein amount comparison. An empty lane (blank) was left in between immunoprecipitations and WCL lanes to detect possible run-over of lanes when loading gel. Western blot analyses verify Y421-Phospho-Cortactin can be detected with Cortactin immunoprecipitation (Experiments completed = 1).

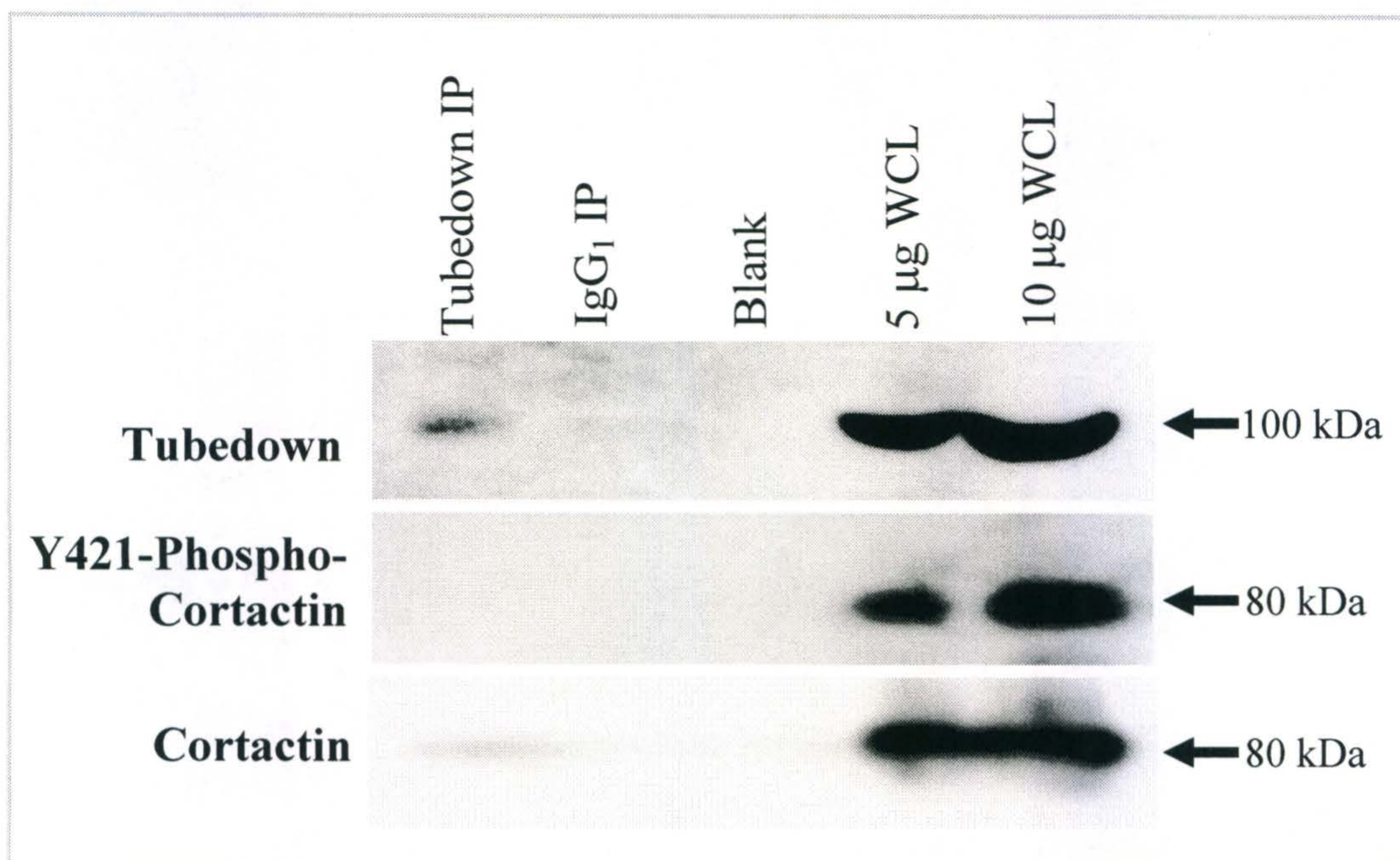


Figure 3. 5 Y421-Phospho-Cortactin, Cortactin, and Tubedown: Western Blot Analyses of Tubedown Immunoprecipitation. Immunoprecipitations (IP) were prepared from IEM cell extracts using Narg1 (Tubedown IP) antibody and IgG₁ negative control (IgG₁ IP) antibody. Immunoprecipitations were analyzed by western blot analyses using Y421-Phospho-Cortactin antibody, Narg1 (Tubedown) antibody, and Cortactin antibody (top, middle, and bottom panels, respectively). Arrows at 80 kDa indicate Y421-Phospho-Cortactin and Cortactin. Tubedown is indicated by an arrow at 100 kDa. Lanes with 35 µg and 50 µg of WCL were used for protein amount comparison. An empty lane (blank) was left in-between immunoprecipitations and WCL to detect possible run-over of lanes when loading gel. Western blot analyses show further evidence of Tubedown and Cortactin's interaction, but suggest no interaction between Tubedown and Y421-Phospho-Cortactin. Representative results are shown (Experiments completed = 10).

3.5 Analysis of Tubedown/c-Src Interaction

To verify that endothelial cells express c-Src, western blot analyses on WCL from IEM and RF/6A endothelial cells were performed with c-Src antibody [Fig. 3.6 and 3.7, WCL lanes]. Western blot analyses with c-Src antibody showed a band at 60 kDa confirming endothelial cells express c-Src.

To determine if Tubedown and c-Src interact together, Tubedown immunoprecipitations were prepared using LE C10-20 (Tubedown) antibody, MI-C755 (Tubedown) antibody, and Narg1 (Tubedown) antibody [Fig. 3.6]. Immunoprecipitations with no antibody were used as control. To test that the Narg1 antibody, which is stabilized by adding bovine serum albumin (BSA), would not cause an artificial band to appear within c-Src molecular weight (60 kDa) the Narg1 antibody alone was tested. Western blot analyses were conducted with Narg1 (Tubedown) antibody and c-Src antibody (top and bottom panels, respectively). Due to use of secondary anti-mouse antibody for western blot procedure, antibodies from immunoprecipitations and possibly BSA from Narg1 antibody preparation were detected during c-Src western blot analyses. Two bands present in the WCL lane with c-Src western blot analysis were sometimes observed [Fig. 3.6]. This is possibly due to degradation of the protein from cell extract. Tubedown immunoprecipitations followed by c-Src western blot analyses showed no band in the migration area of c-Src (60 kDa) suggesting that Tubedown and Src do not interact within RF/6A endothelial cells [Fig. 3.6].

To further validate Tubedown and c-Src do not interact immunoprecipitations were also completed with c-Src antibody from RF/6A endothelial cell extracts [Fig. 3.7].

Western blot analyses of immunoprecipitations were conducted with MI-C755 (Tubedown) (Fig. 3.7, top panel), Narg1 (Tubedown) (Fig. 3.7, middle panel), and c-Src (Fig. 3.7, bottom panel) antibodies. Immunoprecipitations with no antibody were used as control. Immunoprecipitations of c-Src followed by Tubedown western blot analyses showed no band in the migration area of Tubedown (100 kDa) suggesting that Tubedown and c-Src do not interact within endothelial cells [Fig. 3.7].

To confirm antibodies were not interfering with a possible Tubedown and c-Src regions of interaction, stable RF/6A clones harboring pcDNA3.1/Neo/Myc-His constructs containing either *Tubedown* (RF/6A-Tubedown-Myc-His) or *Ard1* (RF/6A-Ard1-Myc-His) coding sequences were used to study the interaction between Tubedown, Ard1 and c-Src. Immunoprecipitations of Tubedown and Ard1 were prepared using Myc-Tag antibodies from either RF/6A-Tubedown-Myc-His or RF/6A-Ard1-Myc-His, respectively [Fig. 3.8]. Control immunoprecipitations were completed with c-Src antibody and Myc-Tag antibody from RF/6A parental endothelial cells. Western blot analyses were completed with Narg1 (Tubedown) antibody, c-Src antibody, and Myc-Tag antibody for Ard1 detection. Narg1 (Tubedown) western blot analysis showed bands for both Tubedown-Myc-His and endogenous Tubedown (108 kDa and 100 kDa, respectively). Immunoprecipitations prepared with the Myc-Tag antibody from RF/6A-Ard1-Myc-His clones detected the interaction between Ard1 and endogenous Tubedown. However, no interactions could be detected between Tubedown and c-Src or Ard1 and c-Src because heavy and light chains of the Myc-Tag antibody left bands in the migration area of c-Src (60 kDa).

Since immunoprecipitations from endogenous lysates could not be completed with the Myc-Tag antibody to detect an interaction between Tubedown and c-Src, *in vitro* immunoprecipitations with Myc-Tag antibody were prepared from ^{35}S -labeled Tubedown-Myc-His or ^{35}S -labeled Ard1-Myc-His TnT lysates. To test that neither Tubedown nor Ard1 interact with c-Src, purified c-Src (Lydon et al., 1992) was incubated with ^{35}S -labeled Tubedown-Myc-His or ^{35}S -labeled Ard1-Myc-His TnT lysates to test their binding affinity [Fig. 3.9]. Immunoprecipitations of Tubedown or Ard1 were prepared with Myc-Tag antibody from ^{35}S -labeled Tubedown-Myc-His or ^{35}S -labeled Ard1-Myc-His lysates generated from TnT. Immunoprecipitation with no antibody from ^{35}S -labeled Tubedown-Myc-His or ^{35}S -labeled Ard1-Myc-His TnT lysates were used as control. Each immunoprecipitation was incubated with 550 ng of purified c-Src. For protein amount comparisons 200 ng of purified c-Src and one tenth of the TnT lysates of ^{35}S -labeled Tubedown-Myc-His or ^{35}S -labeled Ard1-Myc-His used for immunoprecipitations were loaded. Detection of photon emissions from radioactively labeled TnT lysates was completed to test if Tubedown and Ard1 were present in control and immunoprecipitation lanes [Fig. 3.9, Tbdn TnT Lysates, Myc IP (Tbdn TnT Lysates), Ard1 TnT Lysates, and Myc IP (Ard1 TnT Lysates) lanes, respectively]. Western blot analyses were carried out with c-Src antibody for c-Src protein detection [Fig. 3.9]. No c-Src was detected with immunoprecipitation of ^{35}S -labeled Tubedown-Myc-His or ^{35}S -labeled Ard1-Myc-His incubated with purified c-Src, suggesting neither Tubedown nor Ard1 are directly interacting with c-Src. This supports the result using cell extracts presented above.

Other combinations of immunoprecipitations followed by western blot analyses were performed using double concentrations of the LE C10-20 (Tubedown) antibody and double the amount of protein (results not shown). Tubedown and c-Src interactions could not be detected in any of the *in vitro* experiments performed.

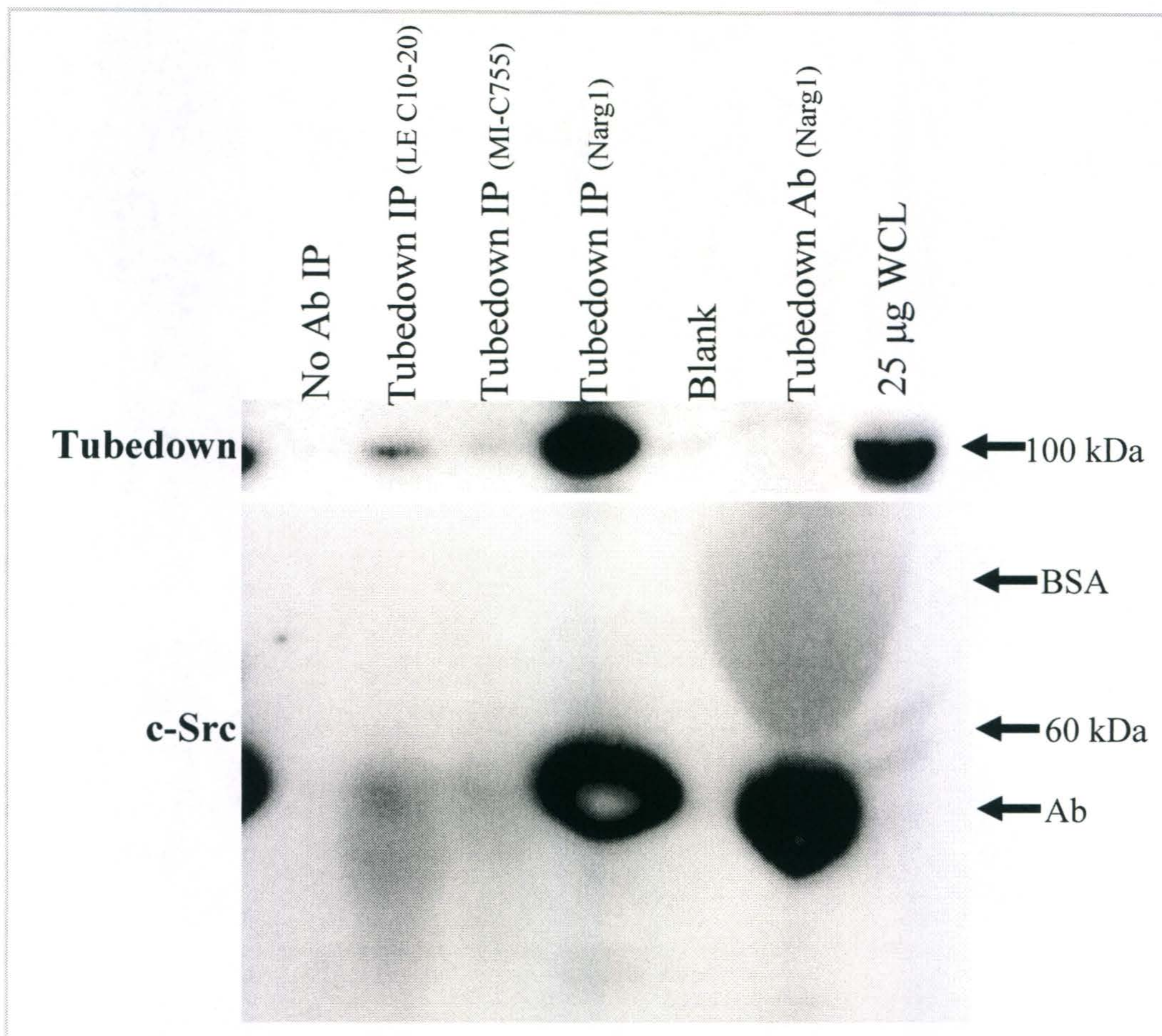


Figure 3. 6 Tubedown and c-Source: Western Blot Analyses of Tubedown Immunoprecipitation. Immunoprecipitations (IP) were prepared from IEM cell extracts. Tubedown immunoprecipitations were prepared using LE C10-20 antibody, MI-C755 antibody, and Narg1 antibody. No antibody (No Ab IP) immunoprecipitation was used as control. Immunoprecipitations were analyzed by western blot analyses using Narg1 (Tubedown) antibody and c-Source antibody antibodies (top and bottom panels, respectively). Arrows at 100 kDa and 60 kDa indicate Tubedown and c-Source, respectively. An arrow above 60 kDa possibly represents BSA that the Narg1 antibody was stabilized with. An arrow below 60 kDa represents heavy chains of antibodies (Ab) from immunoprecipitations. A lane with 50 µg of WCL was used for protein amount comparison. An empty lane (blank) was left in-between immunoprecipitations and WCL to detect possible run-over of lanes when loading gel. C-Source is not co-immunoprecipitating with Tubedown, suggesting Tubedown and c-Source do not interact (Experiments completed = 1).

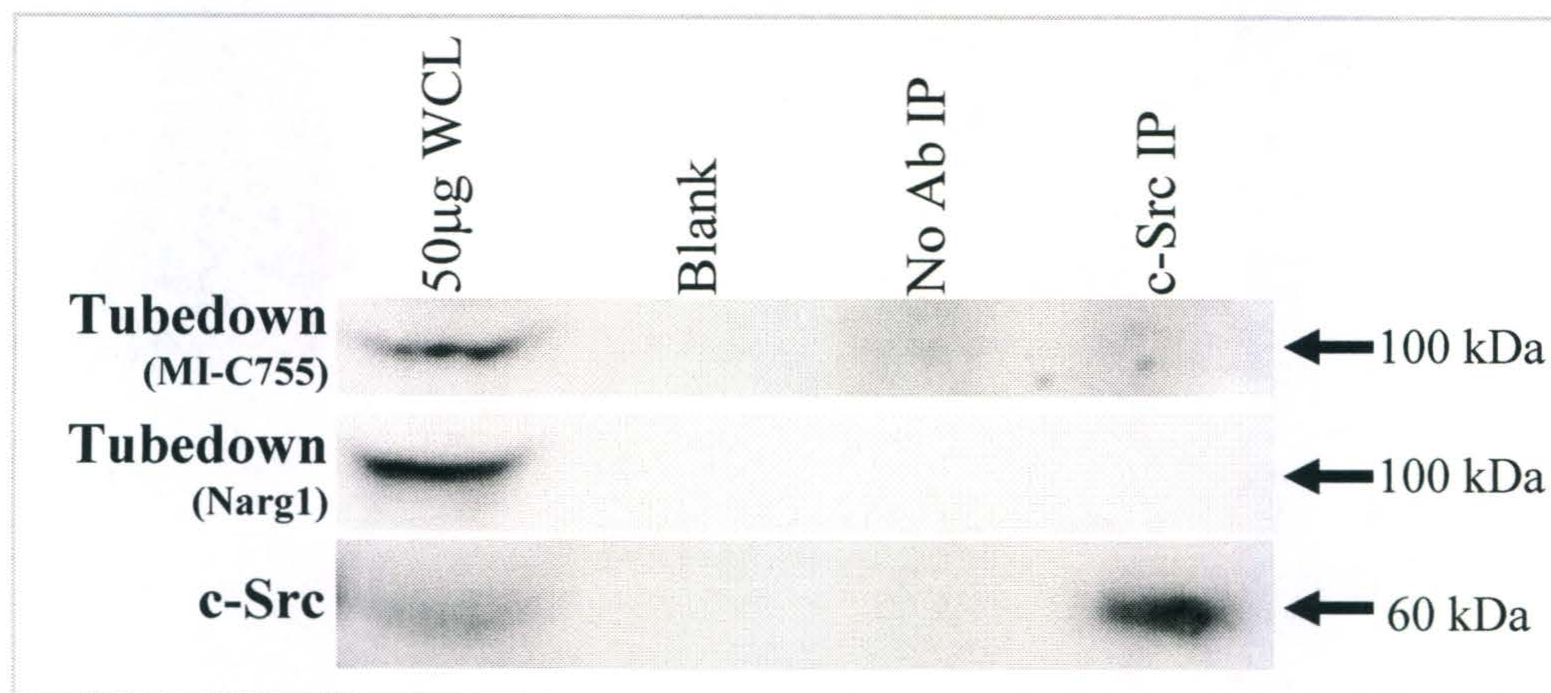


Figure 3. 7 Tubedown and c-Src: Western Blot Analyses of c-Src Immunoprecipitation. Immunoprecipitations (IP) were prepared from RF/6A endothelial cell extracts using c-Src (c-Src IP) antibody or no antibody (No Ab IP) control. Immunoprecipitations were analyzed by western blot analyses using MI-C755 (Tubedown) antibody, Narg1 (Tubedown) antibody and c-Src antibody (top, middle, and bottom panels, respectively). Arrows at 100 kDa and 60 kDa indicate Tubedown and c-Src, respectively. A lane with 50 µg of WCL was used for protein amount comparison. An empty lane (blank) was left in-between immunoprecipitations and WCL to detect possible run-over of lanes when loading gel. Tubedown is not co-immunoprecipitating with c-Src, suggesting Tubedown and c-Src do not interact. Representative results are shown (Experiments completed = 2).

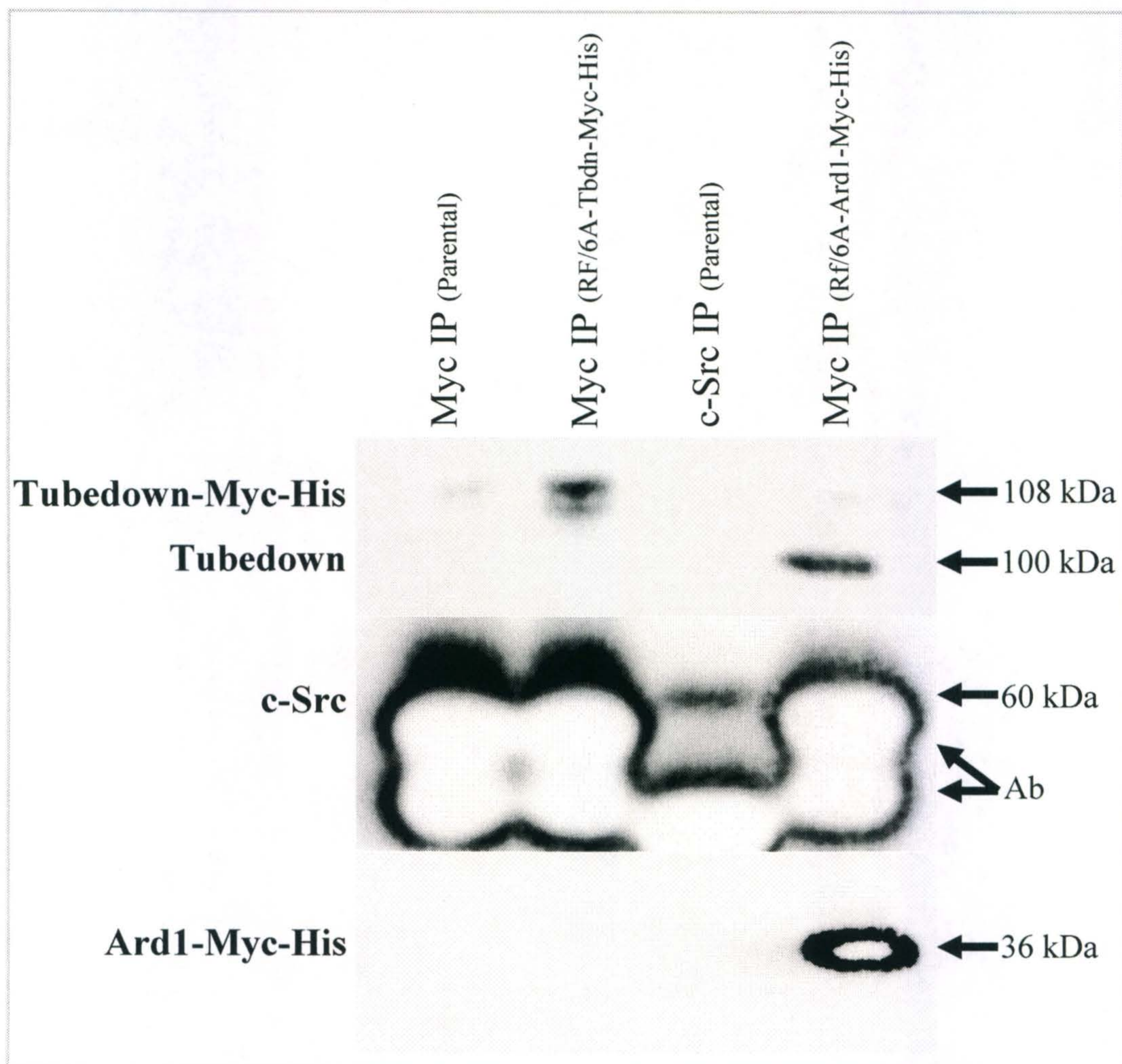


Figure 3. 8 Tubedown and c-Src: Western Blot Analyses of c-Src and Myc-Tag Immunoprecipitations. Immunoprecipitations (IP) were prepared from parental RF/6A endothelial cell extracts using c-Src (c-Src IP) antibody or Myc-Tag antibody (Myc IP) for controls. Immunoprecipitations were also prepared using Myc-Tag antibody from RF/6A Tbdn-Myc-His or Ard1-Myc-His RF/6A cell clones lysates to immunoprecipitate Tubedown and Ard1, respectively. Immunoprecipitations were analyzed by western blotting using Narg1 (Tubedown) antibody, c-Src antibody, and Myc-Tag antibody for Ard1 detection (top, middle, and bottom panels, respectively). Arrows at 108 kDa, 100 kDa, 60 kDa, and 36 kDa indicate Tubedown-Myc-His, Tubedown, c-Src, and Ard1-Myc-His, respectively. An arrow below 60 kDa represents heavy chains of antibodies (Ab) from immunoprecipitations. These results further prove the interaction between Tubedown and Ard1. However, no interaction between Tubedown and c-Src could be detected because heavy and light chains of antibody are in the migration area of c-Src (60 kDa). Representative results are shown (Experiments completed = 2).

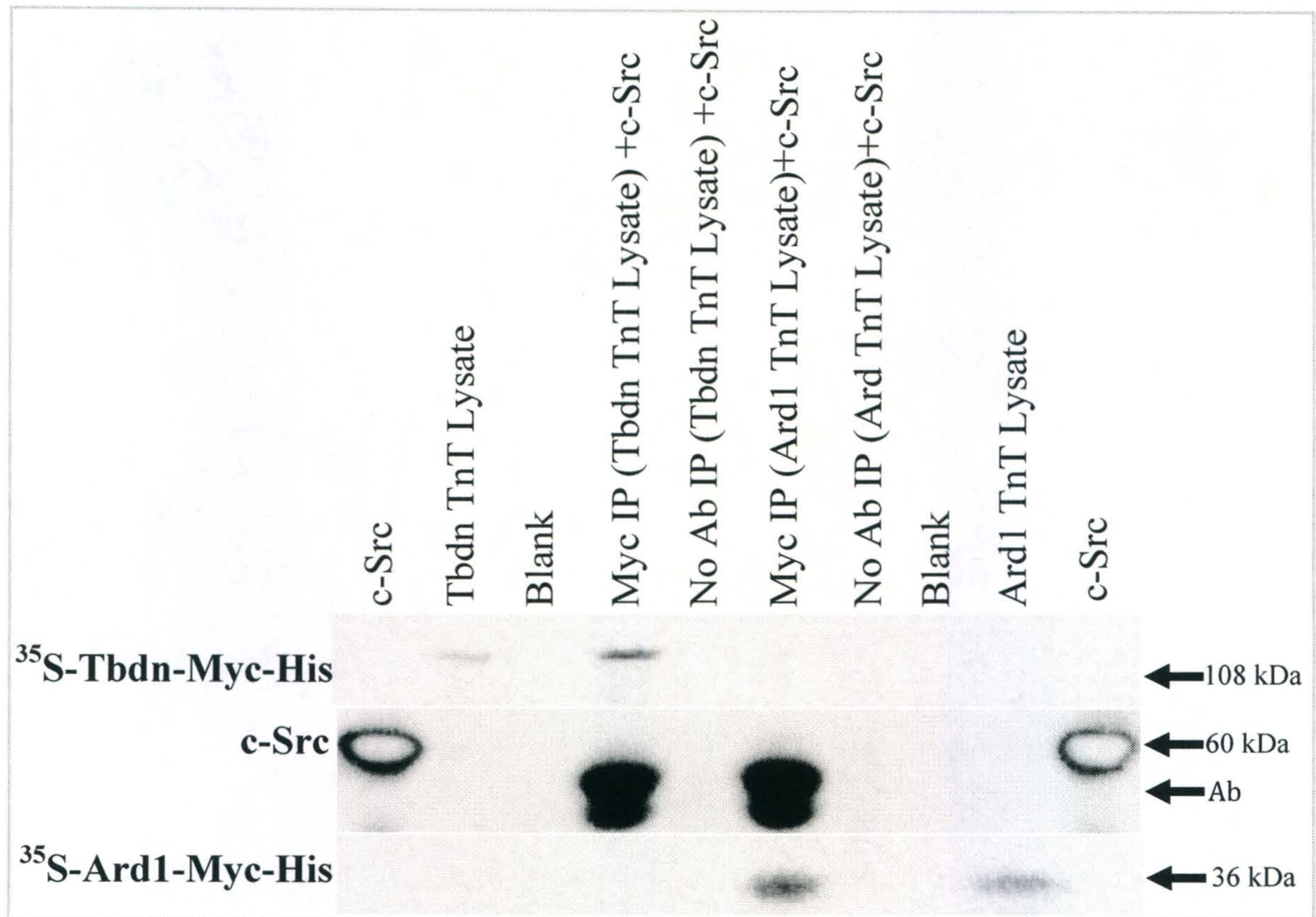


Figure 3. 9 Tubedown, c-Src, and Ard1: Photon Emissions and Western Blot Analysis of ^{35}S -Tubedown-Myc-His and ^{35}S -Ard1-Myc-His Immunoprecipitations Incubated with Purified c-Src. Immunoprecipitations (IP) were prepared from ^{35}S -labeled Tubedown-Myc-His (Tbdn TnT Lysate) and ^{35}S -labeled Ard1-Myc-His (Ard1 TnT Lysate) TnT lysates. ^{35}S -labeled Tubedown-Myc-His was immunoprecipitated with Myc-Tag (Myc IP) antibody and no antibody (No Ab IP) as control. ^{35}S -labeled Ard1-Myc-His was also immunoprecipitated with Myc-Tag (Myc IP) antibody and no antibody (No Ab IP) as control. All immunoprecipitations were incubated with purified c-Src. Purified c-Src (c-Src), ^{35}S -labeled Tubedown-Myc-His (Tbdn TnT Lysate), and ^{35}S -labeled Ard1-Myc-His (Ard1 TnT Lysate) were loaded as controls. Immunoprecipitations were analyzed by western blot analyses using c-Src antibody for c-Src protein detection (middle panel). ^{35}S -labeled Tubedown-Myc-His and ^{35}S -labeled Ard1-Myc-His were analyzed by reading photon emissions from a phosphor screen after 1 week of exposure (top and bottom panels, respectively). Arrows at 108 kDa, 60 kDa, and 36 kDa indicate ^{35}S -labeled Tubedown-Myc-His, c-Src, and ^{35}S -labeled Ard1-Myc-His, respectively. Heavy chains of Myc-Tag antibody from immunoprecipitations are indicated with an arrow under 60 kDa arrow. An empty lane (blank) was left in-between immunoprecipitations and controls to detect possible run-over of lanes when loading gel. No direct interaction between Tubedown nor Ard1 with c-Src could be detected (Experiments completed = 1).

3.6 Analysis of Tubedown/ZO-1 Interaction

To verify ZO-1 could be detected in endothelial cells, western blot analyses of WCL from RF/6A endothelial cells were conducted [Fig. 3.10, WCL lane]. Western blot analysis with ZO-1 antibody shows a band at 225 kDa confirming endothelial cells express ZO-1.

To determine if ZO-1 and Tubedown interact together, immunoprecipitations were prepared using ZO-1 (R40.76) antibody and no antibody as control with RF/6A endothelial cell extracts. Immunoprecipitations were analyzed by western blot using ZO-1(R40.76) (Fig. 3.10, bottom panel) and Narg1 (Tubedown) antibodies (Fig. 3.10, top panel) [Fig. 3.10]. No band was observed around Tubedown's molecular weight (100 kDa) in immunoprecipitations of ZO-1 followed by western blot analyses with antibodies for Tubedown, suggesting that ZO-1 and Tubedown do not form a complex within RF/6A endothelial cells.

Immunoprecipitations were also carried out using ZO-1 (1A12) antibody followed by western blot analyses with ZO-1 (R40.76) antibody and Narg1 (Tubedown) antibody to further detect possible Tubedown and ZO-1 interactions (results not shown). No detection of Tubedown and ZO-1 binding could be detected by immunoprecipitations followed by western blot analyses.

Testing potential ZO-1 redistribution in Tubedown knockdowns to elucidate Tubedown's role in the regulation of ocular endothelial permeability.

3.7 Analysis of ZO-1 Distribution in Tubedown Knockdowns

To determine if Tubedown suppression affects ZO-1 expression and distribution within the cell, transient knockdowns of Tubedown were performed in RF/6A endothelial cells. Transient Tubedown knockdowns were prepared by electroporation of 10-20 nM Tubedown siRNA. Co-transfection of green fluorescent protein (GFP) was used to monitor transfection efficiency. Transient transfection controls were 10-20 nM control siRNA with GFP, GFP only, and non-transfected. The different transfections were conducted in 3 separate experiments. Transfection efficiencies of GFP expressions were calculated for each experiment [Fig. 3.11]. Figure 3.11 shows all samples were efficiently transfected to a similar percentage (40-50%).

Western blot analyses using Narg1 (Tubedown) antibody (Fig. 3.12, top panel) and Tubulin antibody (Fig. 3.12, bottom panel) were completed on WCL of transfected cells to detect percentage of Tubedown suppressed [Fig. 3.12]. Densitometric analyses were completed on western blots of Tubedown and Tubulin from separate transfection experiments revealing a ~90 % decrease in Tubedown expression when compared to GFP only transfected cells ($p < 0.05$, ANOVA) [Fig. 3.13] (Paradis et al, 2002; 2008).

To determine if Tubedown suppression affects ZO-1 expression, western blot analyses were conducted with ZO-1 (R40.76) antibody on WCL from transient and stable knockdowns of Tubedown [Fig. 3.14]. WCL from RF/6A endothelial cells transiently transfected with 20 nM Tubedown siRNA or control siRNA were used for ZO-1 protein

concentration analysis because 20 nM Tubedown siRNA had a slightly higher efficiency to knockdown Tubedown expression 72 hours post transfection [Fig. 3.14]. Western blot analyses with Tubulin antibody were used as loading control. Densitometric analyses were completed on triplicate western blots of ZO-1 and Tubulin from separate transfection experiments, which show no significant changes in ZO-1 level of expression in correlation with Tubedown suppression ($p < 0.05$, ANOVA) [Fig. 3.15, Fig. 3.16].

To detect if suppression of Tubedown affects ZO-1 distribution within a cell transient knockdowns of Tubedown were fluorescently stained with ZO-1 (R40.76) antibody followed by rhodamine red anti-mouse antibody. A stable knockdown clone of Tubedown was used as a positive control for comparison to transient assays. Cells were mounted with medium containing DAPI to view nucleus of cell [Fig. 3.17]. Quantitation of ZO-1 at the cell perimeter revealed a ~50 % decreased in ZO-1 perimeter expression in a stable knockdown of Tubedown (*ASTB#20*). Additionally, a ~40 % decreased in ZO-1 perimeter expression in control siRNA transfected cells when compared to parental RF/6A ($p < 0.05$, ANOVA) [Fig. 3.18].

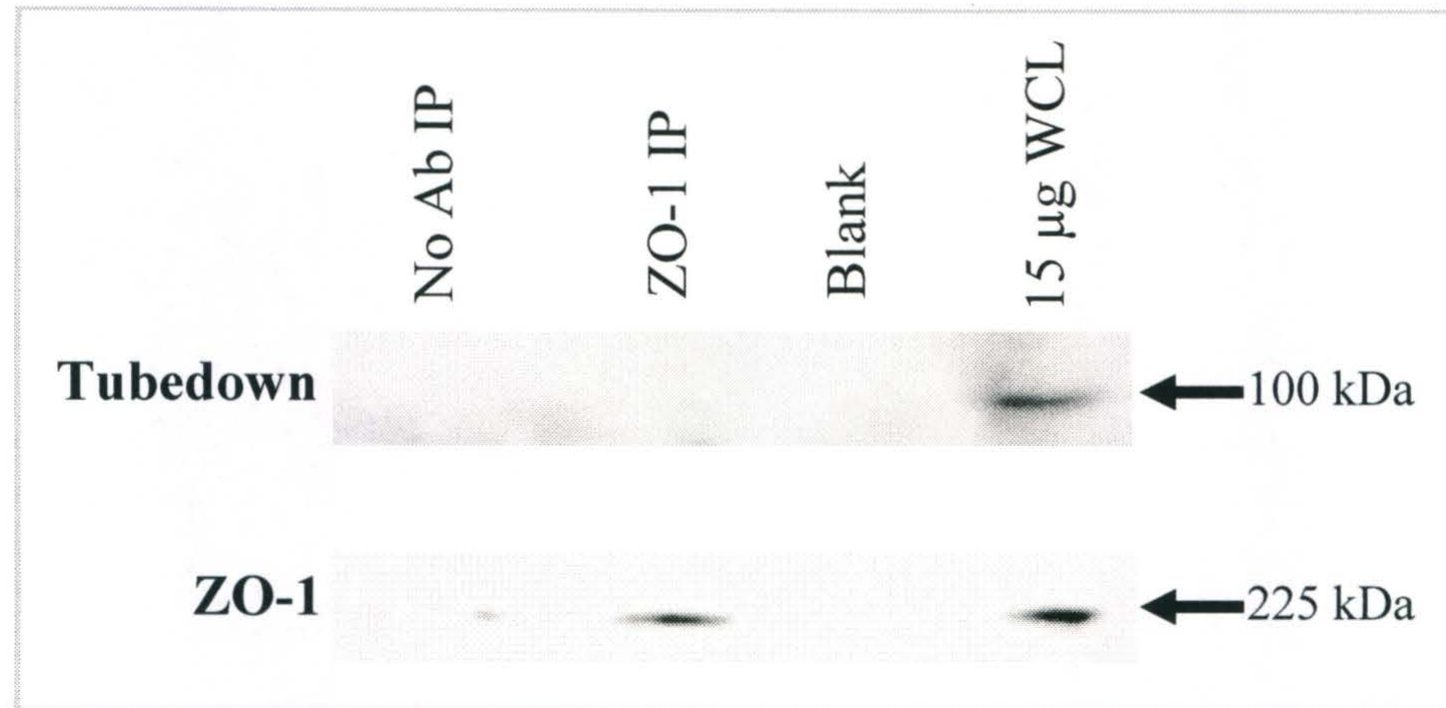


Figure 3. 10 ZO-1 and Tubedown: Western Blot Analyses of ZO-1 Immunoprecipitation. Immunoprecipitations (IP) were performed from RF/6A endothelial cell extracts using ZO-1 antibody (ZO-1 IP) or no antibody (No Ab) control. 15µg of WCL was used for protein amount comparison. Western blot analyses of immunoprecipitations were completed using ZO-1 antibody and Narg1 (Tubedown) antibody. Tubedown and ZO-1 are indicated with arrows at 100 kDa and 225 kDa, respectively. An empty lane (blank) was left in between immunoprecipitations and WCL lanes to detect possible run-over of lanes when loading gel. Tubedown is not co-immunoprecipitating with ZO-1 suggesting no interaction between the ZO-1 and Tubedown. Representative results are shown (Experiments completed = 3).

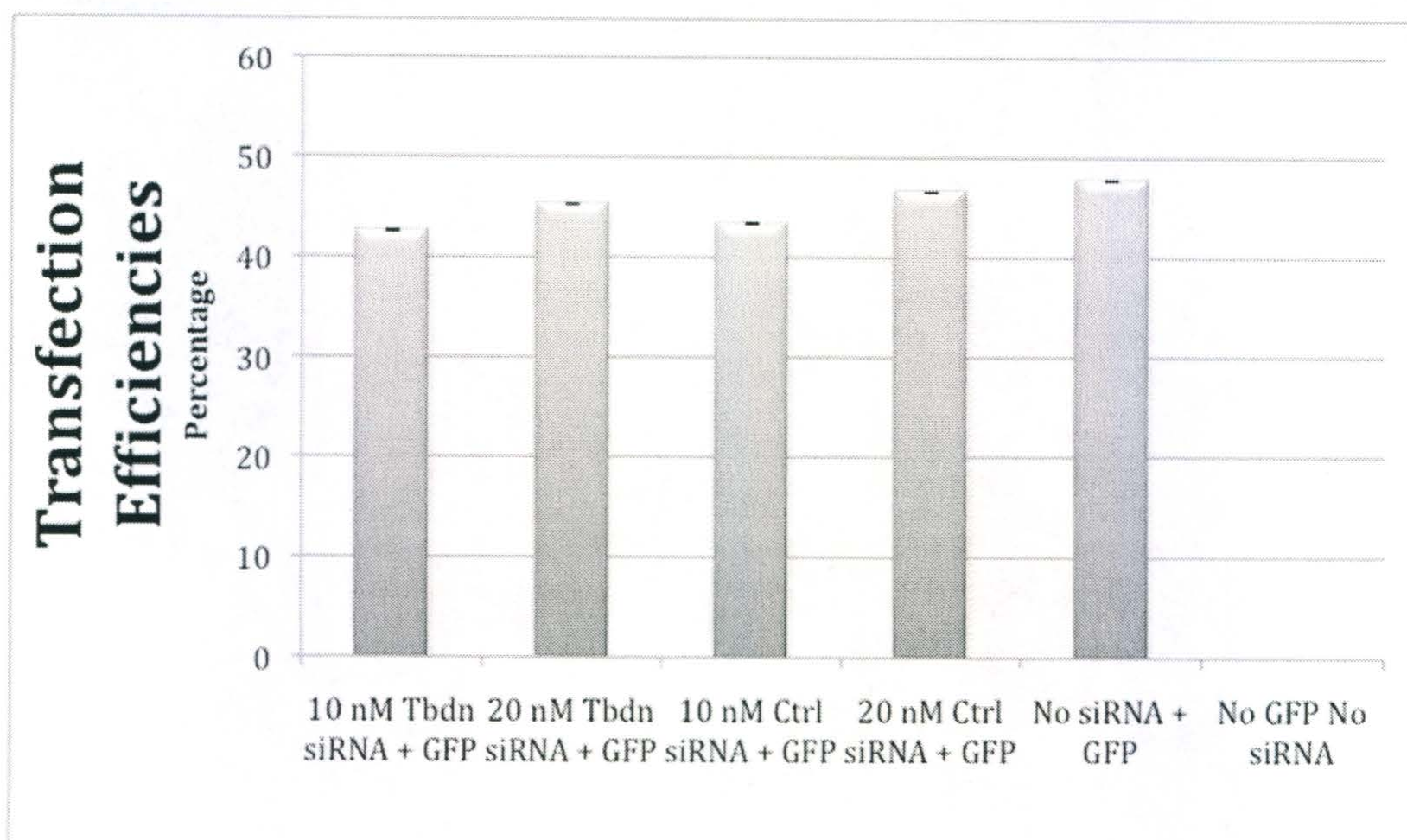


Figure 3. 11 GFP Transfection Efficiencies in Transiently Transfected RF/6A Endothelial Cells. To determine the efficiencies of transient transfections, GFP expression was quantitated through cell count. The chart represents the average transfection efficiency of the 3 experiments with error bars representing +/- standard error (SEM) ($p < 0.05$, ANOVA). Bars represent the percentage of cells that expressed GFP over total number of cells within a 20 mm x 20 mm field (Experiments completed = 3).

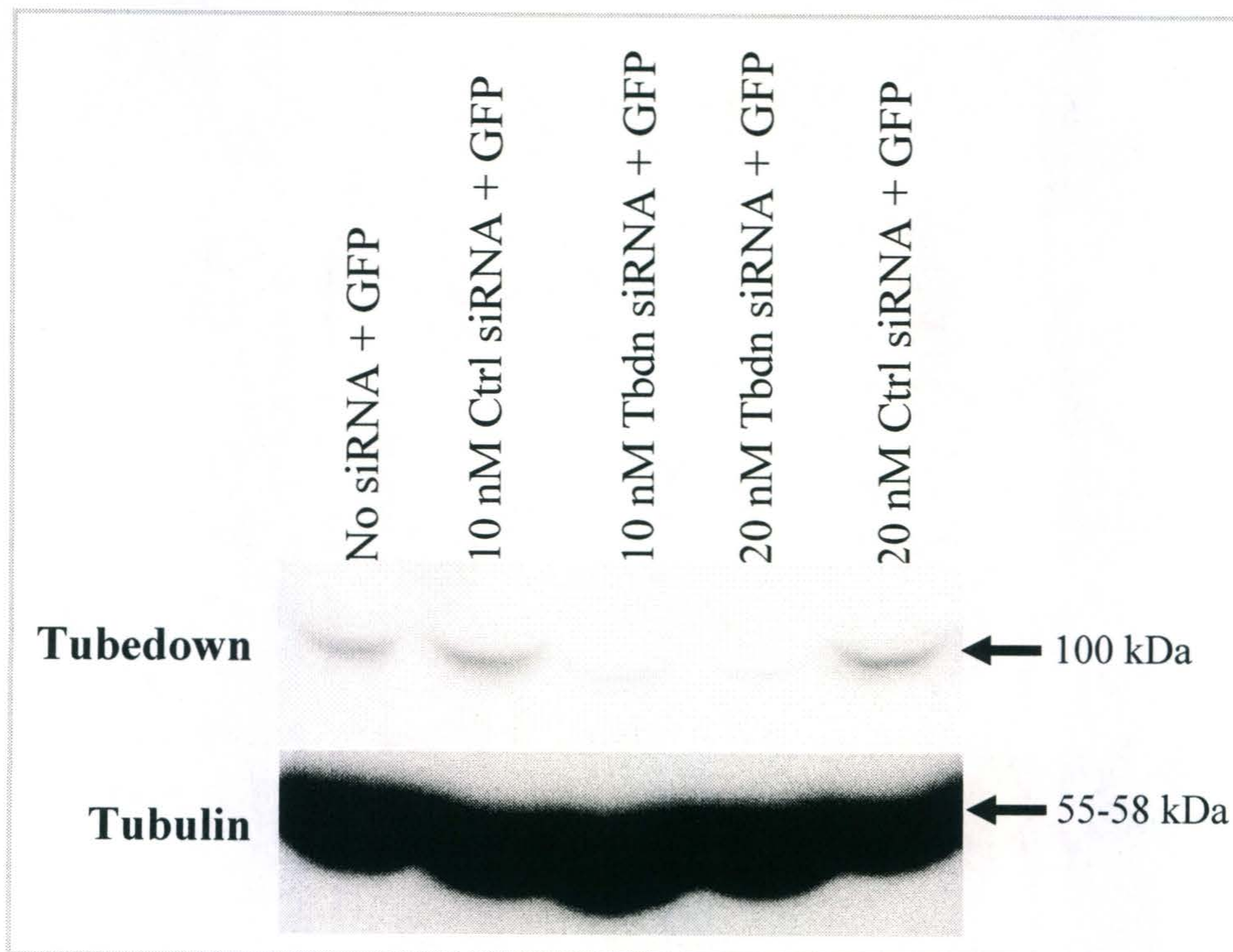


Figure 3. 12 Tubedown and Tubulin: Western Blot Analyses of WCL from Transient Tubedown Knockdowns. Western blot analyses were performed on 75 μ g WCL from triplicate transient transfections of RF/6A endothelial cells. RF/6A endothelial cells were transfected with 10 or 20 nM Tubedown siRNA and GFP (Tbdn siRNA + GFP), 10 or 20 nM control siRNA and GFP (Ctrl siRNA + GFP), and GFP alone (No siRNA + GFP). Western blot analyses were conducted using Narg1 (Tubedown) antibody and Tubulin antibody. Tubedown and Tubulin are indicated with arrows at 100 kDa and 55-58 kDa, respectively. Representative results are shown (Experiments completed = 3).

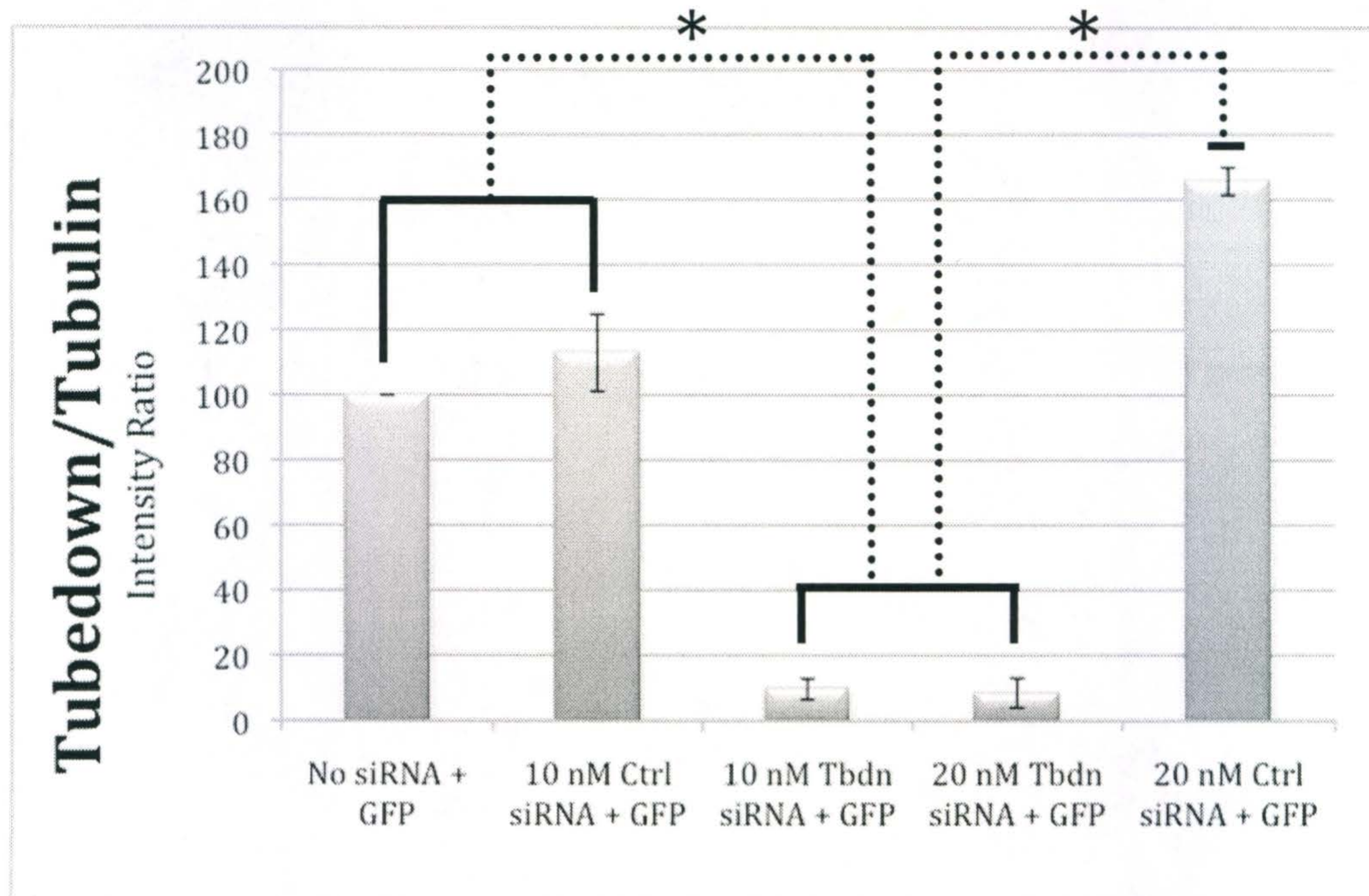


Figure 3. 13 Quantitative Analysis: Tubedown Expression in Transient Tubedown Knockdowns. Densitometric analyses were completed on Tubedown and Tubulin western blots of WCL from triplicate transfections of RF/6A endothelial cells for which a representative is shown in Figure 3.12. RF/6A endothelial cells were transiently transfected with 10 or 20 nM control siRNA with GFP (Ctrl siRNA + GFP), 10 or 20 nM Tubedown siRNA with GFP (Tbdn siRNA + GFP), and GFP alone (No siRNA + GFP). The histogram represents the averages of each of the 3 transfections. Bars represent densitometric analyses of Tubedown over Tubulin band intensities with error bars representing +/- SEM. Significant differences are designated with * ($p < 0.05$, ANOVA).

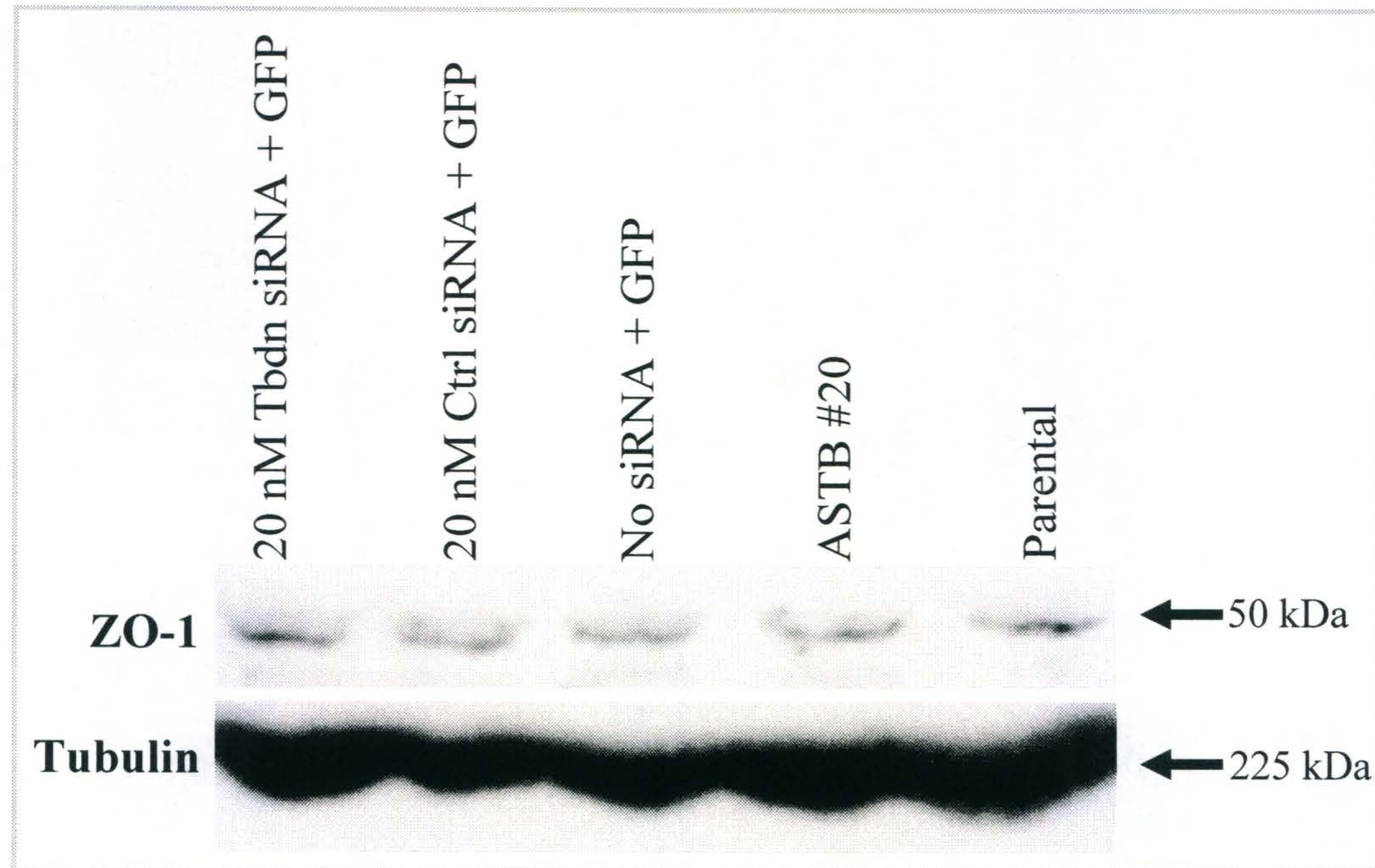


Figure 3. 14 ZO-1 and Tubulin: Western Blot Analyses of WCL from Stable and Transient Tubedown Knockdowns. Western blot analyses were performed on 70 μ g WCL from stable and transient knockdowns of Tubedown in RF/6A endothelial cells. RF/6A endothelial cells were transfected with 20 nM Tubedown siRNA and GFP (Tbdn siRNA + GFP), 20 nM control siRNA and GFP (Ctrl siRNA + GFP), and GFP alone (No siRNA + GFP). *ASTB* clone 20 (*ASTB#20*) was used to detect ZO-1 expression in a stable knockdown of Tubedown. Parental RF/6A endothelial cells without transfection were used for protein amount comparison. Western blot analyses were conducted using ZO-1 and Tubulin antibodies (top and bottom panels, respectively). Tubulin and ZO-1 are indicated with arrows at 55-58 kDa and 225 kDa, respectively. Representative results are shown (Experiments completed = 3).

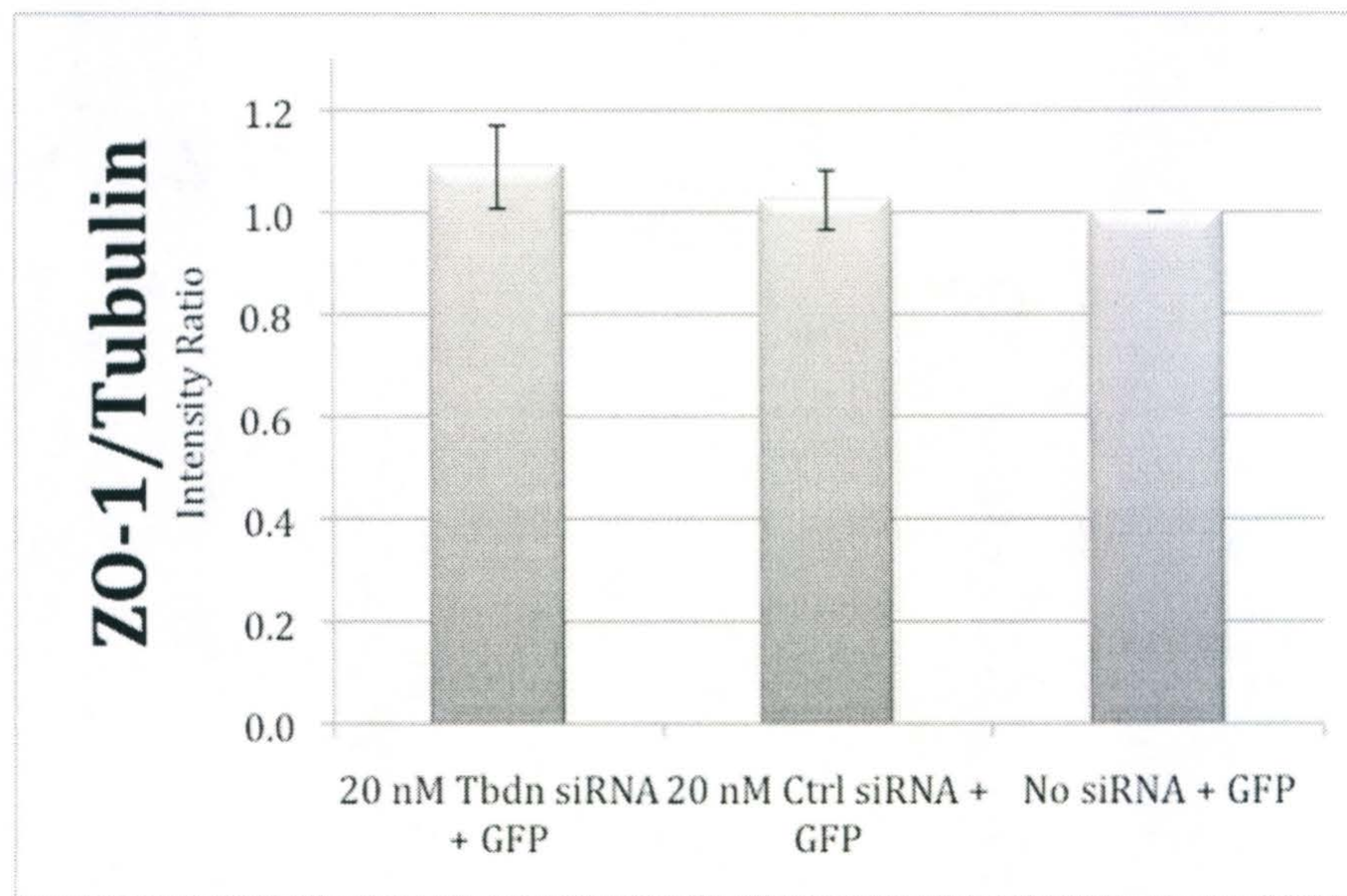


Figure 3. 15 Quantitative Analysis: ZO-1 Expression in Transient Tubedown Knockdowns. Densitometric analyses were completed on ZO-1 and Tubulin western blots of WCL from triplicate transfections of RF/6A endothelial cells. RF/6A endothelial cells were transfected with 20 nM control siRNA with GFP (Ctrl siRNA + GFP), 20 nM Tubedown siRNA with GFP (Tbdn siRNA + GFP), and GFP alone (+ GFP) (Left histogram). Transiently transfected cells were compared to cells transfected with GFP alone. The histogram represents the averages of triplicate experiments. Bars represent densitometric analyses of ZO-1 over Tubulin band intensities with error bars representing +/- SEM for each sample ($p < 0.05$, ANOVA). No significant difference in ZO-1 expression was detected within transiently transfected RF/6A endothelial cells when compared to GFP transient knockdowns of Tubedown.

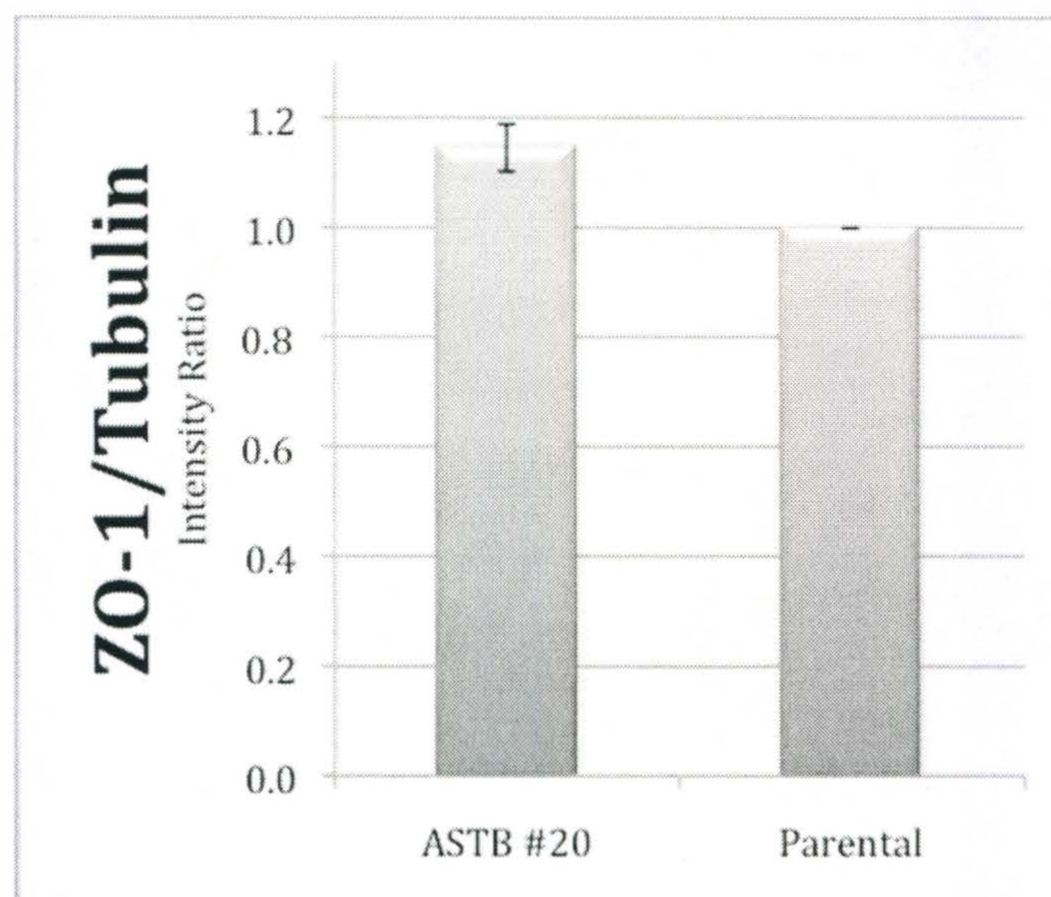


Figure 3. 16 Quantitative Analysis: ZO-1 Expression in a Stable Tubedown Knockdown Clone. Densitometric analyses were completed on ZO-1 and Tubulin western blots of WCL from triplicate transfections of RF/6A endothelial cells. RF/6A endothelial cells were transfected with 20 nM control siRNA with GFP (Ctrl siRNA + GFP), 20 nM Tubedown siRNA with GFP (Tbdn siRNA + GFP), and GFP alone (+ GFP) (Left histogram). Transiently transfected cells were compared to cells transfected with GFP alone. The histogram represents the averages of triplicate experiments. Bars represent densitometric analyses of ZO-1 over Tubulin band intensities with error bars representing +/- SEM for each sample ($p < 0.05$, ANOVA). No significant difference in ZO-1 expression was detected within transiently transfected RF/6A endothelial cells when compared to GFP transient knockdowns of Tubedown.

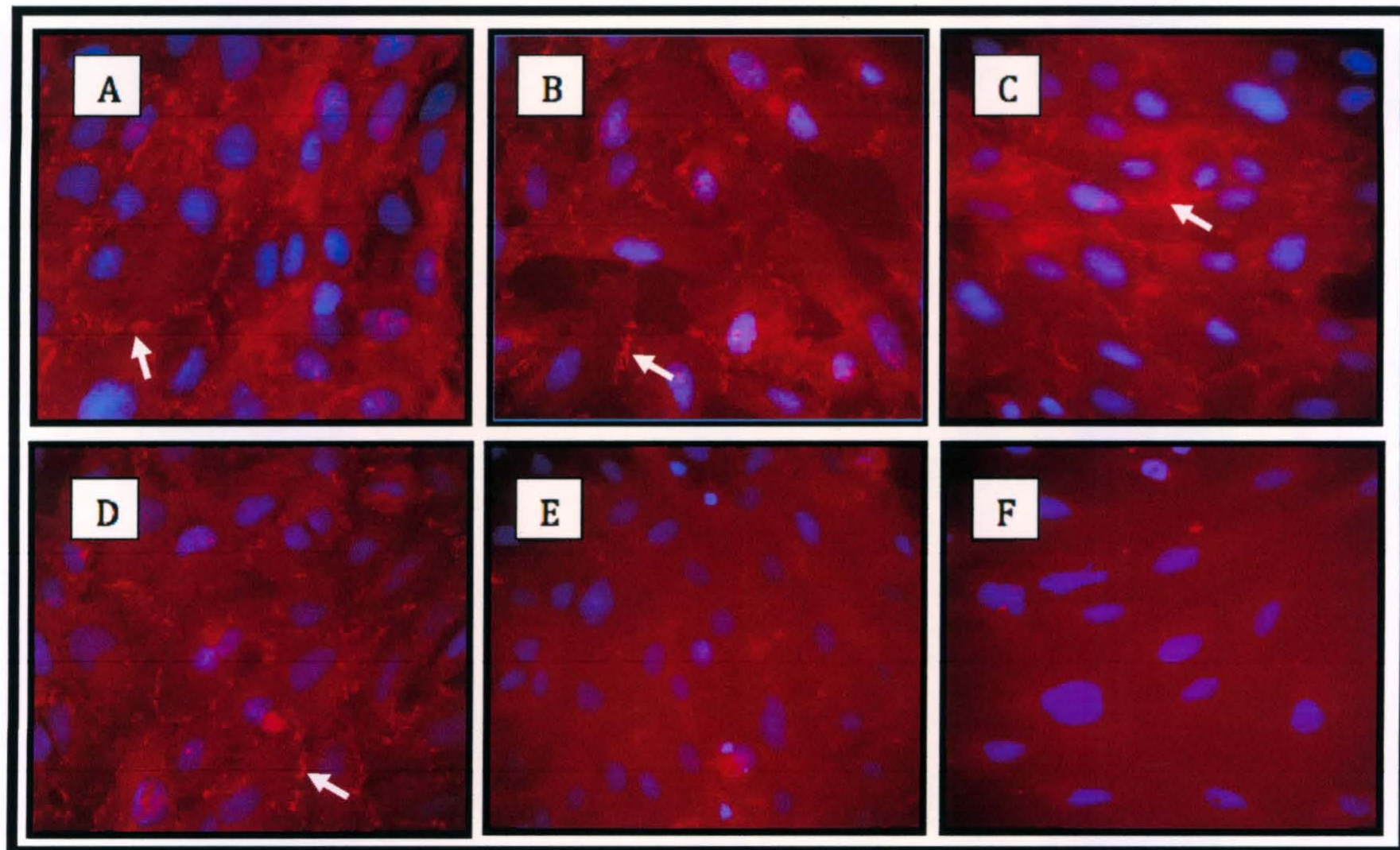


Figure 3. 17 Fluroescent Staining: ZO-1 Distribution in Stable and Transient Tubedown Knockdowns. Fluroescent microscopy analyses on transient or stable knockdowns and corresponding controls are stained for ZO-1 (red) expression pattern. ZO-1 expression distribution is shown in parental RF/6A endothelial cells (A) and a stable Tubedown knockdown clone, *ASTB#20* (B). ZO-1 expression distributrion is also shown in RF/6A endothelial cells transiently transfected with GFP alone (C), 20 nM Tubedown siRNA and GFP (D), or 20 nM control siRNA and GFP (E). RF/6A endothelial cells were also stained using the IgG₁ negative control antibody for comparison (F). All images are a merge of ZO-1 (red) staining and nuclear staining with DAPI (blue). Images shown were taken at 40 X magnification with a 110 μ sec exposure. Arrows show ZO-1 perimeter expression. Representative images are shown (experiments completed = 3).

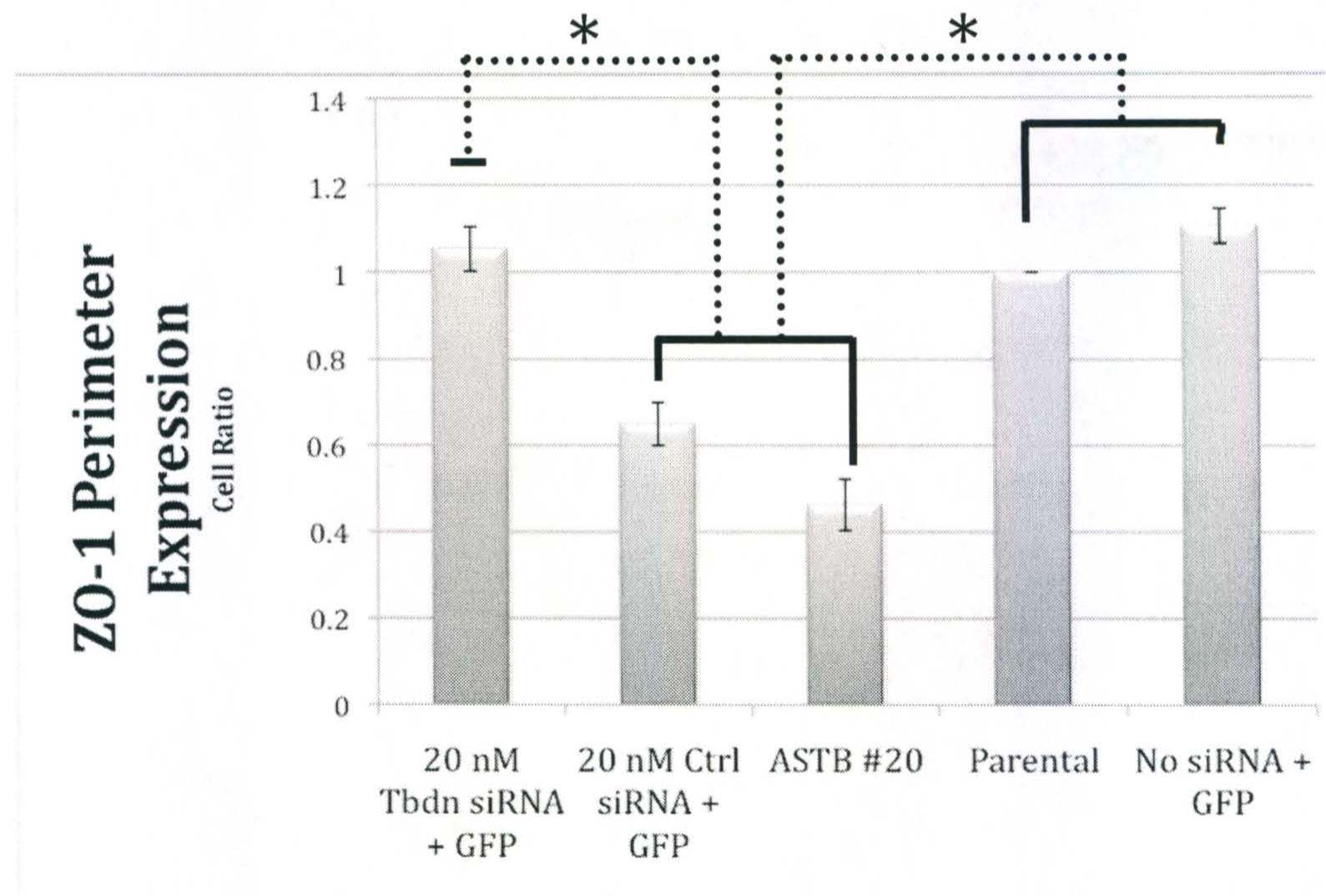


Figure 3. 18 ZO-1 Cell Perimeter Quantitation of Stable and Transient Knockdowns of Tubedown. Fluorescent microscopy analyses on transient and stable knockdowns of Tubedown stained with ZO-1 were quantitated. RF/6A endothelial cells were transiently transfected with 20 nM Tubedown siRNA and GFP (Tbdn siRNA), 20 nM control siRNA (Ctrl siRNA), and GFP alone (No siRNA). Stable knockdown of Tubedown is represented with Tubedown knockdown clone 20 (ASTB#20). Parental RF/6A endothelial cells are used for control (Parental). Quantitation was conducted by counting cells that expressed ZO-1 at the perimeter of the cell where paracellular permeability is regulated. Bars represent the average of three transfections with a minimum of 100 cells counted per bar. Error bars represent +/- SEM of samples. Significant differences are designated with * ($p < 0.05$, ANOVA). ZO-1 perimeter expression is notably decreased in stable knockdowns when compared to parental controls. However, when comparing Tubedown siRNA to control siRNA transfected RF/6A endothelial cells there is a significant difference in ZO-1 perimeter expression. In contrast, comparing Tubedown siRNA to cells only transfected with GFP showed no difference in ZO-1 perimeter expression.

4.0 DISCUSSION

Wet AMD, PDR, and ROP result from abnormal vessel growth within the eye and together they represent the leading causes of blindness in the industrialized world (Konerding, 2004; Sato, 2010). In 2008 there were approximately 50 million blind individuals and three times that amount with some degree of vision loss (Woldeyes and Adamu, 2008). Currently, treatments for neovascular retinopathies are insufficient at eradicating the neovascular progression, do not address the underlying cause of the disease, and cannot adequately repair the resulting damage to the retina (Day et al., 2011; Horster et al., 2011; Kinnunen and Yla-Herttuala, 2012). Defining the mechanisms leading to abnormal neovascularization of eye is a critical step to develop new therapies for neovascular retinopathies.

Drs. Gendron and Paradis' laboratory have identified the Tubedown protein as a key regulator of ocular angiogenesis through regulation of permeability specifically within the retinal-choroidal endothelium (Gendron et al., 2001; Wall et al., 2004; Paradis et al., 2008; Dr. H. Paradis [Memorial University of Newfoundland], personal communication). Furthermore, they have observed a decrease in Tubedown expression in wet AMD, PDR, and ROP correlating to areas of neovascularization seen in patients (Gendron et al., 2001; Gendron et al., 2006; Gendron et al., 2010). Mechanistic investigation to determine how Tubedown regulates the retinal-choroidal endothelial permeability pathways could identify a new target for anti-angiogenic therapeutics, and possibly reveal the underlying pathophysiological cause of neovascular retinopathies. To elucidate Tubedown's involvement in the regulation of permeability, I explored binding

partners for Tubedown with other known protein regulators of the permeability pathways. Investigation of Tubedown interactions with Dynamin, AF-6, Y421-Phospho-Cortactin, c-Src, and ZO-1 were conducted. In addition, I hypothesized that Tubedown may regulate the distribution of ZO-1, a key component of paracellular permeability within endothelial cells.

Dynamin is a known regulator of transcellular permeability. Immunodepletion of Dynamin-2 stops the cinching off of a vesicle at the cell perimeter during endocytosis, essentially abolishing transcytosis in endothelial cells (Cook et al., 1996; Jones et al., 1998). Since stable Tubedown knockdown clones show increased transcellular permeability (Paradis et al, 2008), I speculated that Tubedown might regulate transcellular permeability through an interaction with Dynamin-2. Immunoprecipitation in combination with western blot analyses indicated no interaction between Tubedown and Dynamin-2 within RF/6A or IEM endothelial cells [Fig. 3.2]. These results suggest that Tubedown is not regulating transcytosis through an interaction with Dynamin-2.

Many studies have shown that AF-6 is a regulator of paracellular permeability (Mandai et al., 1997; Yokoyama et al., 2001). AF-6 is required for structural organization of both AJs and TJs in the paracellular permeability pathway (Ikeda et al., 1999; Zhadanov et al., 1999). Stable Tubedown knockdown clones show increased paracellular permeability (Dr. H. Paradis [Memorial University of Newfoundland], personal communication). In addition, immunoprecipitation of Tubedown in combination with mass spectrometry analysis from IEM cells showed ADIP to co-immunoprecipitate with Tubedown, a known binding partner for AF-6 (Dr. H. Paradis

[Memorial University of Newfoundland], personal communication; Fukumoto et al., 2011). Therefore, I hypothesized that Tubedown may regulate paracytosis through an interaction with AF-6. Immunoprecipitation and western blot analyses indicated no interaction between Tubedown and AF-6 in IEM cells [Fig. 3.2]. These results suggest that Tubedown does not regulate paracytosis through an interaction with AF-6.

Our lab has previously concluded that Tubedown interacts with the actin-binding protein Cortactin (Paradis et al., 2008). Cortactin is involved in the regulation of both transcellular and paracellular permeability through its interaction with the actin cytoskeleton (Dudek and Garcia, 2001; Osborn et al., 2006; Zhu et al., 2007). Tubedown's interaction with Cortactin could be the mechanism by which Tubedown regulates paracellular and transcellular permeability in endothelial cells. Phosphorylation of Cortactin has been shown to increase its interaction with the transcellular permeability regulator Caveolin-1 and increase endocytosis overall (Cao et al., 2010). Moreover, multiple studies have shown that increased c-Src kinase activity leads to increased phosphorylation of Cortactin and enhanced transcytosis (Cao et al., 2010; Lambotin et al., 2005; Yang et al., 2006). C-Src phosphorylation of Cortactin is progressive with Y421 being the initial site of tyrosine phosphorylation by c-Src (Huang et al., 1998). I was interested to examine if Tubedown and Cortactin interact when Cortactin is phosphorylated at Y421. Interestingly, no interaction with Tubedown and Y421-Phospho-Cortactin could be detected using immunoprecipitation and western blotting techniques with IEM cells [Fig. 3.4]. Tubedown and Y421-Phospho-Cortactin interactions were investigated in IEM cells because Y421-Phospho-Cortactin has higher

expression levels when compared to RF/6A endothelial cells. As Y421 is believed to be the first tyrosine site phosphorylated on Cortactin, this result suggests that Tubedown does not interact with Cortactin when Y421 is phosphorylated. It is possible that Tubedown binds Cortactin and essentially prevents its tyrosine phosphorylation by either relocation or sequestration of Cortactin keeping it away from kinases like c-Src. Furthermore, Tubedown has been shown to interact with the acetyltransferase Ard1 to mediate acetylation of other proteins (Gendron et al., 2000; Arenesen et al., 2002). In addition, decreased Tubedown expression leads to Ard1 suppression (Paradis et al., 2008). Acetylation has been shown to affect levels of phosphorylation of proteins (Matsuzaki et al., 2005). Acetylation of Cortactin is known to decrease its interaction with actin and subsequently decrease cell migration (Zhang et al., 2009). A second possibility is that Tubedown could regulate transcellular permeability through acetylation of Cortactin subsequently attenuating tyrosine phosphorylation and decreasing transcytosis. This hypothesis is further supported by a recent article by Meiler et al. confirming that acetylation of Cortactin is antagonistic to c-Src tyrosine phosphorylation of Cortactin (Meiler et al., 2012).

C-Src is known to act as a 'switch' in transcellular permeability regulation (Hu and Minshall, 2009). It has been shown to phosphorylate Dynamin, Caveolin-1, and Cortactin, thereby increasing transcellular permeability (Tehrani et al., 2007; Yang et al., 2006; Hu et al., 2008). Previous work in the laboratories of Drs. Paradis and Gendron had suggested that decreased Tubedown expression possibly correlates with an increase in Y416-Phospho-Src (Dr. H Paradis and N. Ho [Memorial University of Newfoundland],

personal communication; Whelan, 2011). Therefore, I hypothesized that Tubedown may interact with c-Src; however, results showed no evidence that Tubedown co-immunoprecipitates with c-Src [Fig. 3.6, Fig. 3.7, Fig 3.8]. Further *in vitro* studies were also conducted to test if Tubedown and c-Src can directly bind. *In vitro* tests showed no direct interaction between Tubedown and c-Src [Fig. 3.9]. These results suggest that Tubedown is not regulating transcellular permeability through an interaction with c-Src within endothelial cells.

ZO-1 has been shown to regulate paracellular permeability in several ways including recruitment of inter-endothelial junctions to the cell perimeter (Ikenouchi et al., 2007; Yamamoto et al., 1997; Umeda et al., 2004; Ebnet et al., 2000; Rimm et al., 1995). I hypothesized that Tubedown may regulate paracellular permeability through an interaction with ZO-1. No interaction between ZO-1 and Tubedown could be detected through immunoprecipitations and western blotting techniques in RF/6A endothelial cells [Fig. 3.10]. These results suggest that Tubedown does not regulate paracytosis through an interaction with ZO-1.

In addition, previous work in the Drs. Paradis and Gendron laboratories had shown stable knockdown clones of Tubedown have decreased ZO-1 expression at the cell perimeter where ZO-1 regulates paracellular permeability (Dr. H. Paradis [Memorial University of Newfoundland], personal communication). The previous work had shown the stable Tubedown knockdown clones did not correlate with a change in ZO-1 overall expression in RF/6A endothelial cells (Dr. H. Paradis [Memorial University of Newfoundland], personal communication), so a change in cellular localization model was

proposed. To further investigate the hypothesis that Tubedown relocates ZO-1 to the cell perimeter a transient Tubedown knockdown protocol was generated. Transfection efficiencies of GFP showed average transfection efficiency (40-50 %). However, siRNA induced knockdown of Tubedown showed a 90 % decrease in Tubedown expression suggesting a transfection efficiency of at least 90 % [Fig. 3.13]. The low GFP transfection efficiencies could be caused by the fact that GFP transfections were completed with super-coiled doubled stranded plasmid. However, transient Tubedown knockdowns were completed with siRNA's. Therefore, the methods of transfection are different.

Transient and stable knockdowns of Tubedown did not correlate with a change of expression for ZO-1 by western blotting techniques [Fig. 3.15, Fig. 3.16]. To test if Tubedown relocates ZO-1 to the cell perimeter, endothelial cells with stable and transient knockdowns of Tubedown were immunofluorescently stained for ZO-1. Oddly, control siRNA transfections showed a significant decrease of ZO-1 expression at the cell membrane when compared to Tubedown siRNA transfections. This could possibly be caused by other protein knockdowns. The control siRNA (SC47) was purchased in 2007, and at the time its sequence had no significant matches when analyzed with BLAST alignment tools, suggesting it would not affect other proteins. In 2012, there are over 100 matches for homology with the control siRNA target sequence. The BLAST algorithm now shows 3 protein homologies with an E-value of 4.4 and 25 protein homologies with an E-value of 16 for the control siRNA target sequence within the rhesus macaque genome. Two of the top five matches of the query BLAST were known genes: G-

coupled purinergic receptor 12 (P2RY12) and metalloproteinase 20 (MMP20) proteins. Using Ensembl genome browser and the Sequencher program the control siRNA SC47 showed homology within exon regions of these genes suggesting potential protein knockdown. Purinergic receptors have been shown to decrease paracellular permeability in human cervical cells by increasing tight junctional resistance (Gorodeski et al., 1998). While no work on P2RY12's effect on ZO-1 expression distribution has been published it is possible that knockdown of P2RY12 could result in change of paracellular resistance affecting ZO-1 expression distribution. The matrix metalloproteinase family (MMP) of proteins are zinc-dependent endopeptidases that degrade extracellular matrix proteins. MMPs have been known to affect paracellular permeability in multiple ways. For example, MMP13 has been shown to enhance permeability of endothelial cells by degrading the extracellular matrix (Lu et al., 2009), and MMP9 can cleave occludin leading to increased endothelial permeability (Xu et al., 2012). Furthermore, MMPs are known to aid in angiogenesis (Witmer et al., 2003). Again, while no work on MMP20's effect on ZO-1 expression distribution has been published it is possible that knockdown of MMP20 would cause decreased ZO-1 perimeter expression. The control siRNA target sequence had a 12 nucleotide homology with both P2RY12 and MMP20 [Fig 4.1 & 4.2]. According to Jackson et al. only an 11 nucleotide homology region is necessary to cause knockdown (Jackson et al., 2003). Thus, the decreased ZO-1 perimeter expression seen in control siRNA is possibly due to multiple protein knockdowns. Therefore, transient knockdowns of Tubedown were compared to RF/6A endothelial cells only transfected with GFP and not control siRNA transient transfections.

```

GENE ID: 703188 MMP20 | matrix metalloproteinase 20 [Macaca mulatta]
(10 or fewer PubMed links)

Score = 24.3 bits (12), Expect = 16
Identities = 12/12 (100%), Gaps = 0/12 (0%)
Strand=Plus/Minus

Query 3      TCCGTTTCATCGT 14
           |||
Sbjct 1268   TCCGTTTCATCGT 1257

```

Figure 4. 1 BLAST Analysis of Control siRNA and MMP20 Homology. Using the BLAST algorithm I found the *MMP20* gene to have homology with our control siRNA (SC47) target construct. Using Ensembl I found the exon regions of *MMP20* and input the data into Sequencher. Sequencher predicts the control siRNA sequence to align with areas of exon 8 and 9 in *MMP20*.

```

GENE ID: 710036 P2RY12 | purinergic receptor P2Y, G-protein coupled, 12
[Macaca mulatta]

Score = 24.3 bits (12), Expect = 16
Identities = 12/12 (100%), Gaps = 0/12 (0%)
Strand=Plus/Plus

Query 1      GATCCGTTTCATC 12
           |||
Sbjct 1180   GATCCGTTTCATC 1191

```

Figure 4. 2 BLAST Analysis of Control siRNA and P2RY12 Homology. Using the BLAST algorithm I found the *P2RY12* gene to have homology with our control siRNA (SC47) target construct. Using Ensembl I found the exon regions of *P2RY12* and input the data into Sequencher. Sequencher predicts the control siRNA sequence to align with an area of exon 3 in *P2RY12*.

Immunofluorescence of ZO-1 in a stable Tubedown knockdown clone (*ASTB*) was used as a positive control, as per previous observations we continued to see decreased ZO-1 expression at the cell perimeter (Dr. H Paradis [Memorial University of Newfoundland], personal communication). However, transient knockdowns of Tubedown (Tbdn siRNA) when compared to GFP transfected RF/6A endothelial cells show no significant differences in ZO-1 perimeter expression [Fig. 3.17]. It is possible that Tubedown affects ZO-1 perimeter distribution overtime, and the 72 hour culture of transient transfections showed no significant difference in ZO-1 distribution because of decreased culture times when compared to stable knockdowns of Tubedown. Maximal decreased Tubedown expression and tight junction formation is observed after 72 hours (Arenesen et al., 2009). However, a limitation to the transient transfection experiments was that Tubedown's effect on ZO-1 perimeter distribution was not observed at 24 or 48 hours. Therefore, the window in which the transient transfection had the highest effect on Tubedown expression and cell-cell contacts were formed may not have been at the time in which the cells were harvested. Furthermore, transient transfection GFP expression and ZO-1 perimeter expression were completed separately. Thus, quantitation of ZO-1 perimeter expression and Tubedown expression were not completed simultaneously, and therefore cell counting of ZO-1 perimeter quantitation may not have been completed on cells that were efficiently knockdown for Tubedown. It must be noted that *ASTB* #20 may be causing multiple protein knockdowns and therefore another protein is causing the relocation of ZO-1 in the stable knockdown clones of Tubedown. Experiments on Tubedown's effect on ZO-1 perimeter expression were exhausted with

materials readily available in the laboratory although no clear conclusion can yet be drawn on whether or not Tubedown exerts an effect on ZO-1 perimeter expression. Additional control siRNA's would need to be designed, and use of multiple knockdown clones of Tubedown would need to be used to conclude if Tubedown does or does not have an effect on ZO-1 distribution within the cell. Also, when completing ZO-1 perimeter quantitation from transient transfections cells should have also been stained for Tubedown expression to determine if cells are efficiently knockdown for Tubedown. Furthermore, re-expression of Tubedown in stable knockdown clones should be completed to observe if ZO-1 perimeter expression is increased with increased Tubedown expression.

The results presented here lead me refute the hypothesis that Tubedown is regulating paracellular permeability through an interaction with AF-6 or ZO-1, or that Tubedown is regulating the transcellular permeability through an interaction with Dynamin-2 or c-Src. Furthermore, Tubedown's effect on ZO-1 perimeter expression is inconclusive. Tubedown in conjunction with Ard1 could possibly be inducing acetylation of Cortactin thereby decreasing its tyrosine phosphorylation aiding in the down regulation of the permeability within the retinal-choroidal endothelium. Tyrosine phosphorylation of Cortactin causes an increase in transcellular permeability (Cao et al, 2010; Lambotin et al., 2005; Yang et al., 2006). Tyrosine phosphorylation on Cortactin is antagonistic to its acetylation (Zhang et al., 2009). C-Src is known to bind and tyrosine phosphorylate Cortactin (Okamura & Resh, 1995). C-Src and Tubedown could be causing a shift in post translation modification balance of Cortactin by inducing

tyrosine phosphorylation and acetylation of Cortactin to regulate transcellular permeability, respectively. Evidence shows that c-Src tyrosine phosphorylates Cortactin to increase transcellular permeability (Cao et al, 2010; Lambotin et al., 2005; Yang et al., 2006), and I speculate Tubedown is acetylating Cortactin thereby attenuating tyrosine phosphorylation and decreasing transcellular permeability [Fig. 4.3].

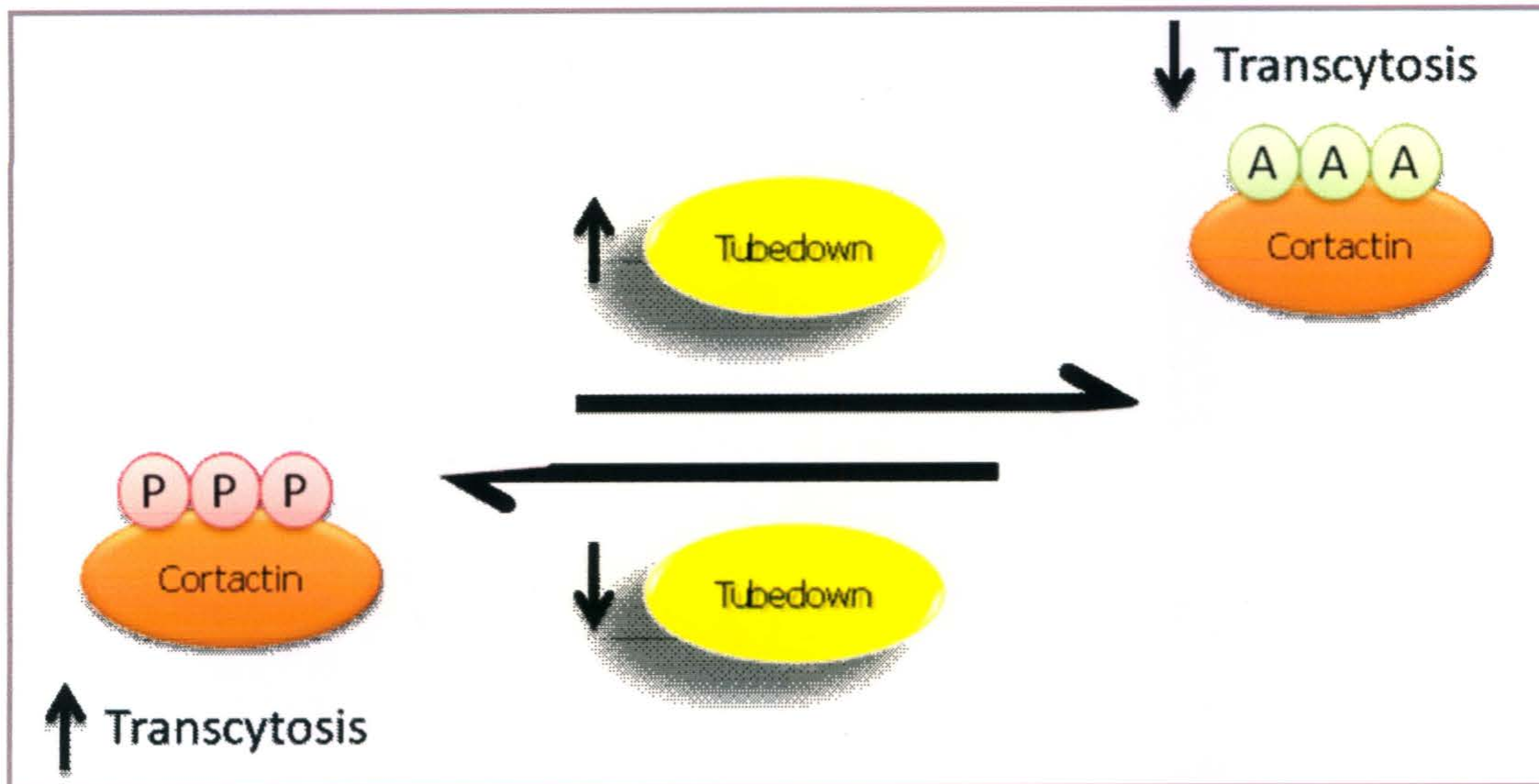


Figure 4. 3 Hypothesized Mechanism for Tubedown's Regulation of Transcytosis. Tubedown is known to decrease transcellular permeability and specifically interacts with non-phosphorylated Cortactin (Paradis et al., 2008). Cortactin tyrosine phosphorylation increases transcellular permeability, and its acetylation is antagonistic to its tyrosine phosphorylation (Cao et al., 202; Meiler et al., 2012). Tubedown may be inducing acetylation of Cortactin, thereby decreasing its tyrosine phosphorylation and attenuating transcytosis.

Tyrosine phosphorylation has been shown to increase both transcellular and paracellular permeability (Staddon et al., 1995; Andriopoulou et al., 1999; Huber et al., 2001). Acetylation has been shown to affect the tyrosine phosphorylation status of proteins (Meiler et al., 2012). I speculate that Tubedown influences acetylation of other regulators of the permeability pathways attenuating tyrosine phosphorylation to decrease permeability. However, this model remains to be explored. While AF-6, ZO-1, and Dynamin are not co-immunoprecipitating with Tubedown it is possible that Tubedown is acetylating these proteins through its interaction with Ard1. ZO-1, Dynamin-2, VE-cadherin, and Occludin are all examples of proteins that can be tyrosine phosphorylated resulting in increased permeability (Rao et al., 2002; Cao et al., 2010). While Tubedown may not directly bind these proteins, it may be inducing their acetylation through its interaction with Ard1 and thereby decreasing their tyrosine phosphorylation. No work has yet been published on whether ZO-1, Dynamin-1, VE-cadherin, or Occludin can be acetylated. Further work to prove Tubedown-Ard1 can induce acetylation of these proteins could be assayed to test the hypothesis that Tubedown is inducing acetylation of permeability regulators while attenuating tyrosine phosphorylation. In addition, assessment of the tyrosine phosphorylation of permeability regulators in Tubedown knockdowns compared to parental cells could be completed to determine if Tubedown is attenuating their phosphorylation state.

Tubedown's mechanism of action in the regulation of permeability pathways within retinal-choroidal endothelial cells still requires further study. In this study, I have been able to exclude possible interactions of Tubedown with Dynamin, AF-6, Y421-

Phospho-Cortactin, c-Src, and ZO-1 within endothelial cell lines. I have provided evidence that Tubedown may regulate transcellular permeability by attenuating Cortactin phosphorylation within endothelial cells. In addition, Tubedown's affect on ZO-1 perimeter expression still remains inconclusive.

5.0 SUMMARY

The cumulative results of the protein interaction investigation suggest the role Tubedown has in regulating permeability pathways within retinal-choroidal endothelial cells does not likely involve interactions between Tubedown and Dynamin, AF-6, c-Src, or ZO-1. The specific interaction of Tubedown with non-phosphorylated Cortactin but not Y421-Phospho-Cortactin suggests that Tubedown may attenuate phosphorylation of Cortactin and subsequently decrease transcytosis.

Stable knockdowns of Tubedown continued to show decreased expression of the paracellular permeability regulator ZO-1 at the cell perimeter. Transiently transfected Tubedown knockdowns suggest no significant difference in ZO-1 perimeter expression. However, the interpretations of knockdowns experiments are in question because of lack of specificity with controls. Therefore, no conclusion can be drawn on Tubedown's effect on ZO-1 perimeter expression.

6.0 REFERENCES

- Age-Related Eye Disease Study Research Group. (2001). A randomized, placebo-controlled, clinical trial of high-dose supplementation with vitamins C and E, beta carotene, and zinc for age-related macular degeneration and vision loss: AREDS report no. 8. *Arch. Ophthalmol.* *119*, 1417-1436.
- Allan, R.K., and Ratajczak, T. (2011). Versatile TPR domains accommodate different modes of target protein recognition and function. *Cell Stress Chaperones* *16*, 353-367.
- Altschul, S.F., Gish, W., Miller, W., Myers, E.W., and Lipman, D.J. (1990). Basic local alignment search tool. *J. Mol. Biol.* *215*, 403-410.
- Arnesen, T., Anderson, D., Baldersheim, C., Lanotte, M., Varhaug, J.E., and Lillehaug, J.R. (2005). Identification and characterization of the human ARD1-NATH protein acetyltransferase complex. *Biochem. J.* *386*, 433-443.
- Arnesen, T., Gromyko, D., Kagabo, D., Betts, M.J., Starheim, K.K., Varhaug, J.E., Anderson, D., and Lillehaug, J.R. (2009). A novel human NatA Nalpha-terminal acetyltransferase complex: hNaa16p-hNaa10p (hNat2-hArd1). *BMC Biochem.* *10*, 15.
- Arnesen, T., Van Damme, P., Polevoda, B., Helsen, K., Evjenth, R., Colaert, N., Varhaug, J.E., Vandekerckhove, J., Lillehaug, J.R., Sherman, F., and Gevaert, K. (2009). Proteomics analyses reveal the evolutionary conservation and divergence of N-terminal acetyltransferases from yeast and humans. *Proc. Natl. Acad. Sci. U. S. A.* *106*, 8157-8162.
- Andriopoulou, P., Navarro, P., Zanetti, A., Lampugnani, M.G., and Dejana, E. (1999). Histamine induces tyrosine phosphorylation of endothelial cell-to-cell adherens junctions. *Arterioscler. Thromb. Vasc. Biol.* *19*, 2286-2297.
- Asaumi, M., Iijima, K., Sumioka, A., Iijima-Ando, K., Kirino, Y., Nakaya, T., and Suzuki, T. (2005). Interaction of N-terminal acetyltransferase with the cytoplasmic domain of beta-amyloid precursor protein and its effect on A beta secretion. *J. Biochem.* *137*, 147-155.
- Bayes, M., Rabasseda, X., and Prous, J.R. (2002). Gateways to clinical trials. *Methods Find. Exp. Clin. Pharmacol.* *24*, 615-643.
- Bazzoni, G., Martinez-Estrada, O.M., Orsenigo, F., Cordenonsi, M., Citi, S., and Dejana, E. (2000). Interaction of junctional adhesion molecule with the tight junction components ZO-1, cingulin, and occludin. *J. Biol. Chem.* *275*, 20520-20526.

Bressler, N.M. (2009). Antiangiogenic approaches to age-related macular degeneration today. *Ophthalmology* 116, S15-23.

Brinker, A., Scheufler, C., Von Der Mulbe, F., Fleckenstein, B., Herrmann, C., Jung, G., Moarefi, I., and Hartl, F.U. (2002). Ligand discrimination by TPR domains. Relevance and selectivity of EEVD-recognition in Hsp70 x Hop x Hsp90 complexes. *J. Biol. Chem.* 277, 19265-19275.

Cao, H., Chen, J., Krueger, E.W., and McNiven, M.A. (2010). SRC-mediated phosphorylation of dynamin and cortactin regulates the "constitutive" endocytosis of transferrin. *Mol. Cell. Biol.* 30, 781-792.

Chang, L.K., Flaxel, C.J., Lauer, A.K., and Sarraf, D. (2007). RPE tears after pegaptanib treatment in age-related macular degeneration. *Retina* 27, 857-863.

Chan-Ling, T., and Stone, J. (1992). Degeneration of astrocytes in feline retinopathy of prematurity causes failure of the blood-retinal barrier. *Invest. Ophthalmol. Vis. Sci.* 33, 2148-2159.

Chappuis-Flament, S., Wong, E., Hicks, L.D., Kay, C.M., and Gumbiner, B.M. (2001). Multiple cadherin extracellular repeats mediate homophilic binding and adhesion. *J. Cell Biol.* 154, 231-243.

Chiang, A., and Regillo, C.D. (2011). Preferred therapies for neovascular age-related macular degeneration. *Curr. Opin. Ophthalmol.* 22, 199-204.

Cook, T., Mesa, K., and Urrutia, R. (1996). Three dynamin-encoding genes are differentially expressed in developing rat brain. *J. Neurochem.* 67, 927-931.

Cook, T.A., Urrutia, R., and McNiven, M.A. (1994). Identification of dynamin 2, an isoform ubiquitously expressed in rat tissues. *Proc. Natl. Acad. Sci. U. S. A.* 91, 644-648.

Cunha-Vaz, J., Bernardes, R., and Lobo, C. (2010). Blood-retinal barrier. *Eur. J. Ophthalmol.* 21, 3-9.

Cunha-Vaz, J.G. (1976). The blood-retinal barriers. *Doc. Ophthalmol.* 41, 287-327.

Day, S., Acquah, K., Mruthyunjaya, P., Grossman, D.S., Lee, P.P., and Sloan, F.A. (2011). Ocular complications after anti-vascular endothelial growth factor therapy in Medicare patients with age-related macular degeneration. *Am. J. Ophthalmol.* 152, 266-272.

Dejana, E., Orsenigo, F., and Lampugnani, M.G. (2008). The role of adherens junctions and VE-cadherin in the control of vascular permeability. *J. Cell. Sci.* 121, 2115-2122.

Diabetic Retinopathy Clinical Research Network, Elman, M.J., Aiello, L.P., Beck, R.W., Bressler, N.M., Bressler, S.B., Edwards, A.R., Ferris, F.L., 3rd, Friedman, S.M., Glassman, A.R., *et al.* (2010). Randomized trial evaluating ranibizumab plus prompt or deferred laser or triamcinolone plus prompt laser for diabetic macular edema. *Ophthalmology* 117, 1064-1077.e35.

Ditzel, J. (1980). Affinity hypoxia as a pathogenetic factor of microangiopathy with particular reference to diabetic retinopathy. *Acta Endocrinol. Suppl. (Copenh)* 238, 39-55.

Dudek, S.M., and Garcia, J.G. (2001). Cytoskeletal regulation of pulmonary vascular permeability. *J. Appl. Physiol.* 91, 1487-1500.

Durham, J.T., and Herman, I.M. (2011). Microvascular modifications in diabetic retinopathy. *Curr. Diab Rep.* 11, 253-264.

Dvorak, H.F., Brown, L.F., Detmar, M., and Dvorak, A.M. (1995). Vascular permeability factor/vascular endothelial growth factor, microvascular hyperpermeability, and angiogenesis. *Am. J. Pathol.* 146, 1029-1039.

Ebnet, K., Schulz, C.U., Meyer Zu Brickwedde, M.K., Pendl, G.G., and Vestweber, D. (2000). Junctional adhesion molecule interacts with the PDZ domain-containing proteins AF-6 and ZO-1. *J. Biol. Chem.* 275, 27979-27988.

Fischer, S., Clauss, M., Wiesnet, M., Renz, D., Schaper, W., and Karliczek, G.F. (1999). Hypoxia induces permeability in brain microvessel endothelial cells via VEGF and NO. *Am. J. Physiol.* 276, C812-20.

Fukumoto, Y., Kurita, S., Takai, Y., and Ogita, H. (2011). Role of scaffold protein afadin dilute domain-interacting protein (ADIP) in platelet-derived growth factor-induced cell movement by activating Rac protein through Vav2 protein. *J. Biol. Chem.* 286, 43537-43548.

Furuse, M., Itoh, M., Hirase, T., Nagafuchi, A., Yonemura, S., Tsukita, S., and Tsukita, S. (1994). Direct association of occludin with ZO-1 and its possible involvement in the localization of occludin at tight junctions. *J. Cell Biol.* 127, 1617-1626.

Furuse, M., Sasaki, H., and Tsukita, S. (1999). Manner of interaction of heterogeneous claudin species within and between tight junction strands. *J. Cell Biol.* 147, 891-903.

Gendron, R.L., Adams, L.C., and Paradis, H. (2000). Tubedown-1, a novel acetyltransferase associated with blood vessel development. *Dev. Dyn.* 218, 300-315.

Gendron, R.L., Good, W.V., Adams, L.C., and Paradis, H. (2001). Suppressed expression of tubedown-1 in retinal neovascularization of proliferative diabetic retinopathy. *Invest. Ophthalmol. Vis. Sci.* 42, 3000-3007.

Gendron, R.L., Good, W.V., Miskiewicz, E., Tucker, S., Phelps, D.L., and Paradis, H. (2006). Tubedown-1 (Tbdn-1) suppression in oxygen-induced retinopathy and in retinopathy of prematurity. *Mol. Vis.* 12, 108-116.

Gendron, R.L., Laver, N.V., Good, W.V., Grossniklaus, H.E., Miskiewicz, E., Whelan, M.A., Walker, J., and Paradis, H. (2010). Loss of tubedown expression as a contributing factor in the development of age-related retinopathy. *Invest. Ophthalmol. Vis. Sci.* 51, 5267-5277.

Gorodeski, G.I., Hopfer, U., and Jin, W. (1998). Purinergic receptor-induced changes in paracellular resistance across cultures of human cervical cells are mediated by two distinct cytosolic calcium-related mechanisms. *Cell Biochem. Biophys.* 29, 281-306.

Head, J.A., Jiang, D., Li, M., Zorn, L.J., Schaefer, E.M., Parsons, J.T., and Weed, S.A. (2003). Cortactin tyrosine phosphorylation requires Rac1 activity and association with the cortical actin cytoskeleton. *Mol. Biol. Cell* 14, 3216-3229.

Horster, R., Ristau, T., Sadda, S.R., and Liakopoulos, S. (2011). Individual recurrence intervals after anti-VEGF therapy for age-related macular degeneration. *Graefes Arch. Clin. Exp. Ophthalmol.* 249, 645-652.

Hu, G., and Minshall, R.D. (2009). Regulation of transendothelial permeability by Src kinase. *Microvasc. Res.* 77, 21-25.

Hu, G., Place, A.T., and Minshall, R.D. (2008). Regulation of endothelial permeability by Src kinase signaling: vascular leakage versus transcellular transport of drugs and macromolecules. *Chem. Biol. Interact.* 171, 177-189.

Huang, C., Liu, J., Haudenschild, C.C., and Zhan, X. (1998). The role of tyrosine phosphorylation of cortactin in the locomotion of endothelial cells. *J. Biol. Chem.* 273, 25770-25776.

Huber, J.D., Witt, K.A., Hom, S., Egleton, R.D., Mark, K.S., and Davis, T.P. (2001). Inflammatory pain alters blood-brain barrier permeability and tight junctional protein expression. *Am. J. Physiol. Heart Circ. Physiol.* 280, H1241-8.

Ikeda, W., Nakanishi, H., Miyoshi, J., Mandai, K., Ishizaki, H., Tanaka, M., Togawa, A., Takahashi, K., Nishioka, H., Yoshida, H., *et al.* (1999). Afadin: A key molecule essential for structural organization of cell-cell junctions of polarized epithelia during embryogenesis. *J. Cell Biol.* 146, 1117-1132.

Ikenouchi, J., Umeda, K., Tsukita, S., Furuse, M., and Tsukita, S. (2007). Requirement of ZO-1 for the formation of belt-like adherens junctions during epithelial cell polarization. *J. Cell Biol.* *176*, 779-786.

Itoh, M., Furuse, M., Morita, K., Kubota, K., Saitou, M., and Tsukita, S. (1999). Direct binding of three tight junction-associated MAGUKs, ZO-1, ZO-2, and ZO-3, with the COOH termini of claudins. *J. Cell Biol.* *147*, 1351-1363.

Jackson, A.L., Bartz, S.R., Schelter, J., Kobayashi, S.V., Burchard, J., Mao, M., Li, B., Cavet, G., and Linsley, P.S. (2003). Expression profiling reveals off-target gene regulation by RNAi. *Nat. Biotechnol.* *21*, 635-637.

Jacob, C., Yang, P.C., Darmoul, D., Amadesi, S., Saito, T., Cottrell, G.S., Coelho, A.M., Singh, P., Grady, E.F., Perdue, M., and Bunnett, N.W. (2005). Mast cell tryptase controls paracellular permeability of the intestine. Role of protease-activated receptor 2 and beta-arrestins. *J. Biol. Chem.* *280*, 31936-31948.

Jones, S.M., Howell, K.E., Henley, J.R., Cao, H., and McNiven, M.A. (1998). Role of dynamin in the formation of transport vesicles from the trans-Golgi network. *Science* *279*, 573-577.

Kennedy, M.B. (1995). Origin of PDZ (DHR, GLGF) domains. *Trends Biochem. Sci.* *20*, 350.

Kinnunen, K., and Yla-Herttuala, S. (2012). Vascular endothelial growth factors in retinal and choroidal neovascular diseases. *Ann. Med.* *44*, 1-17.

Kolb, H. (1995). Simple Anatomy of the Retina. In *Webvision: The Organization of the Retina and Visual System*, Kolb, H., Fernandez, E. and Nelson, R. eds., (Salt Lake City UT):

Komarova, Y., and Malik, A.B. (2010). Regulation of endothelial permeability via paracellular and transcellular transport pathways. *Annu. Rev. Physiol.* *72*, 463-493.

Konerding, M.A. (2004). Ocular angiogenesis: translating preclinical indications to successful clinical development. *Expert Opin. Ther. Targets* *8*, 255-258.

Lambotin, M., Hoffmann, I., Laran-Chich, M.P., Nassif, X., Couraud, P.O., and Bourdoulous, S. (2005). Invasion of endothelial cells by *Neisseria meningitidis* requires cortactin recruitment by a phosphoinositide-3-kinase/Rac1 signalling pathway triggered by the lipo-oligosaccharide. *J. Cell. Sci.* *118*, 3805-3816.

Littleton, J.T., Chapman, E.R., Kreber, R., Garment, M.B., Carlson, S.D., and Ganetzky, B. (1998). Temperature-sensitive paralytic mutations demonstrate that synaptic exocytosis requires SNARE complex assembly and disassembly. *Neuron* 21, 401-413.

Lopez, P.F., Sippy, B.D., Lambert, H.M., Thach, A.B., and Hinton, D.R. (1996). Transdifferentiated retinal pigment epithelial cells are immunoreactive for vascular endothelial growth factor in surgically excised age-related macular degeneration-related choroidal neovascular membranes. *Invest. Ophthalmol. Vis. Sci.* 37, 855-868.

Low, H.H., and Lowe, J. (2010). Dynamin architecture--from monomer to polymer. *Curr. Opin. Struct. Biol.* 20, 791-798.

Lu, D.Y., Yu, W.H., Yeh, W.L., Tang, C.H., Leung, Y.M., Wong, K.L., Chen, Y.F., Lai, C.H., and Fu, W.M. (2009). Hypoxia-induced matrix metalloproteinase-13 expression in astrocytes enhances permeability of brain endothelial cells. *J. Cell. Physiol.* 220, 163-173.

Lua, B.L., and Low, B.C. (2005). Cortactin phosphorylation as a switch for actin cytoskeletal network and cell dynamics control. *FEBS Lett.* 579, 577-585.

Lydon, N.B., Gay, B., Mett, H., Murray, B., Liebetanz, J., Gutzwiller, A., Piwnicka-Worms, H., Roberts, T.M., and McGlynn, E. (1992). Purification and biochemical characterization of non-myristoylated recombinant pp60c-src kinase. *Biochem. J.* 287 (Pt 3), 985-993.

Maberley, D.A., Hollands, H., Chuo, J., Tam, G., Konkak, J., Roesch, M., Veselinovic, A., Witzigmann, M., and Bassett, K. (2006). The prevalence of low vision and blindness in Canada. *Eye (Lond)* 20, 341-346.

Mandai, K., Nakanishi, H., Satoh, A., Obaishi, H., Wada, M., Nishioka, H., Itoh, M., Mizoguchi, A., Aoki, T., Fujimoto, T., *et al.* (1997). Afadin: A novel actin filament-binding protein with one PDZ domain localized at cadherin-based cell-to-cell adherens junction. *J. Cell Biol.* 139, 517-528.

Martinez-Quiles, N., Ho, H.Y., Kirschner, M.W., Ramesh, N., and Geha, R.S. (2004). Erk/Src phosphorylation of cortactin acts as a switch on-switch off mechanism that controls its ability to activate N-WASP. *Mol. Cell. Biol.* 24, 5269-5280.

Mataftsi, A., Dimitrakos, S.A., and Adams, G.G. (2011). Mediators involved in retinopathy of prematurity and emerging therapeutic targets. *Early Hum. Dev.* 87, 683-690.

- Matsuzaki, H., Daitoku, H., Hatta, M., Aoyama, H., Yoshimochi, K., and Fukamizu, A. (2005). Acetylation of Foxo1 alters its DNA-binding ability and sensitivity to phosphorylation. *Proc. Natl. Acad. Sci. U. S. A.* *102*, 11278-11283.
- Mehta, D., and Malik, A.B. (2006). Signaling mechanisms regulating endothelial permeability. *Physiol. Rev.* *86*, 279-367.
- Meiler, E., Nieto-Pelegrin, E., and Martinez-Quiles, N. (2012). Cortactin tyrosine phosphorylation promotes its deacetylation and inhibits cell spreading. *PLoS One* *7*, e33662.
- Meinzel, T., Peynot, P., and Giglione, C. (2005). Processed N-termini of mature proteins in higher eukaryotes and their major contribution to dynamic proteomics. *Biochimie* *87*, 701-712.
- Meyer, C.H., and Holz, F.G. (2011). Preclinical aspects of anti-VEGF agents for the treatment of wet AMD: ranibizumab and bevacizumab. *Eye (Lond)* *25*, 661-672.
- Min, S.W., Cho, S.H., Zhou, Y., Schroeder, S., Haroutunian, V., Seeley, W.W., Huang, E.J., Shen, Y., Masliah, E., Mukherjee, C., *et al.* (2010). Acetylation of tau inhibits its degradation and contributes to tauopathy. *Neuron* *67*, 953-966.
- Minshall, R.D., Tirupathi, C., Vogel, S.M., and Malik, A.B. (2002). Vesicle formation and trafficking in endothelial cells and regulation of endothelial barrier function. *Histochem. Cell Biol.* *117*, 105-112.
- Mullen, J.R., Kayne, P.S., Moerschell, R.P., Tsunasawa, S., Gribskov, M., Colavito-Shepanski, M., Grunstein, M., Sherman, F., and Sternglanz, R. (1989). Identification and characterization of genes and mutants for an N-terminal acetyltransferase from yeast. *EMBO J.* *8*, 2067-2075.
- Nagy, J.A., Dvorak, A.M., and Dvorak, H.F. (2007). VEGF-A and the induction of pathological angiogenesis. *Annu. Rev. Pathol.* *2*, 251-275.
- Ng, E.W., and Adamis, A.P. (2005). Targeting angiogenesis, the underlying disorder in neovascular age-related macular degeneration. *Can. J. Ophthalmol.* *40*, 352-368.
- Nicolo, M., Ghiglione, D., and Calabria, G. (2006). Retinal pigment epithelial tear following intravitreal injection of bevacizumab (Avastin). *Eur. J. Ophthalmol.* *16*, 770-773.
- Nowak, J.Z. (2006). Age-related macular degeneration (AMD): pathogenesis and therapy. *Pharmacol. Rep.* *58*, 353-363.

Odunuga, O.O., Hornby, J.A., Bies, C., Zimmermann, R., Pugh, D.J., and Blatch, G.L. (2003). Tetratricopeptide repeat motif-mediated Hsc70-mSTI1 interaction. Molecular characterization of the critical contacts for successful binding and specificity. *J. Biol. Chem.* 278, 6896-6904.

Okamura, H., and Resh, M.D. (1995). p80/85 cortactin associates with the Src SH2 domain and colocalizes with v-Src in transformed cells. *J. Biol. Chem.* 270, 26613-26618.

Orozco-Gomez, L.P., Hernandez-Salazar, L., Moguel-Ancheita, S., Ramirez-Moreno, M.A., and Morales-Cruz, M.V. (2011). Laser-ranibizumab treatment for retinopathy of prematurity in umbral-preumbral disease. Three years of experience. *Cir. Cir.* 79, 225-232.

Osborn, E.A., Rabodzey, A., Dewey, C.F., Jr, and Hartwig, J.H. (2006). Endothelial actin cytoskeleton remodeling during mechanostimulation with fluid shear stress. *Am. J. Physiol. Cell. Physiol.* 290, C444-52.

Paradis, H., Islam, T., Tucker, S., Tao, L., Koubi, S., and Gendron, R.L. (2008). Tubedown associates with cortactin and controls permeability of retinal endothelial cells to albumin. *J. Cell. Sci.* 121, 1965-1972.

Paradis, H., Liu, C.Y., Saika, S., Azhar, M., Doetschman, T., Good, W.V., Nayak, R., Laver, N., Kao, C.W., Kao, W.W., and Gendron, R.L. (2002). Tubedown-1 in remodeling of the developing vitreal vasculature in vivo and regulation of capillary outgrowth in vitro. *Dev. Biol.* 249, 140-155.

Park, E.C., and Szostak, J.W. (1992). ARD1 and NAT1 proteins form a complex that has N-terminal acetyltransferase activity. *EMBO J.* 11, 2087-2093.

Pei, Y., and Tuschl, T. (2006). On the art of identifying effective and specific siRNAs. *Nat. Methods* 3, 670-676.

Phelps, D.L. (1995). Retinopathy of prematurity. *Pediatr. Rev.* 16, 50-56.

Polevoda, B., Arnesen, T., and Sherman, F. (2009). A synopsis of eukaryotic Nalpha-terminal acetyltransferases: nomenclature, subunits and substrates. *BMC Proc.* 3 Suppl 6, S2.

Predescu, S.A., Predescu, D.N., and Malik, A.B. (2007). Molecular determinants of endothelial transcytosis and their role in endothelial permeability. *Am. J. Physiol. Lung Cell. Mol. Physiol.* 293, L823-42.

Pruitt, K.D., Tatusova, T., Klimke, W., and Maglott, D.R. (2009). NCBI Reference Sequences: current status, policy and new initiatives. *Nucleic Acids Res.* 37, D32-6.

Pylyshyn, Z.W. (2003). *Seeing and visualizing: it's not what you think* (Cambridge, Mass.: MIT Press).

Rajappa, M., Saxena, P., and Kaur, J. (2010). Ocular angiogenesis: mechanisms and recent advances in therapy. *Adv. Clin. Chem.* 50, 103-121.

Rao, R.K., Basuroy, S., Rao, V.U., Karnaky Jr, K.J., and Gupta, A. (2002). Tyrosine phosphorylation and dissociation of occludin-ZO-1 and E-cadherin-beta-catenin complexes from the cytoskeleton by oxidative stress. *Biochem. J.* 368, 471-481.

Rimm, D.L., Koslov, E.R., Kebriaei, P., Cianci, C.D., and Morrow, J.S. (1995). Alpha 1(E)-catenin is an actin-binding and -bundling protein mediating the attachment of F-actin to the membrane adhesion complex. *Proc. Natl. Acad. Sci. U. S. A.* 92, 8813-8817.

Roberts, J.E. (1995). Visible light induced changes in the immune response through an eye-brain mechanism (photoneuroimmunology). *J. Photochem. Photobiol. B.* 29, 3-15.

Rope, A.F., Wang, K., Evjenth, R., Xing, J., Johnston, J.J., Swensen, J.J., Johnson, W.E., Moore, B., Huff, C.D., Bird, L.M., *et al.* (2011). Using VAAST to identify an X-linked disorder resulting in lethality in male infants due to N-terminal acetyltransferase deficiency. *Am. J. Hum. Genet.* 89, 28-43.

Rosenfeld, P.J., Shapiro, H., Tuomi, L., Webster, M., Elledge, J., Blodi, B., and MARINA and ANCHOR Study Groups. (2011). Characteristics of patients losing vision after 2 years of monthly dosing in the phase III ranibizumab clinical trials. *Ophthalmology* 118, 523-530.

Sato, Y. (2010). Anti-angiogenic drugs. *Nihon Rinsho.* 68, 1825-1829.

Schafer, D.A., Weed, S.A., Binns, D., Karginov, A.V., Parsons, J.T., and Cooper, J.A. (2002). Dynamin2 and cortactin regulate actin assembly and filament organization. *Curr. Biol.* 12, 1852-1857.

Schlessinger, J. (2000). New roles for Src kinases in control of cell survival and angiogenesis. *Cell* 100, 293-296.

Schlingemann, R.O., and van Hinsbergh, V.W. (1997). Role of vascular permeability factor/vascular endothelial growth factor in eye disease. *Br. J. Ophthalmol.* 81, 501-512.

Semeraro, F., Morescalchi, F., Parmeggiani, F., Arcidiacono, B., and Costagliola, C. (2011). Systemic adverse drug reactions secondary to anti-VEGF intravitreal injection in

patients with neovascular age-related macular degeneration. *Curr. Vasc. Pharmacol.* 9, 629-646.

Shajahan, A.N., Tirupathi, C., Smrcka, A.V., Malik, A.B., and Minshall, R.D. (2004). Gbetagamma activation of Src induces caveolae-mediated endocytosis in endothelial cells. *J. Biol. Chem.* 279, 48055-48062.

Shima, C., Sakaguchi, H., Gomi, F., Kamei, M., Ikuno, Y., Oshima, Y., Sawa, M., Tsujikawa, M., Kusaka, S., and Tano, Y. (2008). Complications in patients after intravitreal injection of bevacizumab. *Acta Ophthalmol.* 86, 372-376.

Siliciano, J.D., and Goodenough, D.A. (1988). Localization of the tight junction protein, ZO-1, is modulated by extracellular calcium and cell-cell contact in Madin-Darby canine kidney epithelial cells. *J. Cell Biol.* 107, 2389-2399.

Simo, R., and Hernandez, C. (2008). Intravitreal anti-VEGF for diabetic retinopathy: hopes and fears for a new therapeutic strategy. *Diabetologia* 51, 1574-1580.

Staddon, J.M., Herrenknecht, K., Smales, C., and Rubin, L.L. (1995). Evidence that tyrosine phosphorylation may increase tight junction permeability. *J. Cell. Sci.* 108 (Pt 2), 609-619.

Sugiura, N., Adams, S.M., and Corriveau, R.A. (2003). An evolutionarily conserved N-terminal acetyltransferase complex associated with neuronal development. *J. Biol. Chem.* 278, 40113-40120.

Tehrani, S., Tomasevic, N., Weed, S., Sakowicz, R., and Cooper, J.A. (2007). Src phosphorylation of cortactin enhances actin assembly. *Proc. Natl. Acad. Sci. U. S. A.* 104, 11933-11938.

Umeda, K., Ikenouchi, J., Katahira-Tayama, S., Furuse, K., Sasaki, H., Nakayama, M., Matsui, T., Tsukita, S., Furuse, M., and Tsukita, S. (2006). ZO-1 and ZO-2 independently determine where claudins are polymerized in tight-junction strand formation. *Cell* 126, 741-754.

Umeda, K., Matsui, T., Nakayama, M., Furuse, K., Sasaki, H., Furuse, M., and Tsukita, S. (2004). Establishment and characterization of cultured epithelial cells lacking expression of ZO-1. *J. Biol. Chem.* 279, 44785-44794.

Upton, A., Johnson, N., Sandy, J., and Sim, E. (2001). Arylamine N-acetyltransferases - of mice, men and microorganisms. *Trends Pharmacol. Sci.* 22, 140-146.

- Uruno, T., Liu, J., Zhang, P., Fan, Y., Egile, C., Li, R., Mueller, S.C., and Zhan, X. (2001). Activation of Arp2/3 complex-mediated actin polymerization by cortactin. *Nat. Cell Biol.* 3, 259-266.
- van den Berg, A., Mols, J., and Han, J. (2008). RISC-target interaction: cleavage and translational suppression. *Biochim. Biophys. Acta* 1779, 668-677.
- Vestweber, D., Winderlich, M., Cagna, G., and Nottebaum, A.F. (2009). Cell adhesion dynamics at endothelial junctions: VE-cadherin as a major player. *Trends Cell Biol.* 19, 8-15.
- Vogel, S.M., Minshall, R.D., Pilipovic, M., Tiruppathi, C., and Malik, A.B. (2001). Albumin uptake and transcytosis in endothelial cells in vivo induced by albumin-binding protein. *Am. J. Physiol. Lung Cell. Mol. Physiol.* 281, L1512-22.
- Wall, D.S., Gendron, R.L., Good, W.V., Miskiewicz, E., Woodland, M., Leblanc, K., and Paradis, H. (2004). Conditional knockdown of tubedown-1 in endothelial cells leads to neovascular retinopathy. *Invest. Ophthalmol. Vis. Sci.* 45, 3704-3712.
- Wanek, J., Teng, P.Y., Albers, J., Blair, N.P., and Shahidi, M. (2011). Inner retinal metabolic rate of oxygen by oxygen tension and blood flow imaging in rat. *Biomed. Opt. Express* 2, 2562-2568.
- Whelan, M.A. (2011). The role of Tbdn in retinal endothelial cell permeability and retinal homeostasis
- Witmer, A.N., Vrensen, G.F., Van Noorden, C.J., and Schlingemann, R.O. (2003). Vascular endothelial growth factors and angiogenesis in eye disease. *Prog. Retin. Eye Res.* 22, 1-29.
- Woldeyes, A., and Adamu, Y. (2008). Gender differences in adult blindness and low vision, Central Ethiopia. *Ethiop. Med. J.* 46, 211-218.
- Wong, I.Y., Koo, S.C., and Chan, C.W. (2011). Prevention of age-related macular degeneration. *Int. Ophthalmol.* 31, 73-82.
- Wong, T.Y., Chakravarthy, U., Klein, R., Mitchell, P., Zlateva, G., Buggage, R., Fahrback, K., Probst, C., and Sledge, I. (2008). The natural history and prognosis of neovascular age-related macular degeneration: a systematic review of the literature and meta-analysis. *Ophthalmology* 115, 116-126.
- Wong, V., and Gumbiner, B.M. (1997). A synthetic peptide corresponding to the extracellular domain of occludin perturbs the tight junction permeability barrier. *J. Cell Biol.* 136, 399-409.

Xu, R., Feng, X., Xie, X., Zhang, J., Wu, D., and Xu, L. (2012). HIV-1 Tat protein increases the permeability of brain endothelial cells by both inhibiting occludin expression and cleaving occludin via matrix metalloproteinase-9. *Brain Res.* 1436, 13-19.

Yamamoto, T., Harada, N., Kano, K., Taya, S., Canaani, E., Matsuura, Y., Mizoguchi, A., Ide, C., and Kaibuchi, K. (1997). The Ras target AF-6 interacts with ZO-1 and serves as a peripheral component of tight junctions in epithelial cells. *J. Cell Biol.* 139, 785-795.

Yang, L., Kowalski, J.R., Zhan, X., Thomas, S.M., and Luscinikas, F.W. (2006). Endothelial cell cortactin phosphorylation by Src contributes to polymorphonuclear leukocyte transmigration in vitro. *Circ. Res.* 98, 394-402.

Yeh, B., and Ferrucci, S. (2011). Retinal pigment epithelium tears after bevacizumab injection. *Optometry* 82, 152-157.

Yokoyama, S., Tachibana, K., Nakanishi, H., Yamamoto, Y., Irie, K., Mandai, K., Nagafuchi, A., Monden, M., and Takai, Y. (2001). alpha-catenin-independent recruitment of ZO-1 to nectin-based cell-cell adhesion sites through afadin. *Mol. Biol. Cell* 12, 1595-1609.

Zhadanov, A.B., Provance, D.W., Jr, Speer, C.A., Coffin, J.D., Goss, D., Blixt, J.A., Reichert, C.M., and Mercer, J.A. (1999). Absence of the tight junctional protein AF-6 disrupts epithelial cell-cell junctions and cell polarity during mouse development. *Curr. Biol.* 9, 880-888.

Zhang, Y., Zhang, M., Dong, H., Yong, S., Li, X., Olashaw, N., Kruk, P.A., Cheng, J.Q., Bai, W., Chen, J., Nicosia, S.V., and Zhang, X. (2009). Deacetylation of cortactin by SIRT1 promotes cell migration. *Oncogene* 28, 445-460.

Zhu, J., Yu, D., Zeng, X.C., Zhou, K., and Zhan, X. (2007). Receptor-mediated endocytosis involves tyrosine phosphorylation of cortactin. *J. Biol. Chem.* 282, 16086-16094.

